



SCUOLA DI DOTTORATO
UNIVERSITÀ DEGLI STUDI DI MILANO-BICOCCA

School of Medicine and Surgery
Ph.D. Program in NEUROSCIENCE
Curriculum in: Experimental Neuroscience
Cycle: XXXIV

Specific Signatures in Peripheral Blood Monocytes Stratify Multiple Sclerosis Patients Phenotypes

PhD Candidate: SAVINETTI ILENIA

Registration number: 752891

Tutor: Dr. Maria FOTI

Coordinator: Prof. Rosa Maria MORESCO

ACADEMIC YEAR 2020/2021

INDEX

AIM	pag. 1
INTRODUCTION	pag. 2
Overview on Multiple Sclerosis	pag. 2
Etiology	pag. 3
Pathological hallmarks	pag. 4
Diagnosis	pag. 5
Clinical Subtypes	pag. 6
Disease modifying therapies	pag. 8
Immunopathogenesis	pag. 9
Monocytes	pag. 11
Cholesterol	pag. 14
Trained Immunity	pag. 18
Transcriptome and epigenome profiling in MS	pag. 20
MATERIAL AND METHODS	pag. 22
Cells separation	pag. 22
Flow cytometric analysis	pag. 25
RNA isolation	pag. 26
Nanodrop.....	pag. 27
Bioanalyzer	pag. 27
Microarray experiment.....	pag. 27
DNase treatment.....	pag. 28
Reverse Transcription.....	pag. 30
qRT-PCR validation	pag. 32
oxLDL detection	pag. 38
In vitro experiment.....	pag. 39
Statistical analysis.....	pag. 39
RESULTS	pag. 41
MS patients recruitment	pag. 41
Characterization of MS profiles	pag. 44
Data analysis reveals specific subgroups of MS patients	pag. 46
Inflammation Pathway	pag. 53
Cholesterol Biosynthesis Process	pag. 69
MS tested sera overexpress the oxLDL in comparison to HCs.....	pag. 82
Characterization of receptors that may mediate the oxLDL uptake	pag. 84
Putative Trained Immunity Receptors.....	pag. 90

Epigenetic regulation on MS patients	pag. 95
Selection of the suitable in vitro model.....	pag. 98
DISCUSSION.....	pag. 102
BIBLIOGRAPHY	pag. 108

AIM:

Multiple Sclerosis (MS) is an autoimmune disorder in which the central nervous system (CNS) is targeted by the dysregulated activity of the immune system, resulting in progressive neurological dysfunction¹.

MS is heterogeneous in its rate of progression and in clinical symptoms, reflecting the contribution of different factors to a pathogenic autoimmune response². Migration of activated T cells and monocytes into the CNS under the influence of cellular adhesion molecules and proinflammatory cytokines seems critical to initiate and sustain pathology³. Considering these issues, through this PhD work we aimed to:

1) identify transcriptional differences between the different clinical forms of the MS disease, for example between Relapsing Remitting Multiple Sclerosis (RR-MS) and Primary Progressive-Multiple Sclerosis (PP-MS) patients; 2) identify genetic signatures that could stratify MS patients into distinct functional molecular groups; 3) identify potential novel therapeutic targets in MS patients.

Work described in this dissertation has been performed in the Cellular and Molecular Immunology Lab of the School of Medicine and Surgery at the University of Milano Bicocca, headed by Dr. Maria Foti.

INTRODUCTION:

1. OVERVIEW ON MULTIPLE SCLEROSIS

Multiple Sclerosis (MS) is a chronic, heterogeneous, autoimmune and demyelinating disease affecting the Central Nervous System (CNS)⁴. In MS, the immune system attacks the myelinated axons in the CNS, destroying the myelin and leading to impaired electrical conduction and to axonal damage. MS has been known by many names over the last century, but it was Charcot to made the first correlations between the clinical features of MS and the pathological changes noted post-mortem⁵. In particularly, he illustrated the expansions of lesions from ventricles into the cerebral hemispheres, provided earliest insight into the pathology of MS involving both brain and spinal cord⁶. Symptoms of MS may differ greatly from person to person, they may include monocular visual loss due to optic neuritis, double vision due to brain-stem dysfunction, or ataxia to cerebellar lesion⁷, muscle weakness, sensory and sometimes psychiatric problems. Although the etiopathogenesis is still unknown, MS is among the multifactorial diseases in which several elements may be involved in its onset, such as environment, genetic and epigenetic factors (Fig. 1).

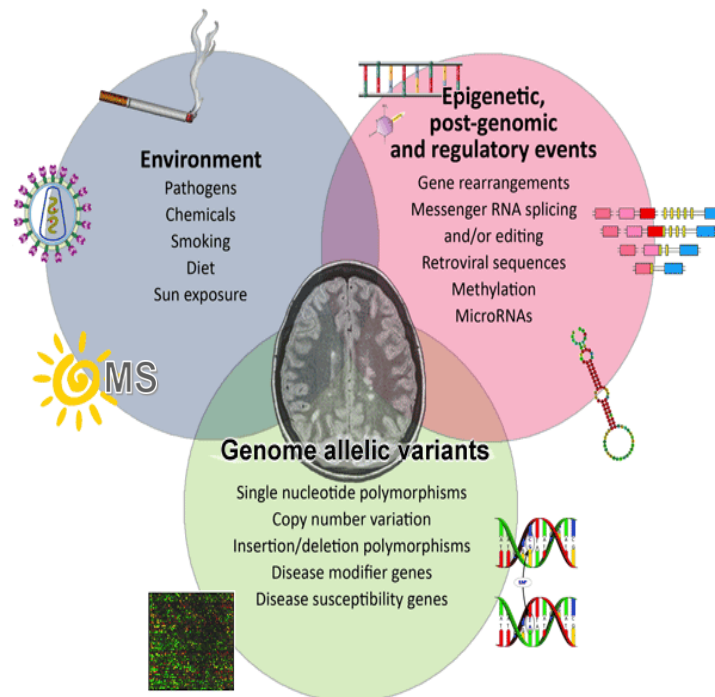


Figure 1. Risk Factors for Multiple Sclerosis. MS is a complex disease in which several factors may have a role. These may include the action of various genes and exposure to chemicals, pathogens, and other external triggers. The study of epigenetic and other regulatory mechanisms linked to MS susceptibility is only beginning to emerge. Credit: J.Oksenberg/UCSF.

2. ETIOLOGY

Multiple Sclerosis typically occurs in adults of 20 to 45 years old and less frequently in childhood or late middle age⁸. It has a heterogeneous prevalence worldwide: highest in North America (140/100,000 population) and Europe (108/100,000), and lowest in East Asia (2.2/100,000 population) and sub-Saharan Africa (2.1/100,000). The global median prevalence of MS has increased from 30/100,000 in 2008 to 33/100,000 in 2013, according to a report by the MS International Federation⁹. Since MS has multiple causes, it is difficult to identify the specific etiology trigger involved in the disease. However, it has been hypothesized that MS has different origins including genetic, immunological, environmental and epigenetic factors. Moreover, gender issues and sexual hormones are among the several factors that have a role in the pathogenesis of MS, as the disease is more common in women in reproductive ages. Alterations in sex hormones may lead to changes in MS symptoms, as observed during pregnancy, menopause, and exogenous hormone administration¹⁰.

Environmental factors. Several studies have been conducted on environmental risk factors for MS. One of the most completed work about this topic is the meta-analysis review published in 2015 by Belbasis and colleagues¹¹. Of the 44 factors included in their analysis, three factors showed a strong association with MS: immunoglobulin G (IgG) seropositivity to Epstein-Barr virus, mononucleosis (which derives from EBV) and smoking. In particular, the risk of developing MS in individuals infected by EBV during their childhood is greater than 15 times compared to those who have not been infected¹². The mechanisms remain unclear, nevertheless the results provide strong correlation between EBV infection and MS. Another discussed risk factor is vitamin D levels¹³: though evidences indicate that lower vitamin D levels are associated with MS risk, the effective impact of vitamin D supplementation on MS activity needs further investigations.

Genetic factors. MS is considered a complex polygenic disease characterized by modest inherited risk for disease susceptibility: the risk rises to 2-3% in subjects with affected parents⁷. The only consistent MS-associated gene is HLA-DRB1 gene on chromosome 6p21; it accounts for 16-60% of the genetic susceptibility in MS⁷. The interesting thing is that the HLA locus was found associated to MS risk both in Relapsing Remitting (RR) and in Primary Progressive patients¹⁴. Moreover, the interleukin-7 receptor alpha chain and interleukin-2 receptor alpha chain have been identified as additional inheritable risk factors accounting for less than 0.4% of the variance risk for developing MS¹⁵. Collectively, the analyses of thousands of cases have identified 110 variants outside the major histocompatibility complex associated with MS susceptibility - these variants often include genes linked to immunological processes, and are always associated with other autoimmune diseases¹⁶.

Epigenetic factors. Although studies of epigenetic changes in MS have only begun in the last decade, a growing body of literature suggests that epigenetic changes may be involved in the development of MS, possibly by mediating the effects of environmental risk factors. To date, small number of studies have addressed the role of epigenetically mediated changes in blood of MS patients. Methylation profiles of mainly CD4⁺, CD8⁺ T cells, B cells, monocytes, and cell-free plasma DNA were reported. The most interesting findings were related to hypomethylation on the IL17A promoter region, which is known to correlate with Th17 cell lineage generation and a decrease in the methylation pattern located in the HLA-DRB1 gene, suggesting that the DRB1 haplotype may influence the association observed between the methylation level at DRB1 CpGs and MS risk^{17,18,19,20}. Monocyte epigenomics was described in one study²¹: the authors found that B cells and monocyte methylation profiles were the most different between relapsing remitting multiple sclerosis (RRMS) and healthy controls. No significant differences were described for CD4 and CD8 T cells. Finally, it has been demonstrated that EAE mouse model treated with the hypomethylating agent 5-aza-2'-deoxycytidine (DAC) ameliorate both clinical and histopathological symptoms²².

3. PATHOLOGICAL HALLMARKS

The pathological hallmarks of MS consist in multiple focal areas of myelin loss within the CNS called plaques or lesions²³. These plaques are not limited to the white matter, as they can be also found in cortical and deep grey matter. The inflammatory infiltrates associated with plaques consist of activated T-cells, macrophages/microglia, plasma cells and B-cells²⁴. In an interesting study of 32 post-mortem brains of patients with MS, it emerged that 26% of the hemispherical lesions were outside the white matter, and in particular that 17% were subcortical lesions²⁵. It has been recently described these lesions more precisely²⁶ and characterized them from the immunological point of view, observing that these types of lesions are less inflammatory. Recently, Kuhlmann et al.²⁷ proposed to classify lesions as: active lesions - for the initial phenotype, which is characterized by the infiltration of CD68⁺ cells (blood-derived monocytes and microglia); mixed lesions – which are commonly seen in progressive patients and are surrounded by a rim of activated microglia/macrophages, whereas showing moderate T-cell infiltrates; and inactive lesions- typical of SPMS, that are sharply demarcated and almost completely depleted of mature oligodendrocytes²⁷. Each one of these lesions can be further separated into active and demyelinating and active and post-demyelinating lesions. This separation refers to the presence of recognizable breakdown products of myelin proteins within macrophages/microglia. MS plaques are frequently histologically classified

as acute, subacute, or chronic without providing an exact definition. During the acute phase plaques appear swollen, then they appear grey during the chronic stage. In addition, during the subacute phase the lesions are full of macrophages, whereas are characterized by gliosis during the chronic period ²⁸. Moreover, chronic inflammation in MS results in the production of Reactive Oxygen Species (ROS) and Reactive Nitrogen Species (RNS) probably promoting mitochondrial damage ²⁹, thus causing metabolic stress, protein misfolding, and a loss of neuronal fitness. Just below is reported a topography of Multiple Sclerosis Lesions (Fig. 2).

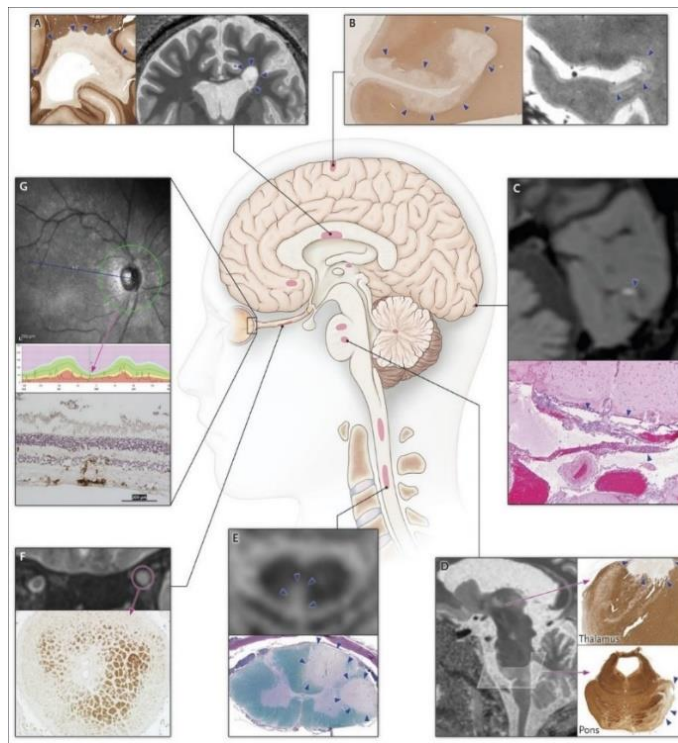


Figure 2. Shown is a schematic of lesions: (A) periventricular white matter, (B) subpial cortex, (C) leptomeninges, (D) thalamus and pons, (E) spinal cord, (F) optic nerve, (G) retina. Credit: Reich et al., *The New England Journal of Medicine*, 378; 2 ;2018.

4. DIAGNOSIS

Diagnostic criteria for MS combining clinical, imaging and laboratory evidence have developed over years, and the most recent revision of these criteria dates back to 2017, called McDonald Criteria.

These criteria include:

- Space dissemination criterion: evidence of at least two different lesions disseminate in different part of CNS
- Time Dissemination criterion: the patient must have undergone at least two different episodes in different dates.

The presence of one or more of these criteria allows a general diagnosis of MS, which may be refined according to the subsequent course of the disease.

Expanded Disability Status Scale (EDSS). The Expanded Disability Status Scale (EDSS) is used to quantify disability in MS patients by monitoring changes over time. It is widely used in clinical trials and in the assessment of people with MS. The neurologist John Kurtzke conceived this method in 1983. EDSS ranges from 0 to 10, considering 10 the maximum level of disability, established by a neurologist.

Values are based on the impairment of:

- pyramidal – weakness or difficulty moving limbs
- cerebellar – ataxia, loss of coordination or tremor
- brainstem – problems with speech, swallowing and nystagmus
- sensory – numbness or loss of sensations
- visual function
- cerebral (or mental) functions

5. CLINICAL SUBTYPES

As stated above, Multiple Sclerosis is a heterogeneous disease in several respects, including the clinical aspect. Indeed, according to the clinical course there are different phenotypes of disease, the main ones are:

Relapsing Remitting Multiple Sclerosis (RRMS): the most common form, affecting about 85% of MS patients (*Multiple Sclerosis Therapeutics. Ed. Jeffrey A Cohen & Richard A Rudick 3 ed. Informa healthcare; 2007*). It is characterized by flare-ups (relapses or exacerbations) period followed by no-symptoms period (remission) - when symptoms improve or disappear (Fig.3).

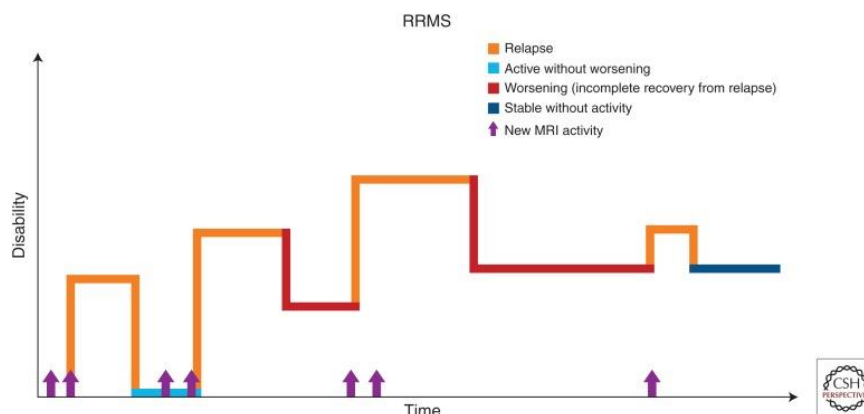


Figure.3. Relapsing Remitting Multiple Sclerosis trend. Credit: National Multiple Sclerosis Society.

Secondary Progressive Multiple Sclerosis (SPMS): Can be defined as an evolution of RRMS, hence it is characterized by at least one relapse followed by progressive clinical worsening over time. Although it is very difficult to predict when such a transition will occur, it has been estimated that approximately 50% of RRMS would pass to SPMS within 10 years, and even the 90% within 25 years (*National Multiple Sclerosis Society*). The course is usually steadily progressive, but in some patients there may be periods of relative stability (Fig. 4).

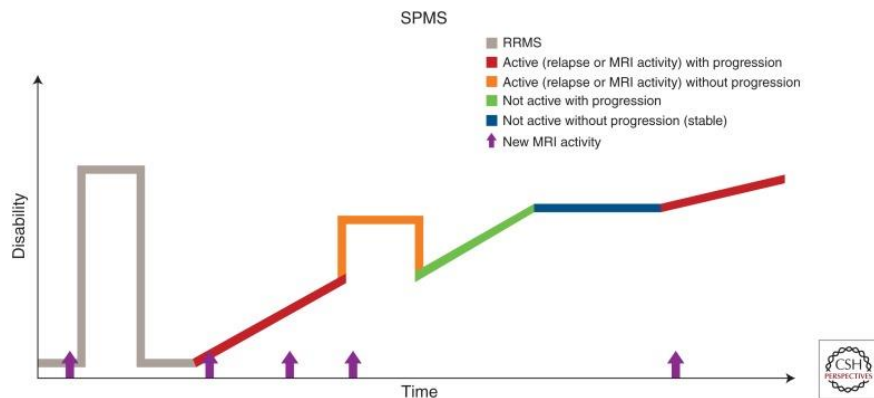


Figure.4. Secondary Progressive Multiple Sclerosis trend. Credit: National Multiple Sclerosis Society.

Primary Progressive Multiple Sclerosis (PPMS): this uncommon form of MS affects approximately 15% of MS patients³⁰. There is a slowly progressive disability from the onset, and clinically the patients present progressive cerebellar dysfunctions. Some patients reach the plateau phase after some time; most, however, progress relentlessly, with no relapses or remissions (Fig.5). While for RRMS the female sex is clearly predominant - counting a sex ratio of 3,5:1 - for PPMS the sex ratio is balanced, probably due to the higher age at the onset for PPMS than for RRMS³¹. This form of MS is more resistant to the drugs typically used to treat the disease, up today Ocrelizumab is the only one drug approved for PPMS.

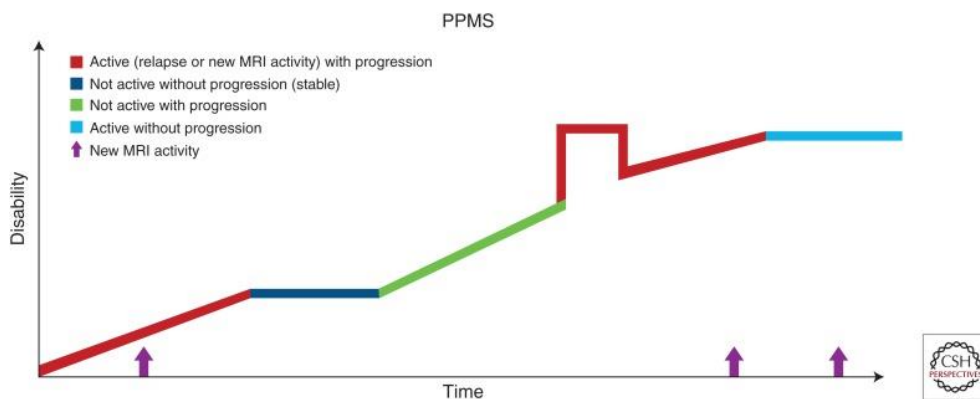


Figure 5. Primary Progressive Multiple Sclerosis trend. Credit: National Multiple Sclerosis Society.

6. DISEASE MODIFYING THERAPIES

Currently, there is still no curative treatment for multiple sclerosis (MS), but during the last 20 years several disease-modifying compounds have been approved for relapsing-remitting MS, and it has been recently approved by both FDA and EMA a new drug that seems to have positive effects for primary progressive patients. FDA and EMA-approved therapeutic agents are described below:

-Interferon β (IFN β): its anti-inflammatory effects are largely believed to result from the inhibition of T-lymphocytes proliferation. Interferon beta is available for MS treatment in recombinant forms, as interferon β -1a or interferon β -1b³². The first is administered by a daily subcutaneous injections, while 1b by intramuscularly way once a week.

-Glatiramer Acetate (GA): GA is a polymer of amino acids that was designed to mimic myelin basic protein (MBP), a major component of CNS myelin. GA reduces antigen presentation and stimulates T cell secretion of cytokines associated with anti-inflammatory or Th2 actions³². In a treatment trial of Clinically isolated syndrome (CIS) with silent MRI lesions, glatiramer acetate treatment was found to significantly prolong time to a second relapse and to reduce the risk of new MRI lesions³². Delivery of GA require frequent intramuscular or daily subcutaneous injections, which can produce many side effects including flu-like symptoms and dermal reactions.

-Mitoxantrone: is a synthetic anthracenedione derivative, and it used in cancer treatment and well as immunomodulatory agent. It is widely used in RRMS patients with a consistent number of relapses and in SPMS patients with a rapid progression of their related symptoms. Side effects such as transient nausea, fatigue, mild hair loss (for days to a week) and menstrual disturbances are frequent (60%–70%)³². Moreover, Mitoxantrone is teratogenic and contraindicated in pregnancy. It is administrated by intravenous injections.

-Dimethyl fumarate: is an immunomodulatory agent with anti-inflammatory properties. Pre-clinical studies indicate that dimethyl fumarate responses are primarily mediated through activation of the nuclear factor (erythroid-derived 2)-like 2 (Nrf2) transcriptional pathway³², but the exact mechanism of action is still unclear. It is administrated orally, 2 times per day.

-Fingolimod: is an oral sphingosine 1-phosphate receptor (S1PR) modulator, to be taken everyday, and represents the first oral drug approved with centralized European procedure in high-activity RRMS, despite treatment with interferon-beta or in case of severe disease³³. Fingolimod inhibits the ability of autoreactive lymphocytes to egress from the lymph nodes towards the CNS¹⁷.

-Natalizumab: is a monoclonal antibody and its mechanism of action is largely through preventing adherence of activated leucocytes to inflamed endothelium, thus inhibiting the migration of inflammatory cells into the CNS³⁴. Natalizumab is administered by intravenous infusion once every

4 weeks, preferably to RRMS with a serious form of the disease. Patients on Natalizumab treatment are at risk for developing a devastating viral infection of the brain, called progressive multifocal leukoencephalopathy.

-Ocrelizumab: is a recently approved B-cell targeted therapy. It consists of a humanised monoclonal antibody designed to selectively target CD20⁺ B-cells³⁵. Based on preclinical studies, this drug binds to CD20 cell surface proteins expressed on certain B cells, but not on stem cells or plasma cells, and therefore important functions of the immune system may be preserved. Ocrelizumab is administered by intravenous infusion in PPMS patients preferably at the onset of the disease.

7. IMMUNOPATHOGENESIS:

For a long time, the CNS was considered a so-called immune-privileged site due to the Blood Brain Barrier (BBB) presence, consisting of endothelial cells tightly closed to each other. However, a fundamental study in mice provides initial evidence for CNS lymphatic vessels lining the dural sinuses, suggesting that the dogma regarding the lack of anatomical connectivity between the CNS and lymphatic system require a re-evaluation³⁶. The multifactorial nature of MS unfolds through a complex, highly multicellular pathophysiological process that evolves throughout the duration of the disease course. Cellular lines that influence MS pathogenesis will now be discussed.

Adaptive Immune System Cells in MS. Genome-wide association studies have identified more than 100 common genetic variants (single nucleotide polymorphism, SNPs) associated with Multiple Sclerosis, mostly in gene loci related to the adaptive immune system³⁷. The presence of T- cells within CNS lesions is detectable in the early stages of MS^{38,39}.

-T cells: Both helper (CD4⁺) and cytotoxic (CD8⁺) T cells have been described in MS lesions. CD4⁺ T cells are more concentrated in the perivascular cuff, whereas CD8⁺ T cells are widely distributed within the parenchyma. CD4⁺ cells trigger the disease in the animal model of MS: their activation and differentiation into Th1 phenotype are crucial processes in the disease's onset⁴⁰. The most likely hypothesis is that myelin damage is initiated by CD4⁺, which reach the CNS and give rise to inflammation⁴¹. Once in CNS, CD4⁺ T cells recruit other adaptive and innate immunity cells, causing myelin and axonal damage resulting in neurological symptoms. Interestingly, CD4⁺ depletion did not correlate with an improvement of MS symptoms, probably because CD4⁺ only drive the initial steps, whereas CD8⁺ represent the prevalent cells populations in MS lesions⁴². At least two CD4⁺ regulatory T cell populations (Treg) have been described: i) T cells expressing the transcription factor FOXP3 - that inhibits in vitro proliferation of effector cells through cell-cell contact⁴³ - and Tr1 cells which inhibit proliferation through the production of IL-10⁴⁴. Treg cells are able to

recognize self-reactive cells and keep under control any autoimmune reactions. In patients with MS, a lower suppressive capacity of Treg cells has been described, which could be both the cause of the disease and the consequence of the inflammatory environment⁴⁵. Tr1 cells have been described more recently and their role has not yet been fully clarified.

CD8⁺ T-cells are found in higher frequency than CD4⁺ T-cells in the white matter and in grey matter cortical demyelinating lesions, and their numbers closely correlate with axonal damage⁴⁶. CD8⁺ T-cells functionality requires expression of Major Histocompatibility Complex (MHC) Class I molecules, which has generally been presumed to be low in the CNS due to its immune-privileged condition. However, most CNS resident cells such as astrocytes, oligodendrocytes and neurons do express MHC class I molecules, at least under inflammatory conditions, making them potential targets for CD8⁺ T-cells.

-B cells: clonally expanded B-cells can be found in the meninges, parenchyma and cerebrospinal fluid (CSF), and produce antibodies that are of diagnostic value. The meninges of patients with secondary progressive disease often contain tertiary lymphoid structures of aggregated plasma cells, B-cells, T-cells and follicular DCs (FDCs)⁴⁷, which are a product of long-term inflammation⁴⁸. By contrast, primary progressive disease is characterized by diffuse meningeal infiltration without such structures⁴⁹. In the absence of known autoantigens, the mechanisms controlling B-cell activation, selection and affinity maturation have been a matter of speculation. However, the recent application of next-generation sequencing technologies has allowed for the characterization of B-cell clonotypes in the peripheral compartments and the CSF of patients with MS, and such studies indicate that antigen-experienced B-cells can undergo maturation in draining cervical lymph nodes before transmigration to the CNS²³. It has been demonstrated that B cells derived from MS patients are able to over produce pro-inflammatory cytokines such as TNF α and IL-6⁵⁰. Moreover, B cells from RRMS patients seem to secrete factors with a toxic impact on rat oligodendrocytes and humans neurons⁵¹. Furthermore, a recent study shown that B cells from MS patients producing low levels of anti-inflammatory cytokines IL10 and faulty in the suppression of Th1 cells. These results suggest that B cells play an important role in the development and pathophysiology of MS. In support of this, B cells were recently chosen as target for the therapeutic treatment of multiple sclerosis: ocrelizumab binds CD20 present on certain B cells surface and induces B cells CD20⁺ depletion.

Innate Immune System Cells in MS. Innate immunity is the first line of defence that comes into play against pathogens and, unlike adaptive immunity, does not act in a targeted and selective way, but in a non-specific way. Its relative simplicity, allows the innate immune system to activate itself in a short time following an infection (within a few hours), providing a first fast response and waiting for the activation of adaptive immunity - which usually takes place in a few days. The innate immune

system is less commonly considered in MS context, although dendritic cells, monocytes, macrophages and microglia - collectively referred to as myeloid cells - have prominent roles in MS pathogenesis. Furthermore, a vicious cycle of interactions between T cells and myeloid cells exacerbates the pathology⁵².

-**Natural Killer cells (NK)**: changes of NK cell functionality in MS were associated with the disease activity, and depletion of NK cells exacerbated the course of the pathology in the experimental autoimmune encephalomyelitis (EAE), the murine model of MS⁵³. The actual role of NK cells in CNS autoimmunity is still not clear.

-**Dendritic cells (DCs)**: are “professional antigen presenting cells” and play an important role in promoting activation and differentiation of naïve T cells. In EAE pathogenesis, the murine model of MS, several studies have suggested the involvement of DCs showing the accumulation of these cells in CNS during inflammation⁵⁴. In addition, in MS patients DCs have an activated phenotype with an increased expression of activation markers and an aberrant secretion of proinflammatory cytokines⁵⁵.

-**Macrophages/Microglia**: They both participate to pathogenesis mechanisms of MS: in EAE model, macrophages reach and infiltrate the CNS, and the residential microglia contribute to the neurological damage⁵⁶. The main difficulty in this context is to distinguish macrophages from residential microglia, since they express many of the same specific markers. Among these, there are CD45, Ionized calcium-binding adapter molecule 1 (Iba1), F4/80 and CD68. To the current knowledge, CD44 is reported to be expressed exclusively by infiltrating cells and⁵⁷, in addition, it has been shown that microglia lack CD169⁵⁸. It has been also demonstrated that quantitative differentiation of markers may help to correctly distinguish among these two cellular types: macrophages express CD11b⁺/CD206high/CD163⁺, while microglia present CD11b⁺/CD206low/CD163⁺ pattern⁵⁹. These discoveries open the door to unraveling their separate contributions, and this could help the development of targeted therapy.

8. MONOCYTES

Monocytes (Mo) are white blood cells, derived from bone marrow, and accounting for the 5-10% of circulating nucleated cells in healthy adult blood⁶⁰. In response to particular stimuli (e.g., infection) monocytes are able to migrate into tissues and differentiate into macrophages (Mφ) or dendritic cells (DC), eliminating the pathogens by phagocytosis, cytokines production and antigen presentation. As suggested by Yona et al.⁶¹, even if the noun is composed by the word “mono”, this cell line is instead characterized by several subgroups. In humans, three major subsets of circulating monocytes (Mo) can be distinguished based on CD14 and CD16 expression⁶². Initially, Mo were identified by their

expression of large amounts of CD14, which is part of the receptor for lipopolysaccharide (LPS). Anyway, the subsequent identification of differential expression of antigenic markers showed that Mo in human peripheral blood are extremely heterogeneous, providing the first clues to the differential physiological activities of monocyte subsets. The 85-90% of total Mo is CD16⁻ and CD14⁺ (classical monocytes), while the minor CD16⁺ Mo subpopulation comprises the remaining 10-15%^{60,63,64}. Furthermore, CD16⁺ can also be divided into cells with high levels of CD14 and low CD16 (intermediate monocytes) and cells with low levels of CD14 and high expression of CD16 (non classical monocytes)⁶⁵. Intermediate monocytes express significantly higher levels of Toll-like receptors (TLRs) 2, 4, and 5 as compared to classical and non classical subsets, indicating a primarily pro-inflammatory function⁶⁶ (Table 1). Furthermore, intermediate monocytes express high levels of CD80, CD86, and HLA-DR suggesting antigen presentation role. Interestingly, the non-classical monocytes also express CD80 and CD86, suggesting an antigen-presenting capability also for this subgroup. Instead, the classical monocytes express higher levels of CD36 and CD163, and low levels of TLRs and co-stimulatory molecules, suggesting that the majority of blood monocytes are primarily phagocytic in nature⁶⁶. Moreover, these subsets of monocytes differ for the expression of chemokine receptor. In particular, CD16⁻ have higher levels of inflammatory CCR1, CCR2, CXCR1 and CXCR2 receptors, as well as CCR7 and CD62L, two proteins involved in migration to lymphoid organs, while CD16⁺ have higher expression of CX3CR1 receptors⁶⁷.

Table 1. Monocytes subsets and their main functions. Human monocytes are classified as classical (CD14⁺⁺/CD16⁻), intermediate (CD14⁺⁺/CD16⁺) and nonclassical (CD14⁺/CD16⁺⁺) monocytes.

Human Monocytes Subsets	Percentage	Molecular Markers	Additional Molecular Markers	Main Role
Classical	85-90% of the total circulating monocytes	CD14 ⁺⁺ /CD16 ⁻	Low levels of TLRs High levels of CD80, CD86	Phagocytosis and Immune Response
Intermediate	The remaining 10-15%	CD14 ⁺⁺ /CD16 ⁺	High levels of TLRs 2, 4, 5 CD80, CD86, HLA-DR	Proinflammatory function and Wound Healing
Non Classical		CD14 ⁺ /CD16 ⁺⁺	High levels of CD80, CD86	Antigen presentation and Patrolling role

Credit:doi:10.3390/biomedicines9070717.

Monocytes in Central Nervous System. In the last years, the role of monocytes and their ability to over cross the BBB during neurodegenerative diseases has been deepened. I have personally investigated this topic during my PhD by writing a review about this issue¹⁷. The exact mechanisms through which monocytes reach the brain are not fully understood, but some processes seem to be

essential: brain becomes highly permeable to circulating peripheral cells, because of injury or during specific disease processes and once into the brain monocytes initiate their contribute to neuroimmune response¹⁷. A fundamental molecule for their recruitment is the chemoattractant factors C-C Motif Chemokine Receptor 2 (CCR2)⁶⁸. This latter is necessary for monocytes' recruitment through monocyte chemoattractant protein-1 (MCP-1- or CCL2) binding, expressed on monocytes surface. Indeed, CCR2 is activated by a plethora of chemokines, but the most powerful activator of its signalling seems to be CCL2, responsible for monocytes transmigration⁶⁹. In addition, it has been demonstrated that in EAE model the expression of CCR2 increases during the acute phase of the disease and, likewise, CCL2 expression correlates with disease's severity⁷⁰. Beside CCR2-CXCL2 axis, also the CD49e ($\alpha 5$ integrin) was reported to be involved in monocytes brain migration. Interestingly, $\alpha 5$ integrin is expressed only on the peripheral monocyte populations but not on CNS-resident myeloid cell populations and it has been demonstrated that $\alpha 5$ integrin antibody treatment significantly reduced the experimental autoimmune encephalomyelitis (EAE) disease severity. Thereby, it suggests that monocytes brain migration is a key factor for instance neurodegenerative disease, and provides a strong rationale for a novel therapeutic approach that specifically targets and inhibits monocyte trafficking into the CNS.

Monocytes and Multiple Sclerosis. In autoimmune disease, monocytes are widely recognized to play an inflammatory and tissue destructive role⁷¹. In EAE model, a correlation between monocyte infiltration into the CNS and progression to the paralytic stage of the disease has been shown⁷². Moreover, depletion of monocytes was shown to significantly inhibit both disease initiation and progression in EAE mice. When examining the frequency and the phenotype of monocyte subsets in peripheral blood and cerebrospinal fluid (CSF) of RRMS, a pivotal role of CD16⁺ emerged⁷³. Untreated RRMS patients have 35% less CD16⁺ in their periphery compared to HCs, whereas RRMS treated with immune-modulating drugs present the same or even higher percentage of CD16⁺ compared to HCs. Flow cytometric analysis of peripheral blood mononuclear cells demonstrated a significant expansion of the nonclassical monocyte population (CD14⁺/CD16⁺⁺) in patients with MS compared to healthy controls. In addition, monocytes of progressive MS produce a high percentage of Interleukin-12 in the blood compared to normal individuals⁷⁴. All these recent findings emphasize the role that monocytes play in MS disease elucidating the role of innate immunity in MS.

Monocytes and Cholesterol. Little is known about the correlation between the cholesterol process and monocytes functions, and how a dysregulation of the cholesterol pathway may have a role on monocytes features. As described above, three different classes of monocytes exist, and it has been shown that intermediate monocytes are elevated in subjects with a cardiovascular disease, and that

this profile correlates with the lipid levels⁷⁵. In addition, subjects with the higher proinflammatory response, were those with the higher cholesterol levels⁷⁵. It has also been demonstrated that in the context of atherosclerosis, cholesterol accumulation may act as priming for monocytes and that modification in cholesterol intracellular metabolic enzymes allow the atherosclerosis progression by affecting monocytes signalling and differentiation⁷⁶. In MS context, it is known that lipid-activated transcription factors liver X receptors may impact the regulation of myeloid and lymphoid cells⁷⁷, but there are no studies strictly related to the monocyte - cholesterol topic. Therefore, through our project we give one of the first contributions about monocytes and cholesterol in Multiple Sclerosis Disease.

9. CHOLESTEROL

Cholesterol is the most important sterol and represents the fundamental element of cellular membranes, where it interacts with the adjacent lipids to regulate the permeability of the bilayer⁷⁸. Furthermore, it represents the precursor of steroid hormones, vitamin D, the oxysterols and bile acids, which in turn regulate the metabolism⁷⁹. In physiological conditions, cholesterol levels and its major metabolites depend on a homeostatic balance between synthesis, absorption, transport, catabolism and excretion processes. Given its importance, both deficiency and excess of cholesterol may be crucial for develop diseases⁸⁰. Often more increased evidence suggest a close relationship between cholesterol metabolism and cardiovascular disorders, several types of cancer and neurodegenerative diseases^{81, 82, 83}.

Biosynthesis of endogenous Cholesterol. The Cholesterol biosynthesis process requires 30 enzymatic reactions, grouped into 3 phases⁸⁴ :

-Mevalonate production. The biosynthesis takes place into the cytosol and begins with the combination of two acetyl-CoAs to form acetoacetyl-CoA. Acetoacetyl-CoA condenses to form 3-hydroxy-3-methylglutaryl-CoA (HMG-CoA) through HMG-CoA synthase (HMGCS1). HMG-CoA is reduced by HMG-CoA reductase (HMGCR) using NADPH to mevalonate⁸⁵. The HMGCR is considered the rate-limiting enzyme of the cholesterol biosynthesis, it follows that it represents the ideal target for regulating the whole process⁸⁵.

-From Mevalonate to Squalene. Mevalonate is phosphorylated to isopentyl pyrophosphate, which is converted to geranyl pyrophosphate and then into farnesyl pyrophosphate through condensation. Then, squalene synthase catalyzes the condensation of two molecules of farnesyl pyrophosphate to obtained squalene⁸⁶.

-Cholesterol. This phase takes place in the endoplasmic reticulum (ER) and provides for the cyclization

of squalene to lanosterol. From lanosterol, through approximately other 20 enzymatic reaction, are formed first lanosterol and desmosterol and then cholesterol⁸⁶.

Regulation: Cholesterol biosynthesis requires a significant energy expenditure, so it needs to be regulated. A crucial player for the regulation process is sterol regulatory element-binding protein 2 (SREBP-2). SREBP2 is normally present in the inactive form linked to SREBP Cleavage-activating protein (SCAP), which in turn is anchored to Insulin induced gene 1 (INSIG1) at Endoplasmic Reticulum (ER) level⁸⁷. In deficiency of intracellular cholesterol, the interaction between SCAP and INSIG becomes weaker, the complex SREBP/SCAP is detached from INSIG and then it moves into the nucleus. Once in the nucleus, it binds the sterol regulating sequences (SRE) present on HMG-CoA-reductase promoter⁸⁸. Thus, the HMGCR gene was activated only when the endogenous cholesterol synthesis is strictly necessary (Fig. 6).

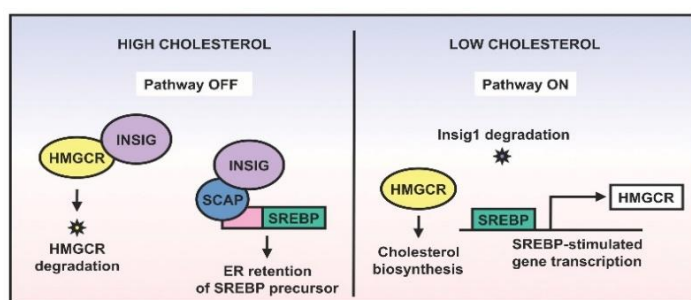


Figure 6. Mechanism of Cholesterol Regulation.

Credit: doi:10.1261/rma.063099.117

Dietary intake: Besides the “de novo” biosynthesis, cholesterol is introduced in humans also by the diet. Around 50% of dietary cholesterol is absorbed through enterocytes in the gut, while the remaining portion is excreted with faeces⁸⁹. However, it depends on the individual and on it is influenced by genetic factors⁹⁰.

Transport: Despite being an amphipathic compound, cholesterol is poorly polar and therefore scarcely soluble in aqueous solution. For this reason, its transport in the plasma needs of complex molecules also known as lipoproteins. Lipoproteins have a basic structure consisting of a central core containing cholesterol esters and triglycerides, surrounded neutral lipids such as cholesterol, phospholipids, and apolipoproteins⁹¹. Plasma lipoproteins are divided into different classes based on size, density, lipid composition, and apolipoproteins.

-Chylomicrons. Relatively large particles and very low density, mainly involved in the transport of dietary triglycerides. They consist of a lipid core surrounded by protein molecules (apoB-48) that give them a higher degree of water solubility. They are produced by the enterocytes and then move

into blood circulation through the lymphatic system ⁹². After distributing their lipid content to the various tissues, the chylomicrons are reduced to cholesterol-rich residues (remnants). Compared to chylomicrons, these remnants are enriched in cholesterol and are pro-atherogenic ⁹¹.

-**Very low density lipoproteins (VLDLs)**. Are very low density lipoproteins rich in triglycerides, synthesized and secreted by the liver. Their half-life is about 6 hours and their degradation gives rise to IDL and LDL.

-**Intermediate Density Lipoproteins (IDLs)**. These lipoproteins are produced by the VLDLs degradation, contain triglycerides and cholesterol in equal parts ^{93,94}.

-**Low-Density Lipoprotein (LDLs)**. Derive from VLDLs and IDLs and represent the main vehicle for cholesterol transport to peripheral tissues.

-**High Density Lipoproteins (HDLs)**. Inversely to the LDLs, HDL are involved in reverse cholesterol transport from peripheral tissues to the liver- so their task is to remove cholesterol from tissues.

They are also called as “good cholesterol”⁹⁵, since have anti-inflammatory and anti-thrombotic properties, which may also contribute to inhibit atherosclerosis.

Cholesterol degradation. As mentioned previously, HMG-CoA reductase catalyzes the rate limiting step of cholesterol biosynthesis. When cholesterol accumulation occurs, the half-life of HMGCR lower from 12h to 1h ⁹⁶. It has been demonstrated that lanosterol and not the cholesterol itself is able to mediate this process, thereby leading to HMG-CoA reductase degradation. Indeed, lanosterol accumulation is able to induce - through INSIG1- the HMGCR ubiquitination and successively its degradation by the proteasome⁹⁷.

Cholesterol: brain and Multiple Sclerosis. Cholesterol is necessary for myelin structure and for its proper functioning and integrity. Under physiological conditions, intact BBB do not lead cholesterol passage from periphery to the brain: this is the reason why cholesterol biosynthesis at brain level is completely independent from that which occur in periphery⁸⁵. In particular, it has been demonstrated that astrocytes produce more cholesterol than neurons in rat model: during the embryonic phase, both astrocytes and neurons synthesize cholesterol necessary for myelinogenesis, but in adult rat neurons lose this ability⁸⁵. In addition, most of the lipoproteins present at the peripheral level are not found at the brain level, always due to the presence of BBB. Instead of classical lipoproteins, at brain level were found the so-called “HDL-like particles”, because of their similarity to plasma HDL ⁹⁸. Again, astrocytes seem to be the main responsible for their production⁹⁸. Another important difference is that the brain cholesterol has a very long half-life: from 6 months to 5 years, contrary to what happens at the plasma level where its half-life consists of few days. Recent data suggest a

role for cholesterol in MS pathogenesis, but it may have a role also as a biomarker of disease activity and progression⁷⁷. In support of this hypothesis, it has been shown that inhibitors of HMGCR enzyme play a role in MS course. Indeed, in a phase II clinical trial high doses of simvastatin improve disease status in secondary progressive MS (SPMS)⁹⁹ - the phase III is still ongoing (<https://www.msociety.org.uk>). Simvastatin can inhibit interferon regulatory factor-4 transcription factor, thereby blocks the secretions of cytokines involved in Th1 and Th17 differentiation in MS. Statins may also act by inhibiting mevalonate production, rather than on cholesterol itself⁹⁹. At today, this treatment seems to be hopeful just for SPMS but not for RRMS, since the association of Simvastatin with beta interferon did not provide better results¹⁰⁰. Other interesting works showed a correlation between dyslipidaemia and high MS disease activity with an impairment of both EDSS and lesions¹⁰¹. In addition, it has been demonstrated that different cholesterol levels are able to clearly distinguish MS patients between healthy volunteers as well as between MS patients at different stage of the disease. Interestingly, these findings are consistent with what will be reported in this dissertation.

Cholesterol and Inflammation. Hypercholesterolaemia determines cholesterol accumulation in immune cells, such as macrophages, establishing inflammatory responses. As a consequence, increase the Toll-like receptor signalling, monocytes and neutrophils production and the inflammasome activation¹⁰². In MS context, it is known that a high-fat/sugar diet, also called “Western diet”, may promote the pathology: in EAE model a high-fat diet exacerbates the pathology¹⁰³. Indeed, this kind of diet leads cholesterol accumulation of white adipose tissue, which can release a plethora of pro-inflammatory mediators. In support of this, cholesterol crystals induce inflammation and inflammasome activation when injected in mice.¹⁰⁴ Piccio and colleagues¹⁰⁵ demonstrated that chronic diet restriction have importantly reduced the MS severity in the animal model of the disease. In addition, Jordan *et al.*¹⁰⁶ demonstrated that intermitting fasting decreased monocytes mobilization and reduced CNS monocytes and relative release of proinflammatory cytokines as well as TNF α and IL1 β ; and of proinflammatory mediators such as CXCL2. Moreover, Materese and colleagues demonstrated that obese RRMS patients release higher levels of proinflammatory cytokines as IL-6 in the CSF, and show higher clinical disability profile¹⁰⁷. In conclusion, a dietary restriction regime seems to be essential to extend lifespan and prevent age-associated diseases, such as neurodegenerative pathologies and to prevent a general inflammatory status.

10. TRAINED IMMUNITY

It will now describe a process known as Trained Immunity (TI), recently discovered and which seems to be at the root of autoinflammatory diseases, such as Hyperimmunoglobulinemia D syndrome (HIDS)¹⁰⁸. Among the various molecules capable of inducing TI there is also the mevalonate, a fundamental intermediate for the Cholesterol Biosynthesis. We assume that in some cases of MS a trained immunity phenotype may be involved¹⁰⁸.

Overview of Trained Immunity. Host immune responses are typically divided into innate immune responses and adaptive immune responses that acting, respectively, in rapid and nonspecific way and in slower but specific way to build up immunological memory. Recently, the dogma according to which only the adaptive immunity can build an immunological memory has been challenged¹⁰⁹. It has been demonstrated that innate immune cells, such as monocytes and macrophages-derived macrophages can mount resistance to reinfections¹⁰⁹. Moreover, in certain mammalian models of vaccination, protection from reinfection has been shown to occur independently of T and B lymphocytes¹¹⁰. All of these observations led to the hypothesis that innate immunity can display an immunological memory, named “trained immunity” or “innate immune memory”¹⁰⁹. In brief, monocytes expose to a primary stimulus and then expose to a secondary stimulus – which can be either a vaccine or infectious- increase the potential of the pro-inflammatory response¹⁰⁹ (Fig. 7). In physiological conditions, these mechanisms are necessary to protect the organism - however, when inappropriately activated, this type of immunity can become maladaptive as in autoinflammatory diseases. The discovery of innate immune memory opens the door for future research to investigate the role of this immunity and its effects on autoinflammatory diseases.

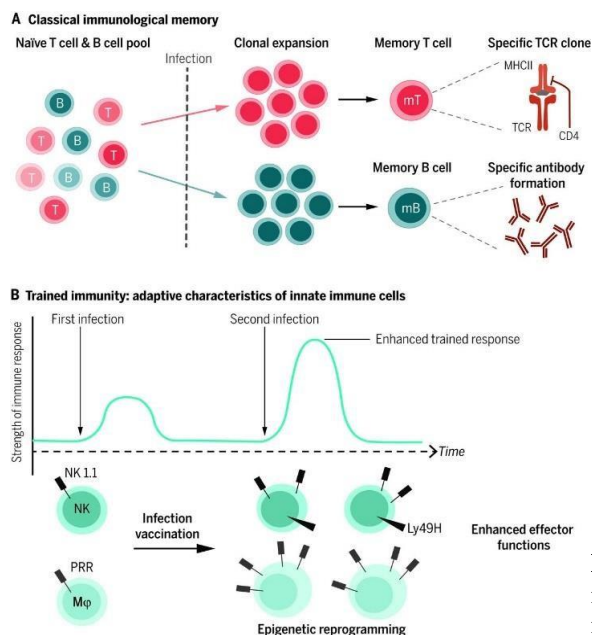


Figure 7. Classical immunological memory versus trained immunity. Image from Trained immunity: a program of innate immune memory in health and disease.

The molecular basis of trained immunity. Recent studies have demonstrated that trained immunity is based on epigenetic reprogramming¹⁰⁹ and on metabolic changes¹¹¹. Histone modifications have shown to be a central process for trained immunity, but also other mechanisms expected to be involved (Fig.8).

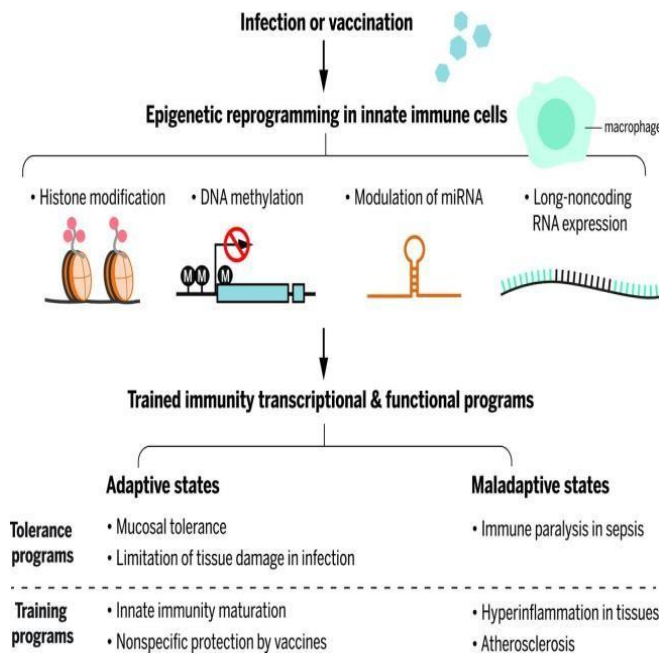


Figure 8. Trained Immunity mechanism. Image from Trained immunity: a program of innate immune memory in health and disease.

The molecular bases of TI are partially defined, but data support the hypothesis of changes in chromatin organization, DNA methylation, reprogramming of cellular metabolism and the expression of long non-coding RNAs^{112,113,114,109}. In vitro experiments in which human monocytes were exposed to β -glucan have shown genome-wide changes at epigenetic level, including histone H3 lysine 4 methylation (H3K4me1), trimethylation (H3K4me3) and H3 lysine 27 acetylation (H3K27ac)¹¹⁵. In addition to these epigenetic modifications, cellular metabolism processes resulted deregulated. In fact, β -glucan exposure determines the switch from oxidative phosphorylation to glycolysis, leading to higher glucose consumption and lactate production¹¹⁶.

The role of metabolic changes in trained immunity. Recent works about Transcriptomic and Metabolomic analyses have demonstrated that metabolic pathways, especially glucose metabolism, are implicated in the context of trained immunity¹¹⁷. In metabolic context, mevalonate plays an important role for TI induction¹⁰⁸: statins administration - which act on HMGCR blocking mevalonate production - inhibits TI process. Hence, mevalonate determines: increased production of pro-inflammatory cytokines such as $\text{TNF}\alpha$, IL-6 and IL-1 β , metabolic shift from oxidative phosphorylation to aerobic glycolysis, mTOR activation through IGF1-R and Akt, and histone

modifications¹⁰⁸. These findings may lead to the development of new therapeutic strategies for the treatment of those diseases in which trained immunity plays a central role.

11. TRANSCRIPTOME AND EPIGENOME PROFILING ON MS:

Transcriptome profiling is one of the most utilized methods to investigate human pathologies at the molecular level. Transcriptome contains the full information about all RNA transcribed by the genome in a specific tissue or cell type, at a particular developmental stage, and under a certain physiological or pathological condition. Thus, transcriptome analysis provides a comprehension of gene structure and function, gene expression regulation and genome plasticity. More importantly, it may disclose the key alterations of biological processes triggering human diseases, thus offering novel instruments useful not only for the comprehension of their underlying mechanisms but also for their molecular diagnosis and clinical therapy¹¹⁸. Several studies have been conducted using Microarray technique to investigate MS disease. For example, it has been identified an association of a single nucleotide polymorphism (SNP) with IL7R and IL2RA genes. A meta-analysis GWAS study, collecting data of 68,284 healthy controls and 47,351 MS patients showed a strong association of 200 autosomal susceptibility variants outside the MHC, one chromosome X variant and 32 independent associations within the extended MHC¹¹⁹. Another well characterized example is the intronic SNP rs1800693 in the gene encoding for tumor necrosis factor receptor super family 1A, which determines the production of soluble form of the TNF receptor. This soluble protein is able to inhibit TNF signalling inside the cells, mirroring somehow the exacerbating effects of TNF-blocking drugs on MS course¹⁴. The transcriptome profiling of MS patients was also used to investigate how the transcriptomes of cell lines involved in MS can be modulated after drugs treatment: this is important to obtain further insights on the effects on molecular signatures thought to be related to the pathophysiology of MS. For example, investigating the effects of IFN β at a molecular level it was possible to classify patients as responders and non- responders at an early stage during on going therapy or even before its initiation¹²⁰. The same was made for Fingolimod treatment, showing that the absolute numbers of naive B cells, memory B cells, and plasmablasts are significantly reduced in the peripheral blood during fingolimod treatment¹²¹.

Despite the great advantages of this technology, there is also to say that gene expression dysregulation in human disorders may be strongly biased by gender. This observation derives from transcriptomic studies available in literature but also from our experience. In particular, for MS disease, transcriptomic profiling of male and female subjects reveals that generally there is a lower

number of Differentially expressed genes (DEGs) in the male group, suggesting that the pathological processes measured in the periphery are sustained by fewer transcriptional changes, regardless the phenotypes of the disease. Likewise, brain aging has been associated with sexual dimorphism in terms of different numbers of gene expression changes in the two genders¹²². However, the transcriptomic analysis has a critical importance to study every single aspect of each disease, and thanks to this technology many forward steps have been made to understand molecular mechanism of a pathology.

microRNAs and Multiple Sclerosis. About the Immune System, miRNAs may affect cytokine secretion, cell activation and immune tolerance¹²³. Studies on PBMC of MS patients revealed interesting results in comparison to healthy controls¹²⁴. The analysis of the expression pattern of 364 miRNAs of MS patients during relapse and remission, demonstrated differences in gene expression patterns not only between MS patients and healthy controls but also between patients with and without relapses. In particular, miR-18b and miR-599 have been shown to be associated with relapse, whereas miR-96 was found to be involved in the remission phase. In other works, vitamin D supplementation improved EAE through the regulation of the miRNA population related to CD4⁺ T cells proliferation, and in another one the upregulation of ebv-miR-BHRF1-2-5p and ebv-miR-BHRF1-3 in RRMS circulation was related to MS risk and increased EDSS score¹²⁵. In peripheral B-lymphocytes isolated from untreated RRMS patients, the levels of 49 miRNAs are reported to be significantly decreased compared with healthy volunteers via microarray analysis; in contrast, no miRNAs increased significantly¹²⁶. Down-regulated miRNAs in B- cells of MS patients include miR-25, miR-106b, miR-93, miR-19b, and miR-181a, which are essential for B-cell development^{127,128}. In addition, it has been shown that miRNAs with anti-inflammatory functions were increased in MS patients, whereas miR-155- which has pro-inflammatory functions- results downregulated¹²⁹. Given these results, is reasonable to consider miRNAs as good potential disease biomarkers and targets of therapy for MS.

MATERIALS AND METHODS

1. CELL SEPARATION

After the Ethical Committee approval, 20 mL of blood per individual were sampled at San Gerardo Hospital (Monza, MB) and delivered to our lab in a few ours. EDTA was used to prevent coagulation. On the same day, blood was treated to obtain PBMCs and then purified CD14⁺ monocytes via positive selection with magnetic beads described below.

Isolation of PBMC from whole blood via density gradient centrifugation. PBMC fraction was obtained by density gradient centrifugation using Lympholyte®-H Cell Separation Media (Cedarlane - Burlington, Canada) following manufacturer instructions. Briefly, whole blood was diluted and then gently layered over the cell separation media and then centrifuged. The Figure 9 illustrates the procedure. Differential migration of cells during centrifugation results in the formation of layers containing different cell types:

- The bottom layer is pellet containing erythrocytes and dead cells
- The layer immediately above contains mostly granulocytes and the Lympholyte® used.
- At the interface between the plasma (top) and the Lympholyte® layer, mononuclear cells are found.

Plasma was stored and PBMCs were then washed and counted in preparation for the next phase.

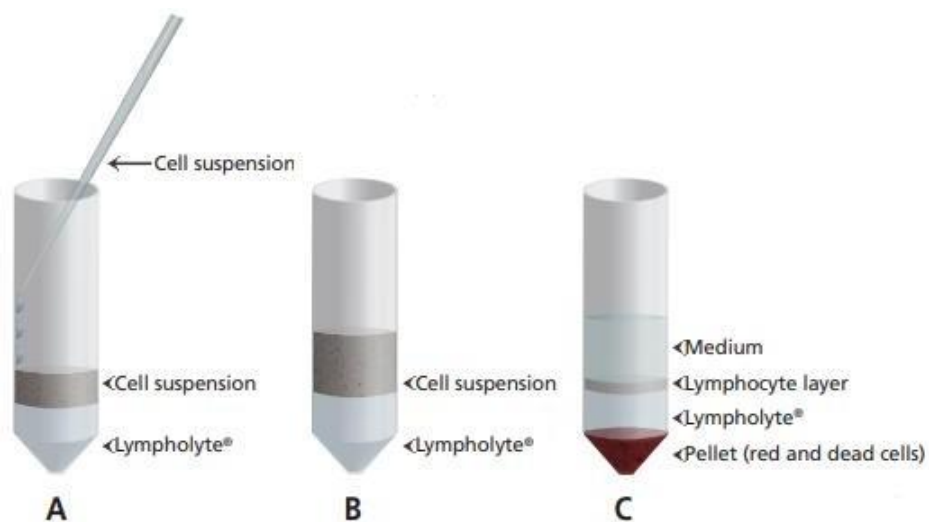


Figure 9. *Lympholyte® Cell Separation Procedure.* (A) Gently layer whole blood over the Lympholyte® making sure not to mix the two layers. (B) Centrifuge the tube for indicated time at the indicated speed. (C) Carefully remove the cells at the interface and transfer in a new tube for washing. Image from: "Lympholyte®- H Cell Separation Media Data Sheet".

Protocol:

1. Dilute blood 1:2 with PBS 1x.
2. Prepare two 50 mL Falcon Tubes with 10 – 12 mL of Lympholyte-H.
3. Carefully layer 25 mL of diluted blood over the Lympholyte-H in each of the Falcon Tubes
4. Centrifuge at 600 rcf for 20' in a swinging-bucket rotor without brake. Four distinct phases should be obtained, starting from the bottom: Blood Cells, Granulocytes+Lympholyte, PBMCs and Plasma.
5. Transfer approx. 10 mL of plasma (Top Phase) in a new 15 mL Falcon Tube. Stop pipetting when about 2 cm above the PBMCs ring.
6. Transfer the PBMCs ring in a new 50 mL Falcon Tube. Be sure to remove the whole ring – aspirate some lympholyte too!
7. Dilute the PMBCs 1:2 with PBS 1x
8. Pellet PBMCs by centrifuging at 296 rcf for 10' at 4°C.
9. Do not throw away supernatant. Instead, transfer it in a new 50 mL Falcon Tube and centrifuge it again at 296 rcf for 10' at 4°C.
10. Resuspend and unite the pellets in 20 mL of PBS 1x
11. Remove Platelets by centrifuging at 296 rcf for 10' at 4°C.
12. Remove the supernatant and resuspend pelleted PBMCs in 5mL of MACS Buffer (PBS 1x, EDTA 2 mM, 0,5% BSA [w/v])
13. Count cells in a haemocytometer diluting them 1:10 (10 μ L of resuspended cells, 80 μ L of PBS 1x, 10 μ L of Trypan Blue)

Magnetic beads positive selection. Starting from PBMC fraction, we then performed a Positive Selection with microbeads using MACS® Technology developed by Miltenyi Biotec (Bergisch Gladbach, Germany). This technology enables the magnetic separation of cell populations based on surface antigens, by labeling epitopes with specific antibodies conjugated to magnetic beads. Due to their small size, the beads do not activate cells and do not have to be removed for any downstream application. The protocol comprises a Magnetic Labelling step, during which cells of interest are magnetically labelled with MACS MicroBeads; a Magnetic Separation Step, by which cells a

separated through a MACS column; and an Elution of Labelled Cells step. s for a separate analysis. Figure 10 overviews the procedure.

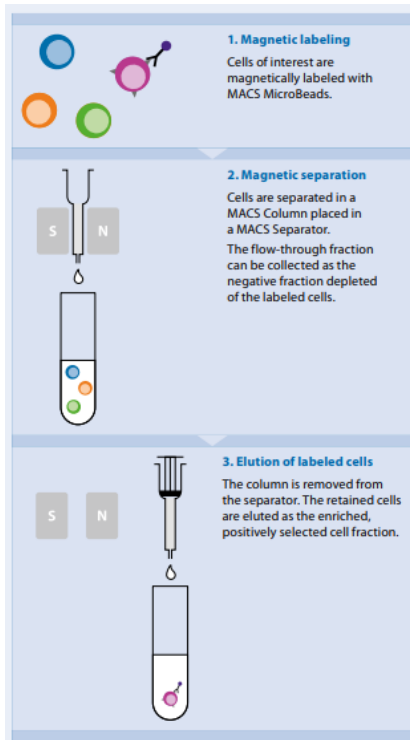


Figure 10. MACS separation overview. Image from: www.miltenyibiotec.com.

Monocytes Isolation procedure:

1. Centrifuge PBMCs at 296 rcf for 10' at 4°C.
2. Resuspend pelleted PBMCs in 20 μ L CD14 Beads + 80 μ L MACS Buffer every 10^7 cells (do not use less than this volume, even if you have less than 10^6 cells). Note: do not vortex to resuspend, but use pipetting instead.
3. Incubate for 15' at 4°C (mix every 7').
4. Add 5 mL of MACS Buffer as washing
5. Centrifuge at 296 rcf for 8' at 4°C
6. While centrifuging mount Miltenyi LS Column on the stand and add 3 mL of cold MACS Buffer, use a 15 mL Falcon Tube as waste.
7. Resuspend pelleted cells in 500 μ L of cold MACS Buffer.
8. Add the sample to the LS column, collect the flow-through as CD14⁻ fraction.
9. Wash three times with 3 mL of cold MACS Buffer, collect the flow-through as CD14⁻ fraction.

10. Remove the LS column from the magnet, and put it above a new 15 mL Falcon Tube.
11. Pipette 5 mL of cold MACS buffer onto the LS Column. Immediately flush out fraction with the magnetically labelled cells by firmly applying the plunger supplied with the column. It contains CD14⁺ cells.
12. Centrifuge CD14⁺ cells at 296 rcf for 8' at 4°C
13. While centrifuging mount Miltenyi MS Column on the stand and add 400 μ L MACS Buffer, use a 15 mL Falcon Tube as waste.
14. Resuspend pelleted CD14⁺ cells in 500 μ L of MACS Buffer.
15. Add the sample to the MS column, collect the flow-through as CD14⁻ fraction.
16. Wash three times with 500 μ L of MACS Buffer, collect the flow-through as CD14⁻ fraction.
17. Remove the MS column from the magnet and put it above a new 15 mL Falcon Tube.
18. Pipette 1 mL MACS buffer onto the MS Column. Immediately flush out fraction with the magnetically labelled cells by firmly applying the plunger supplied with the column. It contains CD14⁺ cells.
19. Count CD14⁺ fraction in a haemocytometer diluting them 1:10 (10 μ L of resuspended cells, 80 μ L of PBS 1x, 10 μ L of Trypan Blue)

2. FLOW-CYTOMETRIC ANALYSIS

After isolation, cell purity was assessed by flow-cytometric analysis. Briefly cells were stained with antibodies for selected surface markers, washed and analysed via the FACS Calibur instrument (BD Biosciences, (Franklin Lakes, New Jersey, USA) available at the Biological Sciences and Biotechnologies department of University of Milano-Bicocca.

Monocytes treatment for FACS.

1. Transfer approx. 2×10^5 CD14⁺ cells in 2 FACS tubes, named Population and Stained
2. Add 500 μ L of PBS 1X and centrifuge at 310 rcf for 5', setting the temperature to +4°C.
3. Remove supernatant sucking through a Pasteur
4. Resuspend "Population" cells in 250 μ L PBS 1X

5. Resuspend “Stained” cells in 50 μL FACS Buffer (PBS1X; 2% FBS; 1mM EDTA; 0.1% Sodium Azide) and add following antibodies:

a. Anti-human CD14 Ab, FITC Conjugated (Miltenyi). Dilute 1:50.

b. Anti-human CD3 Ab, PerCP Conjugated (Miltenyi). Dilute 1:100.

c. Anti-human CD45 Ab, PE Conjugated (BioLegend). Dilute 1:100.

6. Vortex thoroughly.

7. Incubate “Stained” 20’ at +4°C

8. Wash the “Stained” cells twice in 250 μL FACS Buffer. Centrifuge at 310 rcf for 5’, setting temperature to +4°C.

9. Resuspend washed cells in 250 μL FACS Buffer – they are ready for reading.

3. RNA ISOLATION OF MS SAMPLES:

Total RNA Isolation was performed via mirVana™ miRNA Isolation Kit (Ambion), which preserves the small RNA fraction, following manufacturer instruction. Upon isolation from blood, cells were lysed in 600 μL of a denaturing solution which stabilizes RNA and inactivates RNases called mirVana Lysis Buffer. Next, samples are subjected to Acid- Phenol:Chloroform extraction, which provides a robust front-end purification that also removes most DNA. At this point, the procedure for isolation of total RNA is similar to routine glass-fibre binding procedures. Ethanol is added to samples, and they are passed through a Filter Cartridge containing a glass-fibre filter which immobilizes the RNA. The filter is then washed a few times, and finally the RNA is eluted with a low ionic-strength solution, such as RNase Free H₂O. Figure 11 overviews the procedure.

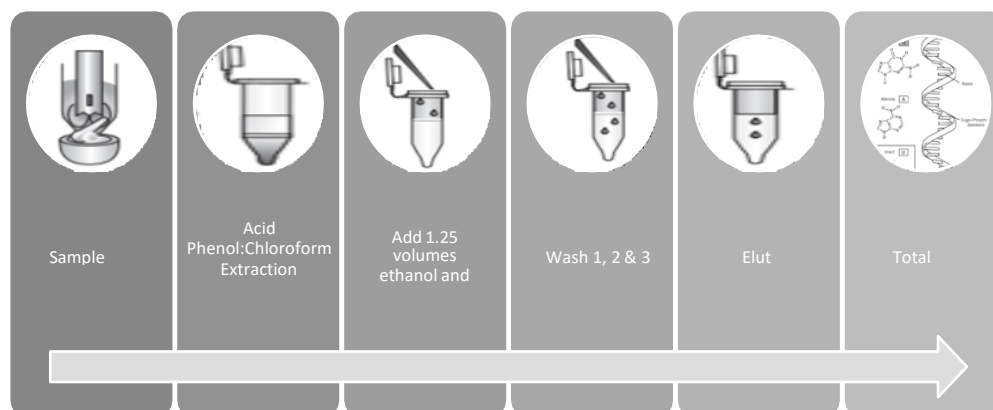


Figure 11. RNA Isolation procedure overview.

To assess the quality of the RNA extract, we performed two kinds of Quality Controls: we quantified RNA contained in our samples through NanoDrop Spectrophotometer which also assured that there was no contamination of Phenols or DNA; and, after that, we performed an electrophoresis analysis through Bioanalyzer to assure samples quality was suitable for further testing.

4. NANODROP SPECTROPHOTOMETRY

To assess quantity and quality of the RNA extracted, every sample was tested through NanoDrop Spectrophotometer, which allows for the analysis of 0.5–2.0 μL samples, without the need for cuvettes or capillaries. Absorbance at 260 nm is proportional to the concentration of the sample. Samples which concentration was below 200 $\mu\text{g} / 3 \mu\text{L}$ were subjected to a SpeedVac Cycle to increase their concentration – for microarray analysis, we needed 200 μg of RNA in about 3 μL . Moreover, the spectrophotometer measures absorbance at 230 nm and 280 nm. 260/230 nm and 260/280 nm ratios are indexes of purity of the RNA extracted – both have to be close to 2.0 for optimal conditions.

5. BIOANALYZER ANALYSIS

Agilent 2100 Bioanalyzer system was used to evaluate quality and integrity of the RNA extracted. This machine performs automated electrophoresis and provides an RNA Integrity Number (RIN) which ranges from 0 to 10 with the latter being the optimal score. Samples with a RIN inferior to 6 should be discarded and not further processed. Just below is shown an example of Bioanalyzer electropherogram one of our samples (Fig. 12).

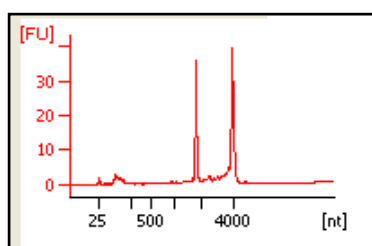


Figure 12. Analysis of RNA from CD14⁺ by Bioanalyzer.

6. MICROARRAY EXPERIMENT: DEGs ASSAY PROCEDURE

As shown in Figure 13, Affymetrix technology requires three phases of sample processing before analysis: synthesis of biotinylated cRNA, Hybridization and Wash and Stain. To perform the microarray experiment, the GeneChip™ 3' IVT PLUS Reagent Kit was used to prepare the samples. This kit allows to prepare RNA samples for gene-expression profiling analysis with GeneChip™ 3' Expression Arrays. The kit generates amplified and biotinylated complementary RNA (cRNA) from

poly(A) RNA in a total RNA sample. During Hybridization, the sample binds to the probes onto the array by sequence complementarity. The wash and stain phase removes non-specific binding and stains the sample with streptavidin-PE. At last, the CCD camera of the imaging station captures an image of the array so the software can assign to each probe a numeric value - called Arbitrary Units - proportional to the expression of the gene.

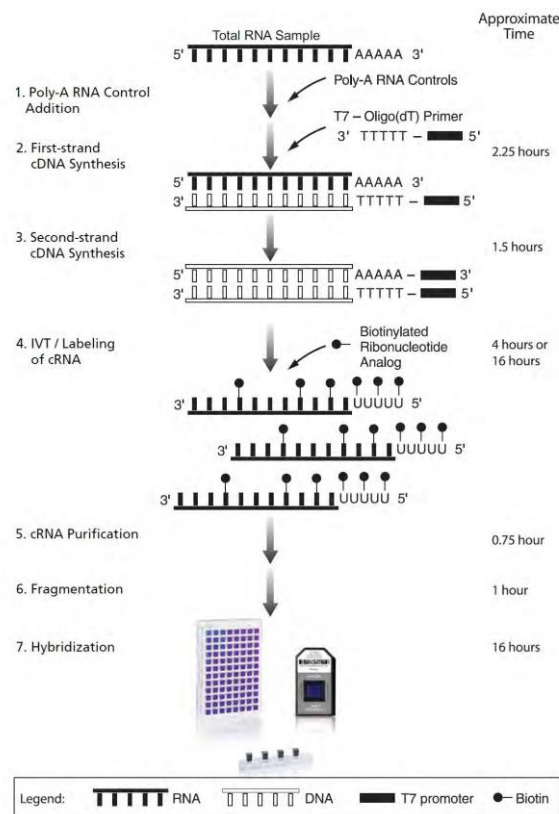


Figure 13: Microarray Experiment Overview. Image from: “GeneChip™ 3' IVT PLUS Reagent Kit USER GUIDE.

7. DNase TREATMENT

All RNA samples, isolated using *mirVana*™ miRNA Isolation Kit (Ambion), were submitted to DNase treatment Digestion using TURBO DNA-free™ DNase Treatment Removal Reagents (Ambion). This procedure is used to remove contaminating DNA from RNA preparations, and subsequently remove the DNase and divalent cations from the sample. The advantage of this protocol consists in the rapid and easy removal of DNase I using a novel method which does not require phenol/chloroform extraction, alcohol precipitation, heating, or the addition of EDTA.

All samples were digested with a final volume based on microliters of each RNA sample (for example: if we have 28 μ L of RNA sample, we used 30 μ L as final volume for DNase digestion). Just below is shown the procedure (Figure 14).

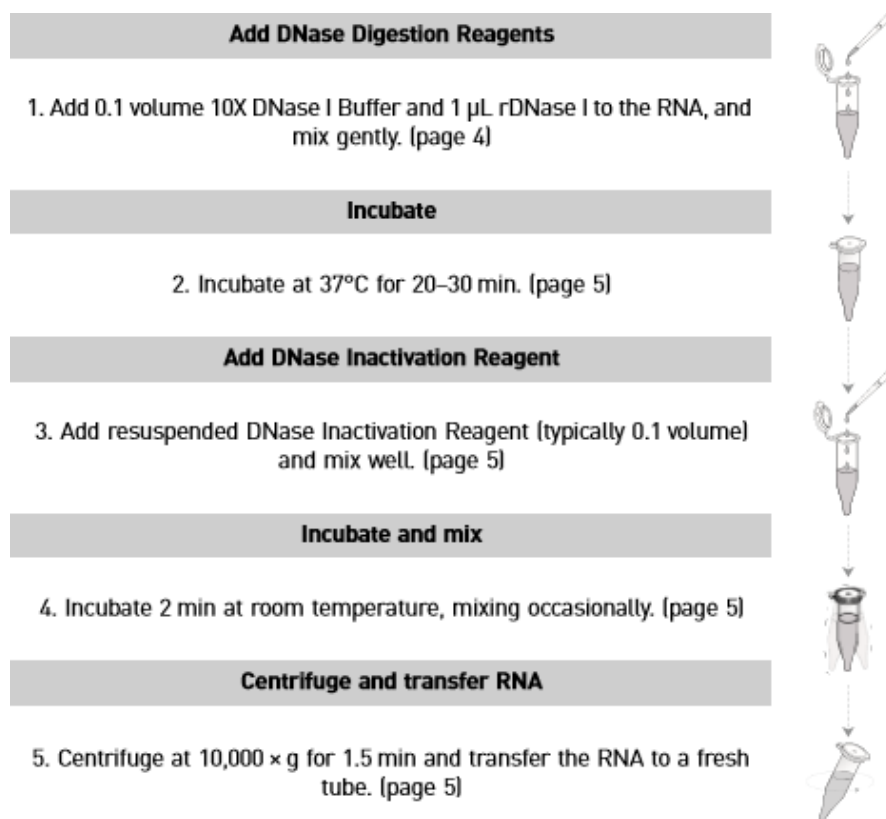


Figure 14. Image from: DNA-free™ Kit DNase Treatment and Removal Reagents User Guide

Protocol

1. Add 0.1 volume 10X DNase I Buffer and 1 μ L rDNase I to the RNA, and mix gently. There are separate DNase digestion conditions depending on the amount of contaminating DNA and the nucleic acid concentration of the sample.

- *Routine DNase treatment*: $\leq 200\mu\text{g}$ nucleic acid per mL

- *Rigorous DNase treatment*: $> 200\mu\text{g}$ nucleic acid per mL or RNA that is severely contaminated with DNA (i.e. $> 2\mu\text{g}$ DNA/50 μ L)

We always performed a *Routine DNase Treatment* so the following procedure refers to that. Use 1 μ L rDNase I (2U) for up to 10 μg of RNA in a 50 μL reaction. These reaction conditions will remove up to 2 μg of genomic DNA from total RNA in a 50 μL reaction volume. If the sample cannot be diluted, simply increase the amount of rDNase I to 2–3 μL (4–6U). It may be possible to successfully remove contaminating DNA from samples containing up to 500 $\mu\text{g}/\text{mL}$ nucleic acid in a 10–100 μL DNA-free™ Kit reaction. However, the efficacy of treating highly concentrated nucleic acid samples

depends on the absolute level of DNA contamination, and residual DNA may or may not be detectable by PCR after 35–40 cycles.

1. Incubate at 37°C for 20–30 min.

2. Add resuspended DNase Inactivation Reagent (typically 0.1 volume) and mix well. Always resuspend the DNase Inactivation Reagent by flicking or vortexing the tube before dispensing it. Use 2 µL or 0.1 volume DNase Inactivation Reagent, whichever is greater. Note: *The DNase Inactivation Reagent may become difficult to pipette after multiple uses due to depletion of fluid from the interstitial spaces. If this happens, add a volume of Nuclease-free Water (supplied with the kit) equal to approximately 20–25% of the bed volume of the remaining DNase Inactivation Reagent, and vortex thoroughly to recreate a pipettable slurry.*

3. Incubate 2 min at room temperature, mixing occasionally. It is important to mix the contents of the tube 2–3 times during the incubation period to redisperse the DNase Inactivation Reagent.

4. Centrifuge at 10,000×g for 1.5 min and transfer the RNA to a fresh tube. This centrifugation step pellets the DNase Inactivation Reagent.

5. After centrifuging, carefully transfer the supernatant, which contains the RNA, into a fresh tube. Avoid introducing the DNase Inactivation Reagent into solutions that may be used for downstream enzymatic reactions, because it can sequester divalent cations and change the buffer conditions.

8. REVERSE TRANSCRIPTION OF MS SAMPLES:

The synthesis of DNA from an RNA template, via reverse transcription, produces complementary DNA (cDNA). Reverse Transcriptases (RTs) use an RNA template and a short primer complementary to the 3' end of the RNA to direct the synthesis of the first strand cDNA, which can be used directly as a template for the Polymerase Chain Reaction (PCR). This combination of reverse transcription and PCR (RT-PCR) allows the detection of low abundance RNAs in a sample, and production of the corresponding cDNA, thereby facilitating the cloning of low copy genes. cDNA synthesis of our samples was performed using High Capacity cDNA Reverse Transcription Kit. We used 900 ng of RNA for each reaction, to have 30 ng/µL. We tested also some samples as RT- (samples without the Reverse Transcriptase enzyme in the MasterMix) to verify the purity of RNA

for the successive qRT-PCR experiments. Just below is reported the table of the component and their volume/reaction of Master Mix for RT+ reaction (Table 2).

Table 2: Master Mix for RT+ considering a final volume of 15 μL . To these 15 μL will be added 15 μL of RNA sample and water, to a total final volume of 30 μL /reaction.

Reagents	μL
10x RT buffer	3
Random Primers	3
25x dNTP Mix (100mM)	1,2
MultiScribe Reverse Transcriptase	0,8
H ₂ O	7

For each reaction, also for the samples with less than 900ng of RNA, we have chosen to use 30 μL as total final volume.

Applied Biosystems recommends using RNA that is:

- Free of inhibitors of reverse transcription and PCR
- Dissolved in PCR-compatible buffer or water
- Free of RNase activity

RNA isolation from ThP1 cells. We used the Takara Script™ RT Master Mix (Perfect Real Time) kit to obtain totRNA from ThP1 cells. The standard mix (Table 3) and the procedure is shown below. Prepare the reverse-transcription reaction solution on ice.

Table 3: Master Mix for RT+ considering a final volume of 10 μL . To these 10 μL will be added RNA sample and water, to a total final volume of 10 μL /reaction.

Reagent	Volume	Final Conc.
5X PrimeScript RT Master Mix (Perfect Real Time)	2 μl	1X
1X total RNA		
RNase Free dH ₂ O up to 10 μl		

2. Perform the reverse-transcription reaction after gently mixing the reaction solution.
3. 37°C 15 min (reverse-transcription), 85°C 5 sec, 4°C.

9. qRT-PCR VALIDATION

Commonly, in qRT-PCR, RNA transcripts are quantified by reverse transcribing them into cDNA first, as described above and then qPCR is subsequently carried out. As in standard PCR, DNA is amplified by 3 repeating steps: denaturation, annealing and elongation. In dye-based qPCR (typically green), fluorescent labeling allows the quantification of the amplified DNA molecules by employing the use of a dsDNA binding dye. During each cycle, the fluorescence is measured. The fluorescence signal increases proportionally to the amount of replicated DNA and hence the DNA is quantified in “real time”. Each sample was tested by using 7500 Real Time System.

qRT-PCR to validate Inflammation Pathway. TNF α , IL1 β , PTX3, CXCL2, CXCL3, CXCL8, KDM6B, CD36, SR-A, OLR1, NLRP3 and DECTIN1 genes were tested on MS patients and HCs. All mentioned primers were taken from literature. All the samples were processed in duplicate and ACT β was selected as housekeeping gene. Gene expression profiling is studied using the Comparative Ct method of relative quantification. This method calculated the Average Ct, the mean of the two technical replicates that have been processed; then the Δ Ct (Average Ct gene- Average Ct housekeeping) and $2^{-\Delta$ Ct were calculated. To testing these genes the TB Green® Premix Ex Taq™ (Tli RNase H Plus) kit was used according to instruction. Each reaction was performed in a final volume of 20 μ L: 5 ng of cDNA (2 μ L) and 18 μ L Master Mix. The standard mix is the following (Table 4):

Table 4: TB Green® Premix Ex Taq™ Master Mix.

Mix	μ l
TB Green	10
Forward Primer 10 μ M	0.4
Reverse Primer 10 μ M	0.4
ROX Dye II	0.4
H ₂ O	6.8

The Real-time qPCR Instrument Parameters were the following (Table 5), according to the instruction of TB Green® Premix Ex Taq™.

Table 5. qRT-PCR steps for PowerUp™ Sybr® Green

Step	Temperature	Duration	Cicle
Initial Denaturation	95°C	30 sec	1
Amplification	95°C	5 sec	40
	60°	34 sec	

The Primer sequences are provided in Table 6.

Table 6. Oligosequences

Gene	Forward	Reverse	Tm °F	Tm °R	2ndry F	2ndry R
ACTb	CATCGAGCACGGCATCGTCA	TAGCACAGCCTGGATAGCAAC	66,1	64,2	Weak	None
TNF α	CCTCTCTCTAATCAGCCCTCTG	GAGGACCTGGGAGTAGATGAG	63,2	61,7	Weak	None
IL1 β	TCTCCGACCACCACTACAGC	GAACCAGCATCTTCCTCAGC	64	62	None	None
PTX3	GTAAATGGTGAACCTGGCGGC	ATTCCCCCGGATGTGACAAG	66,5	68,1	None	Weak
CXCL2	CGCCCAAACCGAAGTCATA	TGCTCAAACACATTAGGCGC	65,8	66,1	None	None
CXCL3	CGCCCAAACCGAAGTCAT	GTGCTCCCCTTGTTTCAGTATCT	66,1	63,3	None	None
CXCL8	ACTGAGAGTGATTGAGAGTGGAC	AACCCTCTGCACCCAGTTTTTC	61,4	66,3	Very weak	None
CD36	CTTTGGCTTAATGAGACTGGGAC	GCAACAAACATCACCACACCA	64,8	66,9	None	None
SR-A	CCAGGTCCAATAGGTCCTCC	CTGGCCTTCCGGCATATCC	64,5	68,7	Weak	Moderate
OLR-1	GGAAATGATAGAAACCCTTGC	CTGGATGAAGTCCTGAACAAT	61,2	60,6	None	Weak
NLRP3	AAAGGAAGTGGACTGCGAGA	TTCAAACGACTCCCTGGAAC	63,9	64	None	Very weak
DECTIN1	TCTTTCCAGCCCTTGTCCTC	CCAGTTGCCAGCATTGTCTT	65,5	65,2	None	None
KDM6B	CTGGAGAGCAAACGGGATG	AGGGTCTTGGTGGAGAAGAGG	65,8	65,7	None	Weak

Oligosequences. Tm: Melting Temperature; 2ndry: secondary structure; F: Forward; R: Reverse.

qRT-PCR of Cholesterol pathway: primers sequences. Real-time qPCR was performed with 7500 Real Time System using PowerUp™ Sybr® Green (Applied Biosystems) Master Mix according to instruction. Primers of CYP51A1, HMGCR, HMGCS1, SQLE and SC4MOL were taken from literature (*Reproductive Sciences 2015, Vol. 22(3) 377-384*), whereas sequences of INSIG1, IDI1

and SC5DL were designed using the Primer3 Plus Software. Each reaction was performed in a final volume of 20 μ L: 5 ng of cDNA (1 μ L) and 19 μ L Master Mix. The standard mix is the following (Table 7):

Table 7. PowerUp™ SYBR® Green Master Mix

Mix	μ L
PowerUp Sybr Green	10 μ L
Primers F+R 10 uM	1 μ L
H ₂ O	8 μ L

The Primer sequences are provided in Table 8.

Table 8. Oligosequences

Gene	Forward	Reverse	Tm ° F	Tm ° R	2ndry F	2ndry R
HMGCS1	AAGTCCAGGCCAGC AGTGA	ATATTCACAGC TCCTGAATGTA CCA	66.2	64.4	None	Weak
HMGCR	CTTGCTTGCCGAGCC TAATGA	ACTAGGCACAG TTCTAGGGCCA TTC	68.4	68.1	Weak	Moderate
IDI1	CCATTAAGCAATCCA GCCGA	CAAGGGAGCCA AGAACGAAT	67	61.4	None	Weak
SQLE	TTGTGATGGGAGTTC AGTACAAGGA	GCCCATCTGCA ACAACAGTCA	67.7	67.5	Moderate	Very weak
SC4MOL	TAAATCTGATCCCTT TCTAT	TGTAAATGTTG AAGCATAGT	61	62.6	Weak	None
CYP51A1	CTACAGTCGCCTGAC AACAC	CCACTTCTCCC CAACTCTC	66	66.7	Weak	None
SC5DL	TGACGGTGATTTTCG TGTCC	CGCCAATCCTA TCCCACAAA	65.2	65.2	Weak	None
INSIG-1	TTGATCGTTCCAGAA GTGGC	CAAGGGAGCCA AGAACGAAT				

Tm: Melting Temperature; 2ndry: secondary structure; F: Forward; R: Reverse.

Relative values of gene expression were normalized to 18s Housekeeping Gene. The primers sequences are shown in Table 9.

Table 9: Housekeeping sequences

Gene	Forward 5'-3'	Reverse 5'-3'	Tm° F	Tm° R	2ndry F	2ndry R
18s	TGACTCAACACGGGAAACC	CGCTCCACCAACTAAGAACG	63.7	64.6	None	None

Tm: Melting Temperature; 2ndry: secondary structure; F: Forward; R: Reverse.

The Real-time qPCR Instrument Parameters were the following (Table 10), according to the instruction of PowerUp™ Sybr® Green:

Table 10: qRT-PCR steps for PowerUp™ Sybr® Green.

Step	Temperature	Duration	Cycle
UDG activation	50°C	2 minutes	Hold
Dual-Lock™ DNA polymerase	95°C	2 minutes	Hold
Denature	95°C	15 seconds	40
Anneal/extend	60°C	1 minute	

Efficiency curve for new primers. IDI1, INSIG1 and SC5DL: Since these 3 primers were designed using Primers3 Plus, and so there are not works in which these sequences were tested, we have assessed efficiency curve to verify their reliability. To test this, we have chosen a sample of which we had sufficiently material and we tested different concentrations of cDNA after serial dilutions. We have tested also housekeeping gene in the same way to have an internal control. In particular, we chosen HC29 concentrated 30ng/μL and then we have diluted the sample 1:1.2 to have 25ng/μL, since we started from 50ng/μL as first concentration to test efficiency. We have tested the following cDNA quantities: 50 ng, 10 ng, 2 ng, 0.4 ng, 0.08 ng (serial dilution of 1:5). The standard primers Mix was the following (Table 11).

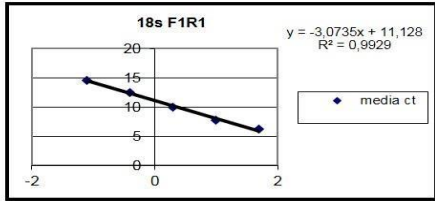
Table 11: Standard Mix for 1,5 sample with an excess of 0,5 sample

Mix	μL
PowerUp Sybr Green	10
Primers F+R 10μM	1
H ₂ O	8

Results of efficiency test. Each primer, 18s as internal control (Fig.15A), IDI1 (Fig.15B), INSIG1 (Fig.15C), SC5DL (Fig.15D) result efficient. The reaction's efficiency was determined considering the slope of the standard curve using the following formula: [Efficiency = $10^{(-1/\text{slope})} - 1$]. An efficiency including between 90 and 110% is considered optimal. Just below are shown the various efficiency curves of each primer and relative dissociation curves (Fig. 15A-D; Fig.16A-D)

A

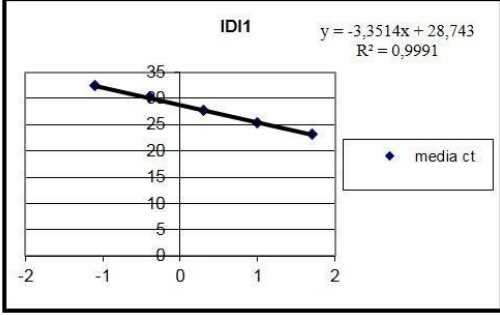
Detector	Reporter	Start	End	Threshold
18S	SYBR	1	3	0,31
	SampleName	Ct	Avg Ct	
	04 RT+ 50ng 18s	6,221	6,256	
	04 RT+ 50ng 18s	6,291	6,256	
	04 RT+ 10ng 18s	7,597	7,705	
	04 RT+ 10ng 18s	7,813	7,705	
	04 RT+ 2ng 18s	9,785	9,966	
	04 RT+ 2ng 18s	10,147	9,966	
	04 RT+ 0.4ng 18s	12,083	12,472	
	04 RT+ 0.4ng 18s	12,86	12,472	
	04 RT+ 0.08ng 18s	14,532	14,614	
	04 RT+ 0.08ng 18s	14,696	14,614	
	B 18s			
	B 18s			



18s F4R4			
ng cDNA	log cDNA	media ct	Efficiency
50	1,69897	6,256	111,00%
10	1	7,705	1,1152513
2	0,30103	9,966	
0,4	-0,39794	12,472	
0,08	-1,09691	14,614	

B

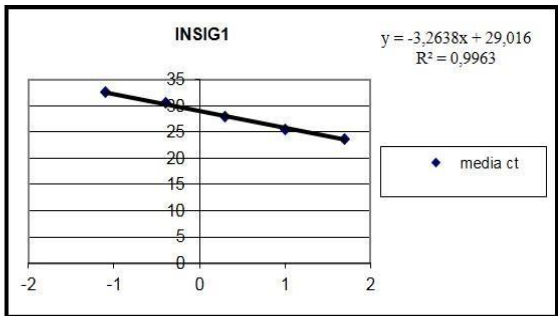
Detector	Reporter	Start	End	Threshold
IDI1	SYBR	3	15	0,31
	SampleName	Ct	Avg Ct	
	50ng	23,142	23,144	
	50ng	23,146	23,144	
	10ng	25,281	25,27	
	10ng	25,26	25,27	
	2ng	27,677	27,663	
	2ng	27,65	27,663	
	0.4ng	30,103	30,207	
	0.4ng	30,312	30,207	
	0.08ng	31,977	32,388	
	0.08ng	32,8	32,388	
	B IDI1			
	B IDI1			



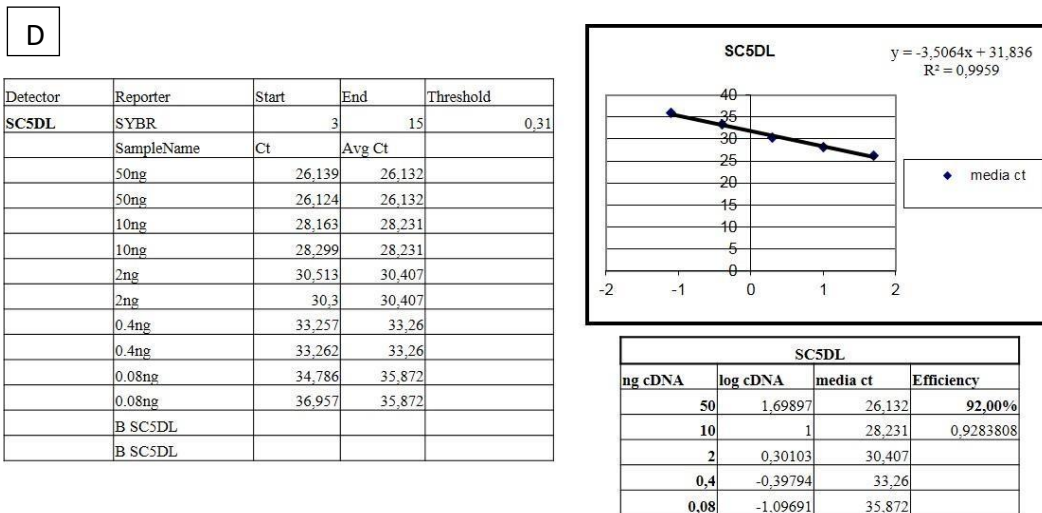
IDI1			
ng cDNA	log cDNA	media ct	Efficiency
50	1,69897	23,144	98,00%
10	1	25,27	0,9878461
2	0,30103	27,663	
0,4	-0,39794	30,207	
0,08	-1,09691	32,388	

C

Detector	Reporter	Start	End	Threshold
INSIG1	SYBR	3	15	0,31
	SampleName	Ct	Avg Ct	
	50ng	23,379	23,712	
	50ng	24,045	23,712	
	10ng	25,125	25,455	
	10ng	25,784	25,455	
	2ng	27,37	27,905	
	2ng	28,44	27,905	
	0.4ng	30,055	30,496	
	0.4ng	30,937	30,496	
	0.08ng	32,323	32,598	
	0.08ng	32,874	32,598	
	B INSIG1			
	B INSIG1			

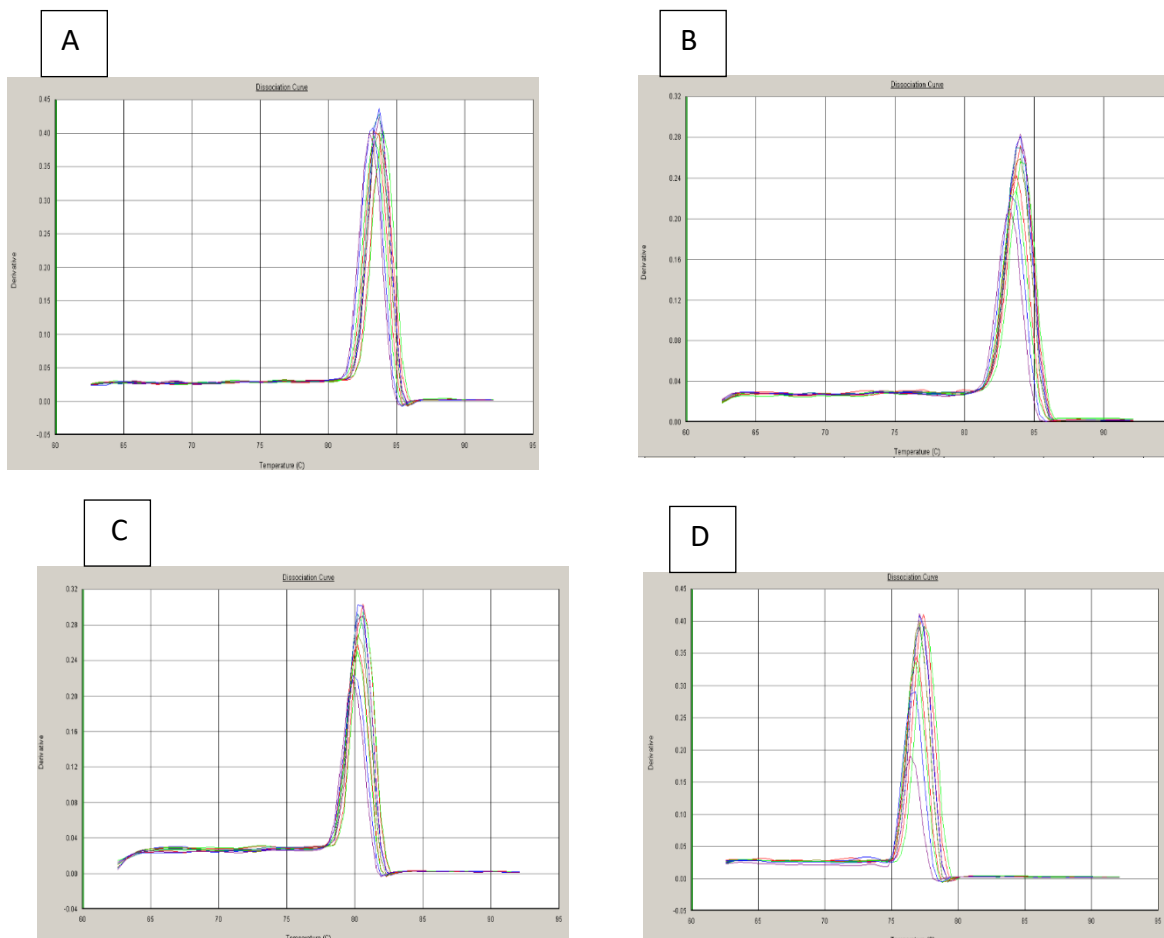


INSIG1			
ng cDNA	log cDNA	media ct	Efficiency
50	1,69897	23,712	102,00%
10	1	25,455	1,0248429
2	0,30103	27,905	
0,4	-0,39794	30,496	
0,08	-1,09691	32,598	



Figures 15. Efficiency curves. A) Efficiency curve of 18s genes. B) Efficiency curve of IDI1 gene. C) Efficiency curve of INSIG1 gene. D) Efficiency curve of SC5DL gene.

Then, we tested whether these primers were able to drive a specific amplification. To do so, we analysed carefully their derivative dissociation profiles – a one peak dissociation profiles indicates that only one fragment is being amplified and so assesses specificity.



Figures 16. Dissociation profiles of each tested primer. (A): 18S ; (B): IDI1; (C) INSIG1; (D) SC5DL.

qRT-PCR to validate *ThP1* experiment. To testing : IDI1, HMGCS1, HMGCR, SQLE, TNF α , IL1 β , NLRP3 and OLR1 genes the TB Green® Premix Ex Taq™ (Tli RNase H Plus) kit was used according to instruction. The sequences are reported in tables 4 and table 6. Relative values of gene expression were normalized to HPRT Housekeeping Gene. The primers sequences are shown in Table 12. Each reaction was performed in a final volume of 20 mL: 20 ng of cDNA (2 μ L) and 18 mL Master Mix.

Table 12: Housekeeping sequences

Gene	Forward	Reverse	Tm° F	Tm° R	2ndry F	2ndry R
HPRT	CCTGGCGTCGTGATTAGTGAT	AGACGTTTCAGTCCTGTCCATAA	66,1	62,5	None	Weak

Tm: Melting Temperature; 2ndry: secondary structure; F: Forward; R: Reverse.

10. DETECTION OF oxLDL in MS PATIENTS

In order to detect whereas oxLDL was present in sera' patients, ELISA test was performed, by using Mercodia oxidized LDL ELISA kit, in according to kit instruction.

Protocol: All reagents and samples must be brought to room temperature before use. Prepare a standard curve for each assay run.

1. Prepare sample buffer 1X solution and dilute samples according to instructions for both processes in the Dilutions of Samples section.
2. Prepare Calibrators, Controls, enzyme conjugate 1X solution and wash buffer 1X solution according to the Reagents section.
3. Prepare sufficient Coated Plate wells to accommodate Calibrators, Controls and samples in duplicate.
4. Pipette 25 μ L of each Calibrator, Control and diluted sample into appropriate wells. All samples should be added to the plate within 20 minutes.
5. Add 100 μ L Assay Buffer to each well.
6. Incubate on a plate shaker (700-900 rpm) for 2 hours at room temperature (18–25°C).

7. Wash 6 times with 700 μ L wash buffer 1X solution per well using an automatic plate washer with overflow-wash function. After final wash, invert and tap the plate firmly against absorbent paper. Do not include soak step in washing procedure.

Or manually:

Discard the reaction volume by inverting the microplate over a sink. Add 350 μ L wash buffer 1X solution to each well. Discard the wash solution, tap firmly several times against absorbent paper to remove excess liquid. Repeat 5 times. Avoid prolonged soaking during washing procedure.

8. Add 100 μ L enzyme conjugate 1X solution to each well.

9. Incubate on a plate shaker (700-900 rpm) for 1 hour at room temperature (18–25°C).

10. Wash as described in 7.

11. Add 200 μ L Substrate TMB.

12. Incubate on the bench for 15 minutes at room temperature, no shaking.

13. Add 50 μ L Stop Solution. Place plate on the shaker for 5 seconds to ensure mixing.

14. Read optical density at 450 nm and calculate results. Read within 30 minutes

11. IN VITRO EXPERIMENT

Briefly, THP-1 monocytes were transferred into a 6-well plate at 3×10^6 cells/well. Then, THP-1 cells were derived to macrophages with 200 ng/ml phorbol 12-myristate 13-acetate (PMA). Prior to Lysophosphatidilcholine (LPC) (Sigma) or other chemical treatment, THP-1 derived macrophages were pre-incubated in RPMI with 1% FBS and 100 U/ml penicillin/streptomycin for 2 h. After this pre-incubation period, the culture medium was changed to the experimental medium supplemented with LPC for 8 h. We used 0.1% methanol as a vehicle control.

12. STATISTICAL ANALYSIS

We compared the resulting metabolic activities of the treatment groups and controls using one-way analysis of variance (ANOVA) and Tukey's multiple-comparison post-test. Differences between

groups were considered to be significant at a P value of <0.05 . Statistical analyses were performed with GraphPad Prism 7.04 (GraphPad Software, Inc., San Diego, CA).

RESULTS

1. MULTIPLE SCLEROSIS PATIENT RECRUITMENT

The purpose of the present research project is the identification and characterization of the genetic signatures for disease activity and progression in Multiple Sclerosis (MS). Specifically, we aimed to identify the transcriptional differences between the different clinical forms such as Relapsing Remitting (RRMS) and Primary Progressive (PPMS) of MS compared to Healthy Controls (HCs).

Cohort: 52 samples of MS patients, both male and female, were collected by collaborators at the MS center (U.O. Sclerosi Multipla IRCCS S. Maria Nascente Fondazione Don Gnocchi), while 57 samples of age-matched HCs, were obtained through the blood donation center in Vimercate (Milano). These samples regroup the first and the second cohort of patients recruited for the microarray analysis and the validation phase respectively.

In particular, the 1st cohort of patients was named as **cohort 1** and was selected from different clinical subgroups: RRMS and PPMS. For this study, we have analysed in total with microarray technology:

- 25 samples Primary-Progressive (PP): 12 female, 13 male
- 27 samples Relapsing-Remitting (RR): 21 female, 6 male
- 57 samples healthy controls: 27 female, 30 male

We have obtained the data for a total of 33 female samples (13 HC, 13 RRMS, 7 PPMS) for the microarray analysis, 16 female samples of cohort 1 (5 HC, 10 RRMS, 1 PPMS) were used also for the first part of the validation phase.

The recruited RRMS samples had a sex ratio of 3.5:1 (Female to male) whereas the PPMS samples sex ratio was 1:1. This is in line with the reported data about the MS sex difference frequencies¹³⁰. Due to the well-known sex-based gene expression effect¹³¹, the Bioinformatics analysis has been performed by dividing the different groups first based on sex. Therefore, the data derived from female samples will be presented.

The selection criteria for the HC subjects were as following:

- No familiarity with Multiple Sclerosis or other Autoimmune Diseases
- Being not a smoker

-No evident infection at the time of blood collection

The selection criteria for the MS patients (MSP) were as following:

-If possible, no immunomodulatory or immunosuppressive drug treatment for at least 3 months before blood collection

-If possible, no comorbidity

-No steroid treatment for at least 4 weeks before blood collection

-No evident infection at the time of blood collection

-Diagnosis based on McDonald Criteria and confirmed via MRI

Table 13 summarizes the main characteristics of the cohort 1 of MS and HC subjects recruited in this study.

Table 13. Characteristics of HCs and MS subjects from the cohort 1.

Phenotype	Sex	Age	EDSS	Disease duration	Treatment	Comorbidity
HC3	Female					
HC11	Female					
HC13	Female					
HC27	Female					
HC29	Female					
HC31	Female	49				
HC32	Female	44				
HC33	Female	44				
HC37	Female	41				
HC41	Female	47				
HC52	Female	40				
HC53	Female	40				
HC61	Female	53				
SMP7 (RR)	Female	NA	2	NA		
SMP10 (RR)	Female	39	NA	NA		
SMP11 (RR)	Female	55	3	25		Hashimoto thyroiditis
SMP12 (RR)	Female	51	7	31	AZA, Mito	
SMP13 (RR)	Female	22	0	6		
SMP17 (RR)	Female	43	6	10	AZA, methotrexate	LES
SMP18 (RR)	Female	55	5.5	27	AZA	hypertension
SMP22 (RR)	Female	39	2.5	12	AZA, GA	
SMP2 (RR)	Female	38	1	NA		

SMP16 (RR)	Female	28	1	4		
SMP27 (RR)	Female	58	6.5	16	IFN	
SMP28 (RR)	Female	49	5	1		
SMP29 (RR)	Female	50	2.5	2		
SMP3 (PP)	Female	64	7	18		
SMP4 (PP)	Female	73	7.5	38		
SMP6 (PP)	Female	60	7	25	Mito (2006)	
SMP15 (PP)	Female	53	6.5	15		
SMP24 (PP)	Female	68	6	13	Eutirox for hypothyroidism	
SMP25 (PP)	Female	76	8	NA		
SMP26 (PP)	Female	70	6.5	NA		

HC: healthy controls, RR: Relapsing-Remitting; PP: Primary Progressive; SMP: Multiple Sclerosis Patient; IFN: Interferon Beta; Mito: Mitoxantrone; AZA: Azathioprine; GA: Glatiramer Acetate. EDSS: Expanded Disability Status Scale; NA: Not Applicable/Available.

Just below is reported the table of the mean values of all samples, relative to age, EDSS and disease duration. (Table 14).

Table 14. Clinical characteristics of cohort 1 HCs, treatment-naïve patients with RRMS and PPMS included in the peripheral blood monocyte analysis

Phenotype	Nr of patients/controls	Sex	Mean Age \pm St. Dev	Mean EDSS \pm St. Dev	Mean Duration (years) \pm St. Dev
HC	13	female	44.7 \pm 4.35	NA	NA
RR	13	female	44 \pm 9.47	3.5 \pm 1.63	13.4 \pm 9.21
PP	7	female	66 \pm 7.34	7 \pm 0.7	21.8 \pm 1

HC: Healthy controls, RR: Relapsing-Remitting, PP: Primary- progressive. EDSS: Expanded Disability Status Scale; NA: Not Applicable/Available; St. Dev: Standard Deviation; Nr: number.

For the second part of the validation phase, we recruited a 2nd cohort, named as **cohort 2**, of MS patients and HCs. This cohort was composed by 7 HCs, 8 RRMS and 7 PPMS patients.

Table 15 reports the table with these samples characteristics.

Table 15. Characteristics of HCs and MS subjects from the cohort 2.

Phenotype	Sex	Age	EDSS	Disease Duration	Treatment	Comorbidity
HC30	Female	47				
HC35	Female	37				
HC38	Female	38				
HC39	Female	40				
HC40	Female	49				
HC46	Female	48				
HC57	Female	41				
SMP44 (RR)	Female	50	1	6	NA	
SMP59 (RR)	Female	49	6.5	25	IFN, GA	

SMP69 (RR)	Female	40	1.5	14	IFN, GA	
SMP70 (RR)	Female	44	1	6	IFN	Endometriosis, Hypertension
SMP71 (RR)	Female	42	1	16	NA	
SMP72 (RR)	Female	58	6.5	36	Gabapentin, Clonazepam	
SMP73 (RR)	Female	50	2.5	12	IFN, GA	
SMP74 (RR)	Female	42	6	24	IFN, GA, AZA, Mitoxantrone	
SMP47 (PP)	Female	52	6	5	Vit D	Epilepsy
SMP48 (PP)	Female	47	5	9	Depakin, Vin-pat	Epilepsy
SMP51 (PP)	Female	59	7	30	NA	
SMP63 (PP)	Female	55	7.5	16	NA	
SMP65 (PP)	Female	64	7.5	14	NA	
SMP66 (PP)	Female	63	6.5	39	Bacoflen, Amantadina	
SMP68 (PP)	Female	56	7	7	AZA	Raynaud Syndrome

HC: Healthy controls, RR: Relapsing-Remitting, PP: Primary-progressive, MS_P: Multiple Sclerosis Patient; IFN: Interferon Beta, Mito: Mitoxantrone; AZA: Azathioprine; GA: Glatiramer Acetate, VitD.: Vitamina D. EDSS: Expanded Disability Status Scale; NA: Not Applicable/Available.

Just below is reported the table of the mean values of all samples, relative to age, EDSS and disease duration. (Table 16).

Table 16. Clinical characteristics of cohort 2 HCs, treatment-naive patients with RRMS and PPMS included in the peripheral blood monocyte analysis.

Phenotype	Nr of patients/controls	Sex	Mean Age \pm St. Dev	Mean EDSS \pm St. Dev	Mean Duration (years) \pm St. Dev
HC	7	female	43 \pm 5,01	NA	NA
RR	5	female	46.8 \pm 5.98	3.25 \pm 2.06	17.3 \pm 10.3
PP	7	female	56.5 \pm 6.02	6.6 \pm 0.9	17 \pm 12.72

HC: Healthy controls; RR: Relapsing-Remitting; PP: Primary Progressive; EDSS: Expanded Disability Status Scale; NA: Not Applicable/Available; St. Dev: Standard Deviation; Nr: number.

As it can be noticed, the cohort 2 of PPMS patients has lower mean of age (56.5 \pm 6.02 vs 66 \pm 7.34), lower mean disease duration (17 \pm 12.72 vs 21.8 \pm 1) and EDSS score mean (6.6 \pm 0.9 vs 7 \pm 0.7) compared to the cohort 1.

2. CHARACTERIZATION OF MS MOLECULAR PROFILES THROUGH WHOLE GENE EXPRESSION ANALYSIS

A Genome-wide approach has been conducted to study the gene expression in MS patients. Affymetrix platform has been used to perform the microarray analysis. For this experiment, as reported previously, a total of **7 PPMS**, **13 RRMS** samples plus **13 HC** samples have been profiled. A total amount of 10 mL of peripheral blood was collected and submitted to CD14⁺ cell purification protocol.

To determine whether to use positive or negative selection strategies, a series of preliminary experiments have been performed. Briefly, monocytes were isolated by positive selection using CD14⁺ magnetic beads and by negative selection using the Rosette procedure followed by CD61 micro beads to remove megakaryocytes. Figure 17 reports a Fluorescence-Activated Cell Sorting (FACS) analysis, and shows the results obtained by positive and negative selection procedures. The higher percentage of pure cells (94% vs 82%) were obtained by the positive selection. The CD69 staining verified that the positive selected cells were not activated by the procedure as compared to negative selection (data not shown). Therefore, the positive selection has been used to perform the microarray experiments.

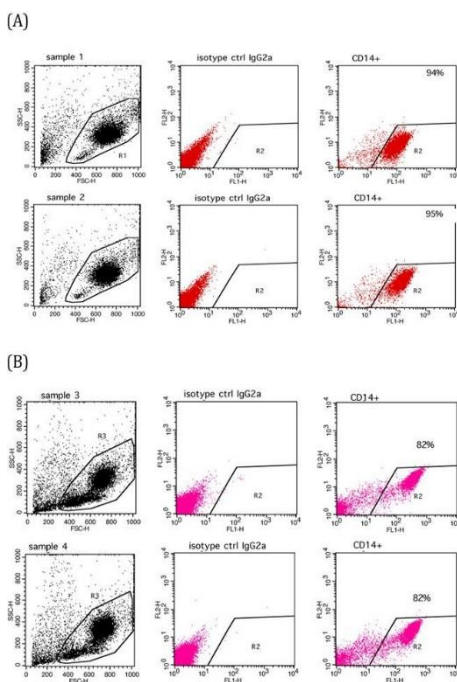


Figure 17. Positive selection is associated with increased cell purity. (A) FACS analysis of CD14⁺ cells following the positive selection procedure or (B) FACS analysis of CD14⁺ cells following the negative selection. Data representative from one experiment are shown. CD14⁺: Cells stained with the anti-CD14 antibody, IgG2a: isotype control antibody.

The percentage and purity of CD14⁺ was obtained after FACS analysis, by staining the cells with the human anti-CD14 antibody. Table 17 reports the final results obtained by the purification method used. In general, the percentage of monocytes in the peripheral blood analyzed ranged from 8% to 17%.

Table 17. Mean values of the cohort 1 samples and summary of CD14+ Percentage

Phenotype	Mean PBMC ± St. Dev	Mean%CD14+
HC	2.14E+07 ± 1.18E+07	10.94
RR	1.71E+07 ± 6.61E+06	7.15
PP	1.59E+07 ± 5.74E+06	9.13

HC: Healthy controls, RR: Relapsing-Remitting; PP: Primary-Progressive. PBMC: Peripheral blood mononuclear cells.

The table below reports the mean values relative to CD14⁺ percentage obtained in cohort 2 samples. (Table 18).

Table 18. Mean values of cohort 2 HC, RR and PP samples and summary of CD14⁺ Percentage

Phenotype	Mean PBMC ± St. Dev	Mean%CD14 ⁺
HC	8.60E+06 ± 2.48E+06	8.49
RR	4.10E+07 ± 1.25E+06	8.32
PP	5.74E+07 ± 1.94E+07	10.88

HC: Healthy controls, RR: Relapsing-Remitting, PP: Primary-Progressive, PBMC: Peripheral blood mononuclear cells, SMP: Multiple Sclerosis Patient; PBMC: Peripheral blood mononuclear cells; St. Dev: Standard deviation.

In general, RRMS patients have a lower percentage of CD14⁺ cells than both HCs and PPMS patients. After the cell purification protocol, totRNA enriched with microRNA was extracted by using mir-Vana™ miRNA Isolation Kit. The detailed protocols of these procedures are reported in Materials and Methods. After totRNA quality controls analysis, the 33 female samples were labeled and hybridized (according to the Affymetrix protocol) on the HGU219 array strips which contains a total of 49,386 human genes.

3. DATA ANALYSIS REVEALS SPECIFIC SUBGROUPS OF MS PATIENTS

From the hybridization of the strips, raw data were generated as .Cel files and analyzed with the Partek Genomic Suite 6.0 Software, a Bioinformatic tool which uses the Statistical Algorithm called RMA (Robust Multichip Analysis) to generate the raw expression data. Briefly, this algorithm performs the background correction, the quantile normalization and the median polish summarization, to analyze the raw images and associate each probe with a number that represents the correspondent Arbitrary Unit (AU) of fluorescence. Subsequently, a Principal Component Analysis (PCA) was performed as quality control; in fact, the PCA analysis is used to determine the quality of replicate samples and the extent of changes observed between HC and MS samples. This analysis also allows the identification of the possible outlier samples within the different groups. From this analysis, we observed that the samples were very variable and that two subgroups of RR samples (renamed as RR1 and RR2) were selected (green and violet circles) (Fig.18).

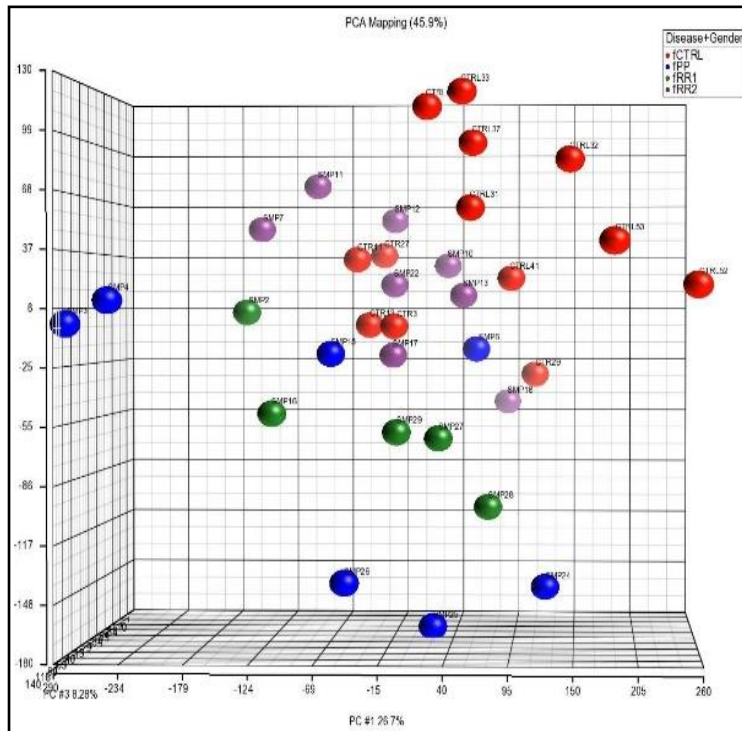


Figure 18. The PCA 3D image reveals two subgroups of RRMS. Red: female Healthy controls (fCTRL n=13), Blue: female Primary-Progressive patients (fPP n=7), Green: female Relapsing-Remitting patients type 1 (fRR1 n=5), Violet: female Relapsing-Remitting patients type 2 (fRR2 n=8).

Table 19 reports the samples names associated to the subgroups RR1 and RR2.

Table 19. Subdivision of total samples (HC, RR1, RR2, PP).

fHC (13)	fRR2 (8)	fRR1 (5)	fPP (7)
HC3	SMP7	SMP2	SMP3
HC11	SMP10	SMP16	SMP4
HC13	SMP11	SMP27	SMP6
HC29	SMP12	SMP28	SMP15
HC31	SMP13	SMP29	SMP24
HC32	SMP17		SMP25
HC33	SMP18		SMP26
HC37	SMP22		
HC41			
HC52			
HC53			
HC61			

fHC: female Healthy Controls, fRR2: female Relapsing- Remitting type 2; fRR1: female Relapsing-Remitting type 1, fPP: female Primary Progressive; SMP: Multiple Sclerosis patients.

After PCA analysis, the next step was to identify the DEGsthrough the ANOVA test with (FDR) or without (pValue) the Bonferroni correction. In particular, the following parameters of Fold Change (Fc)=2 and False Discovery Rate (FDR)=0.05 have been applied. Table 20 summarizes the results obtained by this analysis.

Table 20. Results of the Statistical Test obtained by comparing the different groups of samples.

	Fc2; FDR 0.05	Fc2, pV 0.05
fPPvsfHC	1491 (1463 up)	1686 (1644 up)
fRR1vsfHC	658 (646 up)	989 (932 up)
fRR2vsfHC	-	77 (60 up)
fPPvsfRR1	-	215 (189 up)
fPPvsfRR2	857 (785 up)	1302 (1157 up)
fRR1vsfRR2	394 (323 up)	936 (663 up)

fHC: female Healthy controls; fRR1: female Relapsing-Remitting type 1; fRR2: female Relapsing- Remitting type 2; fPP: female Primary Progressive. Fc: Fold change; FDR: False Discovery Rate; pV: pvalue; up: upregulated.

The ANOVA results confirm what it was suggested by the PCA analysis: we were able to detect the biggest variability in terms of DEGs between PP and HC and the division of RR samples in two subgroups. Moreover, no DEGs have been found with $Fc=2$ and $FDR=0.05$ in PPvsRR1 and HCvsRR2, indicating that the two groups of samples are very similar to each other. Only with a pV of 0.05 we have been able to select some DEGs between these pairs, but only 215 of which 189 were upregulated, and 77 of which 60 were upregulated, out of the total number of 49,386 genes. As shown in Table 12, 1491 DEGS are selected when PP monocytes are compared to those of the HCs, indicating that PP monocytes undergo a strong genetic reprogramming with most of the genes (1463) up-regulated. In addition, DEGs analysis revealed also that the subgroup of RR1 patients is modulating about 658 DEGs, again suggesting that this group of patients is characterized by monocytes expression changes that are not present in the HCs or in the RR2 group of subjects. The Venn Diagram between these two lists of DEGs shows that 439 on 658 genes of RR1 group are indeed upregulated in the PP subjects (data not shown).

After the DEGs selection, we performed the Functional Annotation analysis. Through the Gene Ontology (GO) analysis, it was possible to organize these DEGs in the three functional classes of the database (biological process, molecular function and cellular component). We present here, the annotation based on the biological process (BP) (Fig.19 and Fig.20) of the DEGs list obtained by comparing PP and RR1 against the HCs samples. For each functional class is assigned an enrichment score, calculated using a chi-square test, comparing the proportion of the gene list in a group to the proportion of the genes that are present in a specific annotated group. For example, if a functional group has an enrichment score over 1, the functional category is over represented in that group.

The BPs that are most enriched in the DEGs list of PP were the following: Biological regulation, Immune system process and Metabolic process (Fig.19). Instead, the BPs that were most enriched in the DEGs list of RR1 were: Biological regulation, Metabolic process and Immune system process (Fig.20).

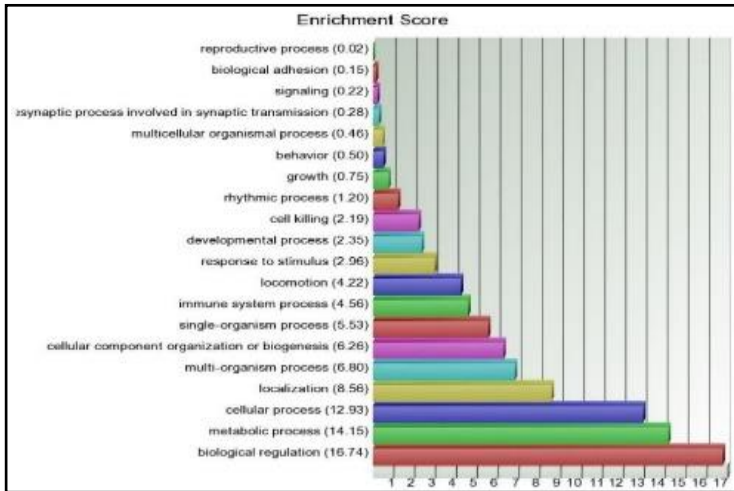


Figure 19. Biological Processes (BP) and GO-Enrichment scores. The data report the BP that are significantly enriched in the comparison fPP vs fHC (Fc2; FDR0.05). The annotation of 1491 DEGs is shown.

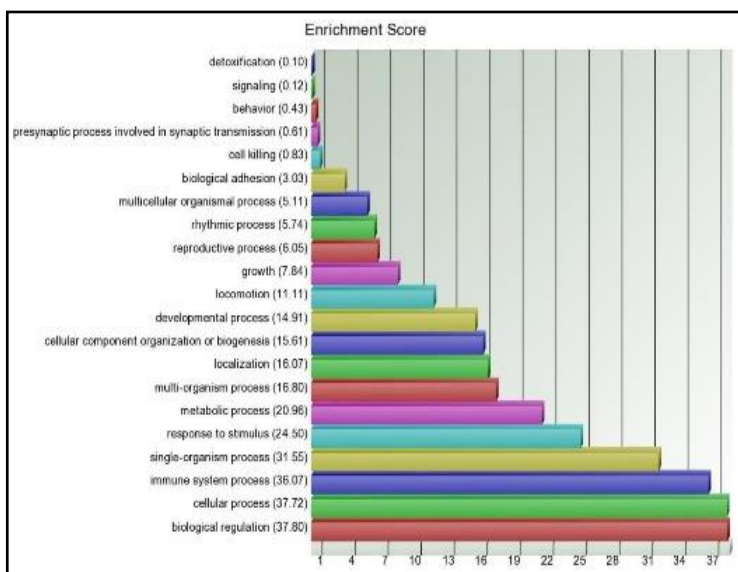


Figure 20. Biological Processes (BP) and GO-Enrichment scores. The data report the BP that are significantly enriched in the comparison fRR1 vs fHC (Fc2; FDR0.05). The annotation of 658 DEGs is shown.

For the comparison RR2vsHC, it was not possible to apply the FDR statistical test but instead we had to apply the pValue of 0.05 without the Bonferroni correction. In this case, it has been possible to identify only 77 DEGs (60 up-regulated). So, it follows that we were not able to detect an Enrichment score because the number of DEGs was not sufficiently high or present in any relevant GO annotation. These data strongly suggest that the RR2 monocytes show a gene expression program that is very similar to the HCs monocytes.

Next, we analyzed the BPs with the higher enrichment scores and we identified and characterized the following BPs: **Cell Cycle**, **Anti-apoptosis**, **Inflammation** and **Cholesterol Biosynthesis**. To display the direction of the gene changes compared to the HCs, the DEGs of these functional classes were analyzed through Hierarchical clustering. The heat maps of the selected BPs are shown in Figures 21-24.

The analysis of the **Cell cycle** genes (Fig.21) indicates a clear upregulation in MS patients, especially in the group of PP (with the exception of SMP6) and RR1. Several cell cycle genes are most regulated in some PP and RR1 subjects compared to the others. In particular, the cell cycle related genes CDKN1C, RIF1, POGZ, RPS6KB1, USP16, KIAA0174, USP9X and PTP4A1 were mostly upregulated in the RR1 patients SMP16 and SMP2 and in the PP patients SMP3, SMP4 and SMP15 in comparison to the other RR1 and PP samples. In the same way, we can observe how the genes NEK1, VASH1, HAUS8, DDIT3, MAP3K8, CDKN1A and CKS2 are mostly induced in the RR1 patients SMP27 and SMP29; and in the PP patients SMP24, SMP25 and SMP26. In summary, the analysis of the most changed genes in this class suggested that the PP and RR1 monocytes induce the upregulation of genes directly involved in cell proliferation including CDKN1A, CYLD, MAPK6, PTP4A1.

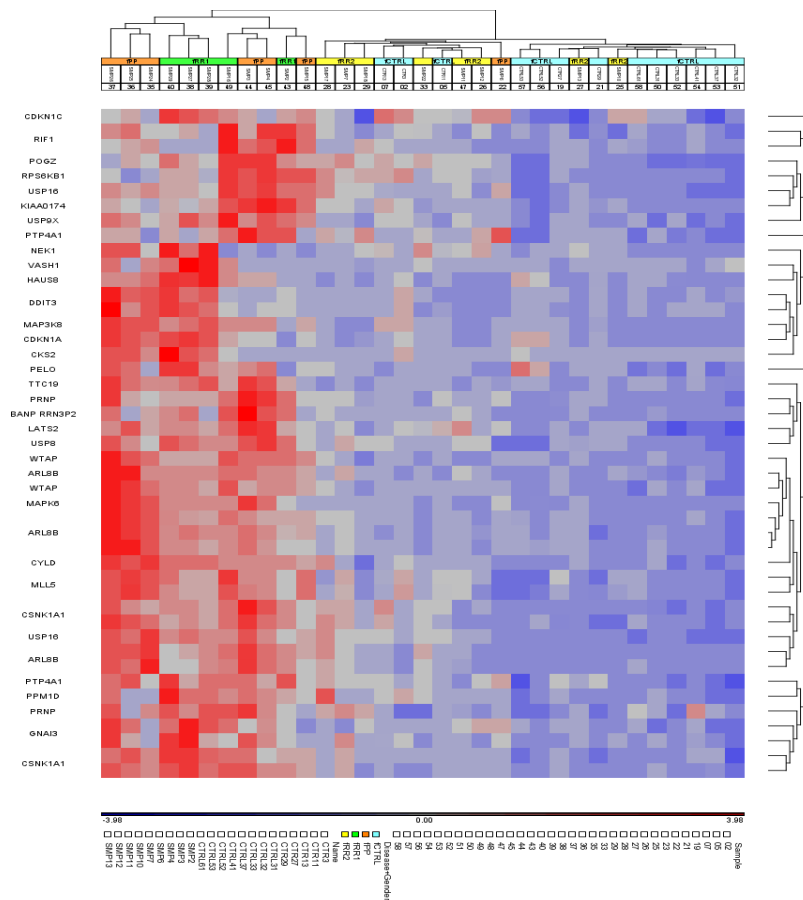


Figure 21. PP and RR Monocytes regulate Cellular Proliferation. List of genes that are significantly upregulated (Red) and downregulated (Blue) within the Cell cycle associated GO terms in PP and RR1 monocytes compared to HCs and RR2 monocytes. DEGs were selected based on $F_c=2$ and $FDR=0.05$. PP n=7; RR1 n=5; RR2 n=8; HC n=13.

The analysis of the **anti-apoptosis** genes is shown in Figure 22. Also in this case, it is possible to appreciate the upregulation of this BP in the PP and RR1 patients compared to the HCs and RR2 groups. The detection of the signalling pathways associated with anti-apoptosis strongly suggests that monocytes from the MS phenotype PP and RR1 potentially raise their life span to enhance the inflammatory response, this phenotype is consistent with a cell memory type of induction.

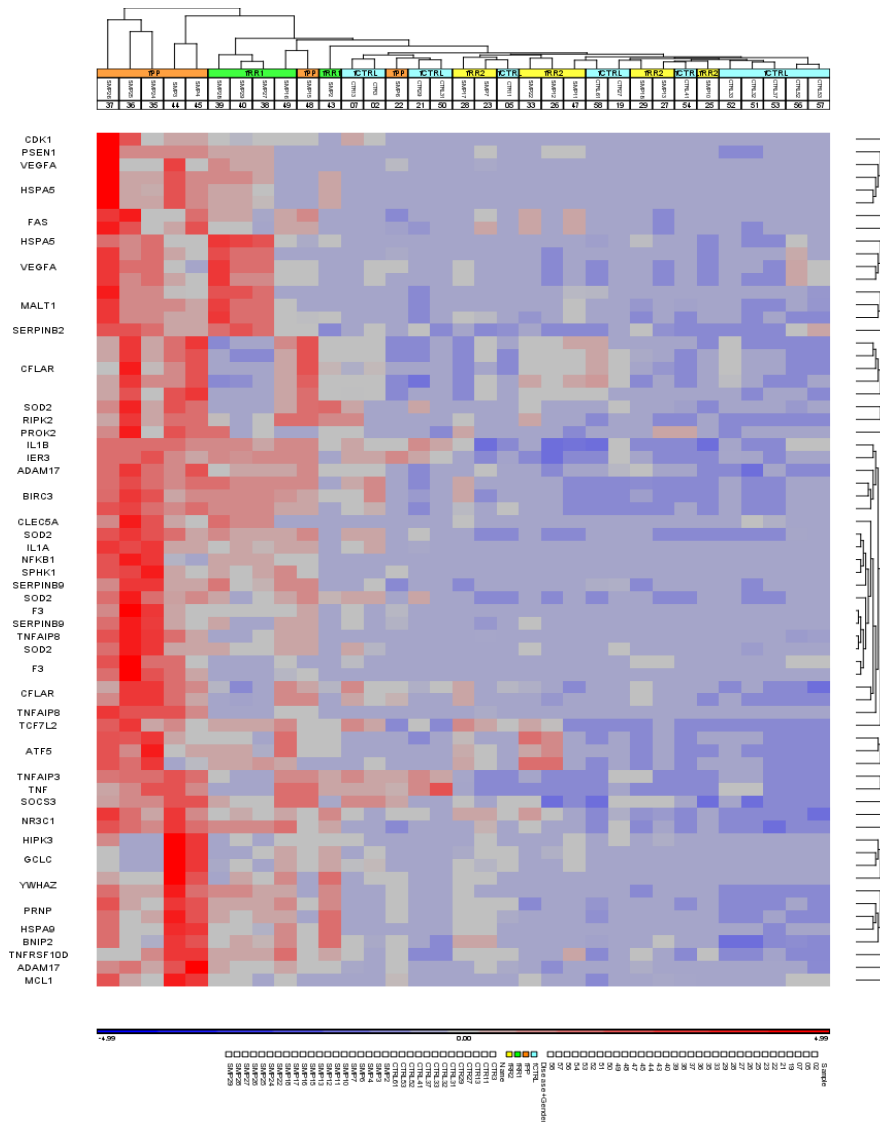


Figure 22. PP and RR Monocytes regulate the gene of Anti-apoptotic response. List of genes that are significantly upregulated (Red) and downregulated (Blue) within the Anti-Apoptotic response associated GO terms in PP and RR1 monocytes compared to HCs and RR2 monocytes. DEGs were selected based on $F_c=2$ and $FDR=0.05$. PP $n=7$; RR1 $n=5$; RR2 $n=8$; HC $n=13$.

The analysis of the **Inflammatory Process** genes is shown in Figure 23. Interestingly, these genes are expressed more strongly in the PP and RR1 patients' monocytes. The mostly upregulated genes in most of the PP patients and in most of the subgroup of RR1 patients are those encoding the inflammatory cytokines $IL1\beta$, $IL1\alpha$ and $TNF\alpha$, the inflammatory chemokines $IL8$, $CXCL2$, $CCL4$, $CCL20$ and $CXCL3$ whereas the cytokine $IL6$, and the chemokines $CXCL1$, $CCL7$ are strongly upregulated only in PP patients SMP24, SMP25 and SMP26 (Fig.23). Interestingly, beside the inflammatory cytokines and chemokines genes, the genes $NLRP3$ (a component of the inflammasome), $CLEC7A$ (the fungus Dectin-1 receptor) and the gene $OLR1$ (the oxLDL receptor) are all strongly induced indicating that the activation status of monocytes is amplified in the PP and RR1 subgroups of patients compared to HCs and RR2. These data clearly suggest that the monocytes from PP and RR1 patients

are triggered to have an enhanced inflammatory response in the monocytes' compartment of the peripheral blood.

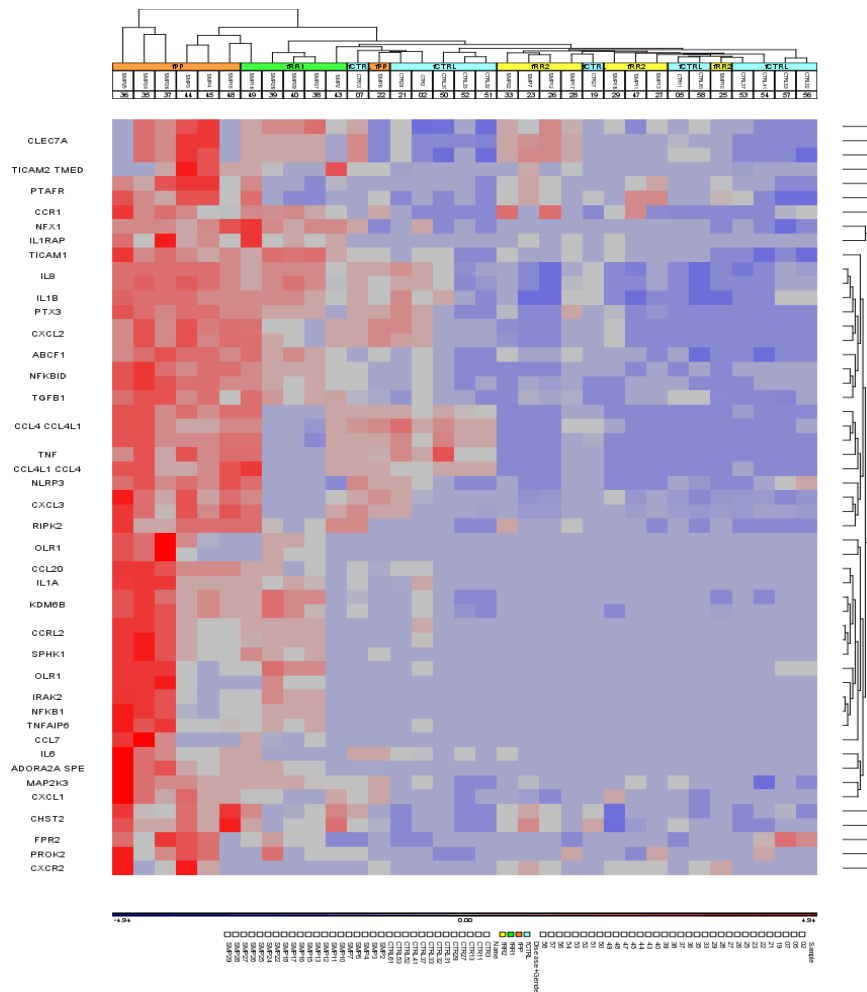


Figure 23. PP and RR1 Monocytes regulate the gene of the Inflammatory Response. List of genes that are significantly upregulated (Red) and downregulated (Blue) within the Inflammatory Response associated GO terms in PP and RR1 monocytes compared to HCs and RR2 monocytes. DEGs were selected based on $F_c=2$ and $FDR=0.05$. PP $n=7$; RR1 $n=5$; RR2 $n=8$; HC $n=13$.

Finally, we observed the regulation of genes associated with metabolic processes. Specifically, we concentrated our attention on the **Cholesterol Biosynthesis Process** as one of the BPs that was most potently induced in MS monocytes. Figure 24A reports the complete analysis of the microarray data relative to this BP. The Cholesterol Biosynthesis Process is clearly induced in most of the PP samples with the exception of sample SMP6, and in RR1 samples with the exception of sample SMP2 (Fig. 24A). The figure 24B and figure 24C report the box plot analysis of the expression values of the microarray experiment. Most of the genes in this pathway are regulated within the PP and RR1 group of samples although with a different statistical significance (Fig. 24B). The gene *INSIG1* was the highly expressed compared to the other genes in the family, and therefore, it was reported in Figure 24C.

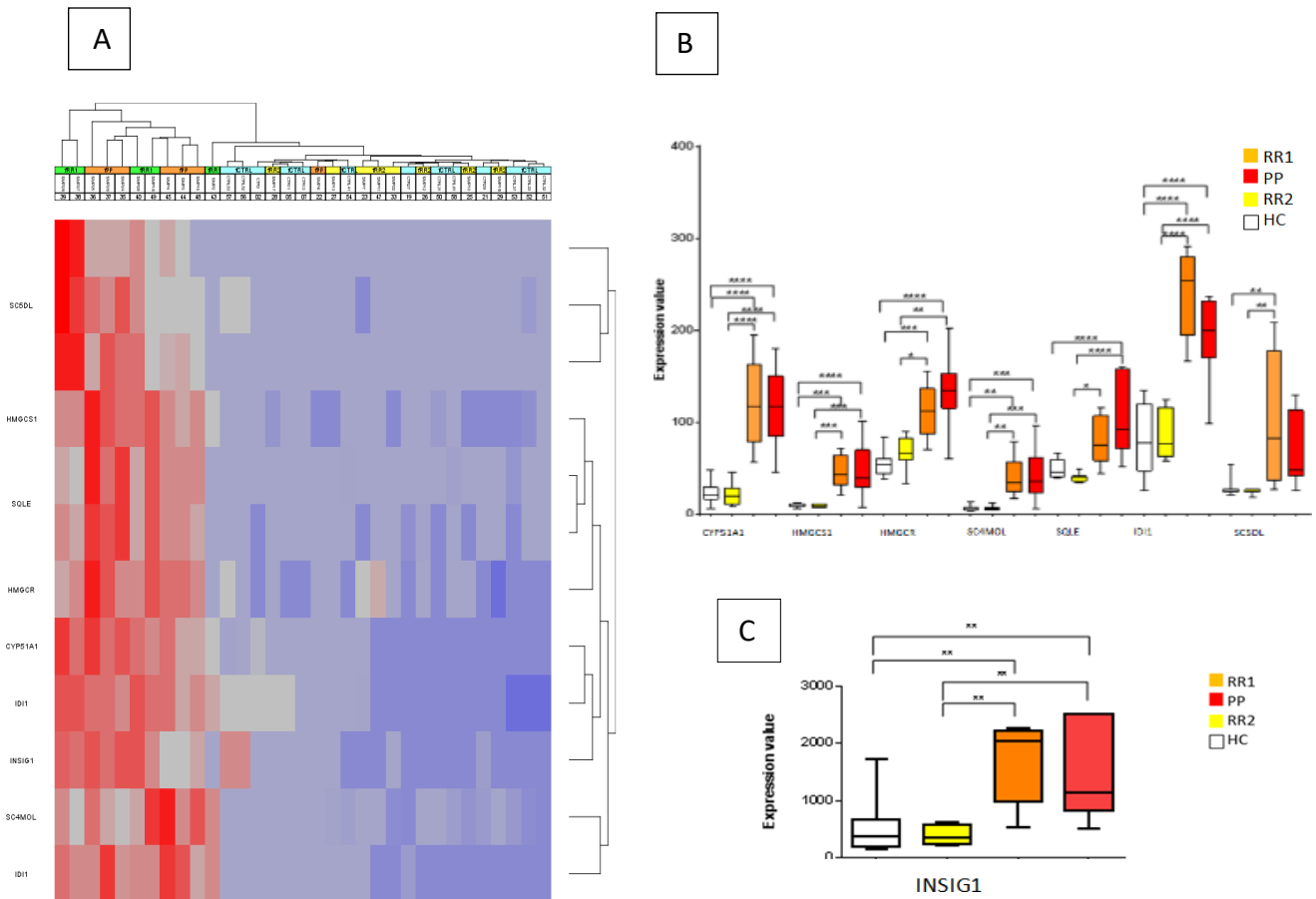


Figure 24. PP and RR1 Monocytes regulate the gene of Cholesterol Biosynthesis Process. A) List of genes that are significantly upregulated (Red) and downregulated (Blue) within the Cholesterol Biosynthesis Process associated GO terms in PP and RR1 monocytes compared to HCs and RR2 monocytes. DEGs were selected based on $Fc=2$ and $FDR=0.05$; B) Box Plot of the cholesterol genes(CYP51A1, HMGCS1, HMGCR, SC4MOL, SQLE, IDI1, SC5DL) expression Arbitrary Units; C) Box Plot of the cholesterol gene (INSIG1) expression Arbitrary Units. PP n=7; RR1 n=5; RR2 n=8;HC n=13. * $p<0.05$, ** $p<0.01$, *** $p<0.001$, **** $p<0.0001$.

In each analysed process, the PPMS patients SMP6 was not clustering with the same phenotypic PP group and the same happens for the RR1 patients SMP2. Whereas for SMP2 the clinic data does not help to understand its trend, for SMP6 it might depend on a previous immunomodulating treatment.

4. INFLAMMATION PATHWAY IS STRONGLY DEREGULATED IN COHORT 1

Among the biological processes identified by microarray analysis, we focused our attention on Cholesterol and Inflammation pathways. The former represents the most defined pathway, the latter is interesting not only for the deregulation of classical proinflammatory genes, but also for the upregulation of the genes NLRP3 (a component of the inflammasome), CLEC7A (the fungus Dectin-1 receptor) and OLR1 (the oxLDL receptor) (Fig.23). All three of them are strongly induced, indicating that the activation status of monocytes is amplified in the PP and RR1 subgroups of patients compared

to HCs and RR2. These data clearly suggest that the monocytes from PP and RR1 patients are triggered to have an enhanced inflammatory response in the monocytic compartment of the peripheral blood. Again, these genes result expressed more strongly in the PP and RR1 patients' monocytes. The gene mostly upregulated in most of the PP and RR1 patients were those encoding TNF α , CXCL8, CXCL2, CCL4, CCL20 and CXCL3 whereas the cytokine IL6, and the chemokines CXCL1, CCL7 were strongly upregulated only in PP patients SMP24, SMP25 and SMP26. From this point on, the validation of the Inflammation pathway will be divided into two distinct parts: the first one is related to the proinflammatory genes encoding cytokines or chemokines, while the second one is related to the receptors molecules CD36, SR-A and OLR1 - which are able to bind oxLDL – and DECTIN-1, NLRP3- which are putative receptors linked to Trained Immunity process.

In addition, the PTX3 gene - which encodes a member of the pentraxin family- and KDM6B gene- involved in H3K27 di- or trimethylation- have been tested.

Additional HCs recruitment. Since it is known that inflammatory genes are modulated by several variables such as environmental stress factors, to testing TNF α , IL1 β , CXCL2, CXCL3 and CXCL8 we selected HCs to include for further analysis by taking advantage of microarray results. To have the same a substantial number of healthy controls, for this experiment we recruited other 9 HCs. However, these HCs were also tested for the validation of the other genes involved in this pathway (KDM6B, CD36, SR-A, OLR1, NLRP3 and DECTIN1). Table 21 reports the main characteristics of these HCs. Since two new controls have the same nomenclature as two already used controls, the new ones were named HC11N and HC13N.

Table 21. Characteristics of additional Healthy Controls used for qRT-PCR validation.

Sample	Sex	Age
HC01	Female	28
HC02	Female	36
HC03	Female	55
HC04	Female	40
HC05	Female	48
HC10	Female	49
HC11N	Female	49
HC13N	Female	41
HC14	Female	43

HC: Healthy Controls.

4.1. THE CYTOKINES TNF α , IL1 β AND THE PTX3 GENE ARE MOST UPREGULATED IN RR1 MS FROM COHORT 1 THAN IN PATIENTS OF COHORT 2

Tumor necrosis factor-alpha (TNF α) is an important mediator of the immunological response. Several

studies have demonstrated its involvement in pathological hallmarks of MS, both in human and in EAE model: TNF α activity increased during active disease with peaks during relapses. However, fully understand the TNF α role in MS is an ongoing challenge, due to its complexity in terms of signaling¹³².

IL-1 β plays an important role in EAE and perhaps in MS: IL-1 β -deficient mice show an improvement of their symptoms; whereas in human, IL-1 β at high level was found both in the blood and in CNS lesions of MS patients¹³³. In addition, several MS therapeutic drugs were used to affect IL-1Ra and/or IL-1 β production, such as type I IFN, glatiramer acetate and natalizumab.

Pentraxin 3 (PTX3) is a fundamental component of the innate immunity, acting as a regulator of inflammation process¹³⁴. In MS context, it has been demonstrated that during relapse, plasma PTX3 levels increase in comparison to healthy individuals. In addition, during the remission phase, plasma PTX3 levels were remarkably lower¹³⁵. This allows thinking that plasma PTX3 quantification may be a potential biomarker of MS course.

Just below is reported the Table 22, containing the main characteristics and the updated clinic data about cohort 1 MS patients tested for TNF α , IL1 β and PTX3 genes.

Table 22. cohort 1 information.

Phenotype	Age	EDSS	Disease duration	Treatment	Comorbidity	Updated clinic (EDSS; relapses)
HC11						
HC27						
HC32	44					
HC41	47					
HC35	37					
HC52	40					
HC53	40					
HC57	41					
HC01	28					
HC02	36					
HC03	55					
HC04	40					
HC05	48					
HC10	49					
HC11N	49					
HC13N	41					
HC14	43					
SMP16 (RR1)	28	1	4			1; rel: 2011
SMP27 (RR1)	58	6.5	16	IFN		8

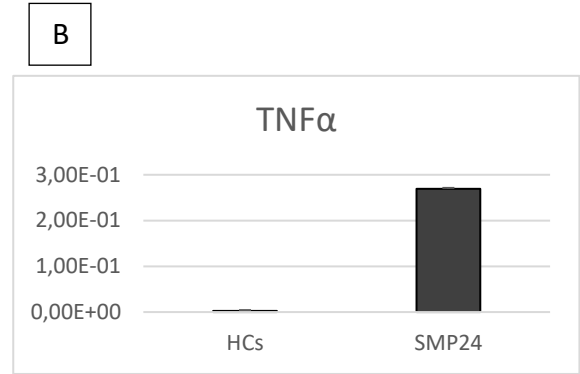
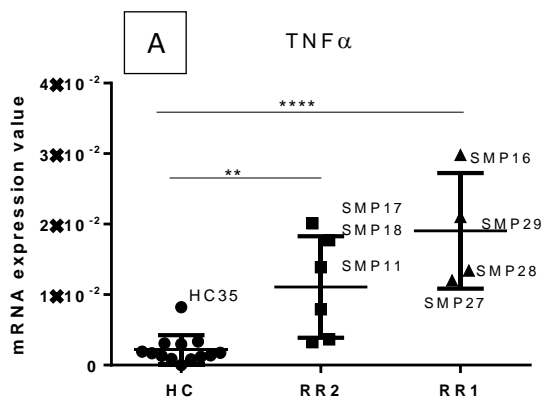
SMP28 (RR1)	49	5	1			5; rel: 2011,2012,2013,2014
SMP29 (RR1)	50	2.5	2			1; rel: 2011,2012,2016
SMP24 (PP)	68	6	13	Eutirox	Hypothyroidism	6.5
SMP11 (RR2)	55	3	25		Hashimoto Thyroiditis	3; rel: 2011
SMP12 (RR2)	51	7	31	AZA, Mito		6.5
SMP13 (RR2)	22	0	6			1; rel: 2010,2016 (x2) ,2017
SMP17 (RR2)	43	6	10	AZA, Methotrexate	LES	6
SMP18 (RR2)	55	5.5	27	AZA	Hypertension	5.5; rel: 2016
SMP22 (RR2)	39	2.5	12	AZA, GA		7; rel: 2017

HC: Healthy controls; RR1: Relapsing Remitting 1; RR2: Relapsing Remitting 2; PP: Primary Progressive; SMP: Multiple Sclerosis Patient; EDSS: Expanded Disability Status Scale; IFN: Interferon beta; Mito: Mitoxantrone; AZA: Azathioprine; GA: Glatiramer Acetate; LES: Systemic Lupus Erythematosus; rel: relapse.

Since we were able to test only **1 PP** of the cohort 1 (SMP24), it was not included in the statistical analyses, but its expression values were reported as histogram in comparison to HCs subjects.

For the **TNF α** gene were tested **12 HCs** (HC11, HC53, HC57, HC01, HC02, HC03, HC04, HC05, HC10, HC11, HC13, HC14), **4 RR1** (SMP16, SMP27, SMP28, SMP29), **6 RR2** (SMP11, SMP12, SMP13, SMP17, SMP18, SMP22), **1 PP** (SMP24).

TNF α is statistically overexpressed in RR1 MS and in RR2 MS. Nevertheless, three RR2 MS patients show higher TNF α expression indicating monocytes activation (Fig.25A). Indeed, clinical data revealed that additional autoimmune diseases affect SMP11 and SMP17 (Hashimoto Thyroiditis and LES respectively), whereas SMP18 is hypertensive. In addition, clinical data show that both SMP11 and SMP18 had a relapse in 2011 and 2016 respectively, while the SMP17 remained stable but with a high EDSS value (EDSS of 6.0). Regarding RR1 patients, TNF α is higher expressed in SMP16 and SMP29, which had one relapse (2011) and three relapses (2011, 2012, 2016) respectively. Instead, SMP27 shows the lowest level. Despite a high EDSS, SMP27 has a longer duration of the disease than other RR1 patients. The PP SMP24 over-expresses the gene in comparison to all HCs tested (Fig 25B).



Tukey's multiple comparisons test	Mean Diff.	95.00% CI of diff.	Significant?	Summary	Adjusted P Value
HC vs. RR2	-0.008887	-0.0152 to -0.002574	Yes	**	0.0053
HC vs. RR1	-0.01685	-0.02417 to -0.009542	Yes	****	<0.0001
RR2 vs. RR1	-0.007968	-0.01622 to 0.0002877	No	ns	0.0597

Figure 25. Statistical analysis of TNF α in cohort 1 subjects. A) Dot plot of tested samples, B) Histogram obtained by the mean of each HC tested for TNF α , and SMP24 mRNA expression value. HCs: healthy controls; RR2, Relapsing Remitting 2; RR1, Relapsing Remitting 1; SMP: Multiple Sclerosis Patients. ** pV = 0.005, ****pV < 0.0001.

For IL-1 β were tested **4 HCs** (HC11, HC41, HC01, HC02), **3 RR1** (SMP27, SMP28, SMP29), **6 RR2** (SMP11, SMP12, SMP13, SMP17, SMP18, SMP22), **1 PP** (SMP24).

IL1 β is regulated differently among patients: in particular, as for TNF α , RR2 MS patients SMP11, SMP12 and SMP13 have the lowest levels. As for TNF α , patients SMP12 and SMP13 show the lower expression profile among RR2, and SMP27 among RR1 (Fig.26A). PP patients SMP24 over-expresses IL-1 β gene in comparison to tested HCs (Fig.26B).

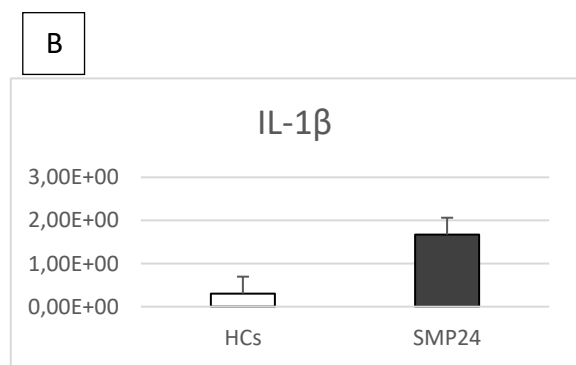
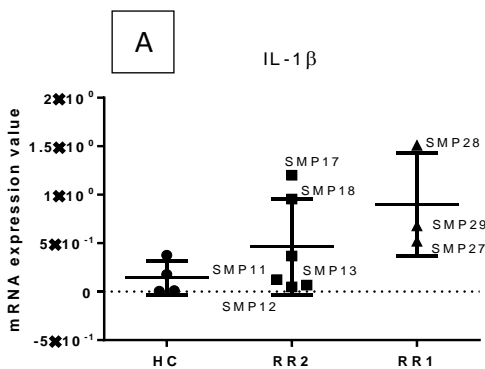
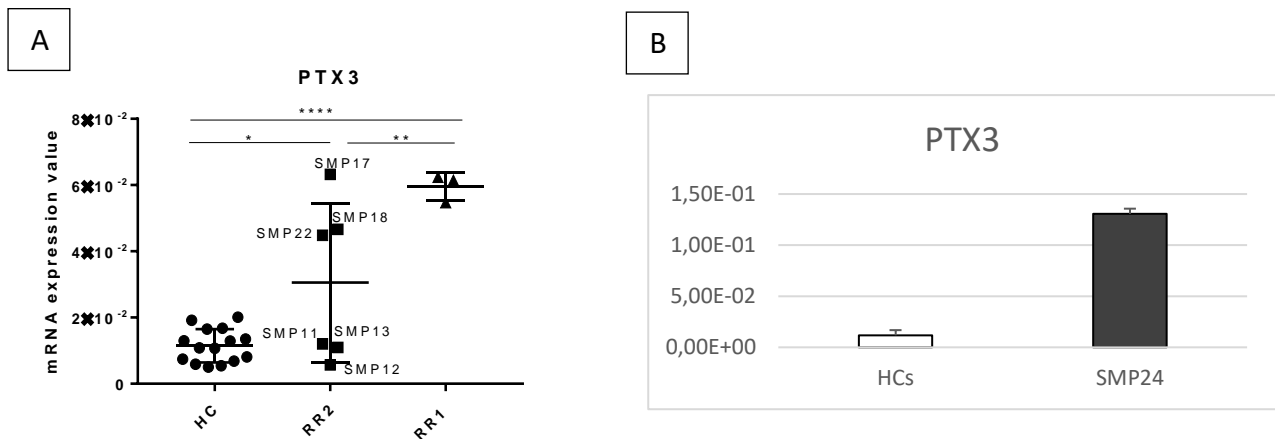


Figure 26. Statistical analysis of IL1 β in cohort 1 subjects. A) Dot plot of tested samples, B) Histogram obtained by the mean of each HC tested for IL1 β , and SMP24 mRNA expression value. HCs: healthy controls; RR2: Relapsing Remitting 2; RR1: Relapsing Remitting 1; SMP: Multiple Sclerosis Patient.

The gene PTX3 was tested in **15 HCs** (HC11, HC27, HC32, HC41, HC52, HC53, HC01, HC02, HC03, HC04, HC05, HC10, HC11, HC13, HC14), **3 RR1** (SMP27, SMP28, SMP29), **6 RR2** (SMP11, SMP12, SMP13, SMP17, SMP18, SMP22), **1 PP** (SMP24).

PTX3 is induced in RRMS and interestingly it is able to define two groups in RR2 MS patients: those that express high levels (SMP17, SMP18, SMP22) and those that do not regulate this gene (SMP11, SMP12, SMP13) (Fig.27A). SMP24 up-regulates the PTX3 gene (Fig.27B).



Tukey's multiple comparisons test	Mean Diff.	95.00% CI of diff.	Significant?	Summary	Adjusted P Value
HC vs. RR2	-0.01907	-0.03424 to -0.003896	Yes	*	0.0124
HC vs. RR1	-0.04802	-0.06789 to -0.02815	Yes	****	<0.0001
RR2 vs. RR1	-0.02895	-0.05116 to -0.006739	Yes	**	0.0095

Figure 27. Statistical analysis of PTX3 in cohort 1 subjects. A) Dot plot of tested samples, B) Histogram obtained by the mean of each HC tested for PTX3, and SMP24 mRNA expression value.

HCs, healthy controls; RR2, Relapsing Remitting 2; RR1, Relapsing Remitting 1; SMP: Multiple Sclerosis Patient.

*pV < 0.03; ** pV = 0.009; ****pV < 0.0001.

TNF α and PTX3 were additionally tested on MS samples from cohort 2. To verify whether TNF α and PTX3 were indeed overexpressed in MS monocytes, we tested their upregulation on RR and PP samples derived from cohort 2.

The Table 23 report the main characteristics and the updated clinic data about cohort 2 MS patients tested for TNF α and PTX3 genes.

Table 23. Cohort 2 information.

Phenotype	Age	EDSS	Disease duration	Treatment	Comorbidity	Updated clinic (EDSS; relapses)
HC11						
HC27						
HC32	44					
HC41	47					
HC35	37					
HC52	40					
HC53	40					
HC57	41					
HC01	28					
HC02	36					
HC03	55					
HC04	40					
HC05	48					
HC10	49					
HC11N	49					
HC13N	41					

HC14	43					
SMP44 (RR)	50	1	6	NA		1
SMP59 (RR)	49	6,5	25	IFN, GA		8; rel: 2009,2010,2011,2013
SMP69 (RR)	40	1,5	14	IFN, GA		2,5; rel: 2013,2017
SMP70 (RR)	44	1	6	IFN	Endometriosis, Hypertension	45; rel: 2013 (x2), 2014, 2017
SMP71 (RR)	42	1	16	NA		3; rel: 2012,2013
SMP72 (RR)	58	6,5	36	Gabapentin, Clonazepam		
SMP73 (RR)	50	2,5	12	IFN, GA		
SMP74 (RR)	42	6	24	IFN, GA, AZA, Mitoxantrone		
SMP47 (PP)	52	6	5	Vit D	Epilepsy	7,5
SMP48 (PP)	47	5	9	Depakin, Vinpat	Epilepsy	6; rel: 2015
SMP51 (PP)	59	7	30	NA		8
SMP63 (PP)	55	7,5	16	NA		7,5
SMP65 (PP)	64	7,5	14	NA		8
SMP66 (PP)	63	6,5	39	Bacoflen, Amantadina		6.5
SMP68 (PP)	56	7	7	AZA	Raynaud Syndrome	7

HC: Healthy controls; RR: Relapsing Remitting; PP: Primary Progressive; SMP: Multiple Sclerosis Patient; EDSS: Expanded Disability Status Scale; IFN: Interferon beta; Mito: Mitoxantrone; AZA: Azathioprine; GA: Glatiramer Acetate; LES: Systemic Lupus Erythematosus; rel: relapse.

For **TNF α** were tested **12 HCs** (HC11, HC53, HC57, HC01, HC02, HC03, HC04, HC05, HC10, HC11, HC13, HC14), **8 RR** (SMP44, SMP59, SMP69, SMP70, SMP71, SMP72, SMP73, SMP74), **7 PP** (SMP47, SMP48, SMP51, SMP63, SMP65, SMP66, SMP68).

The figures A, B and C represent the statistical analysis of the validated samples for TNF α gene. Since TNF α expression levels from RR patients SMP71, SMP44 and SMP59 were higher, their data are reported as individual charts (Figures 28A and 28B).

Clinic data report that patient SMP44 remained stable over time, while patient SMP59 had a worsening of EDSS from 6.5 to 8, and several relapses. To appreciate the differences between the other RR and PP, the successive analysis was performed by removing SMP71, SMP44 and SMP59 (Figure 28C). The new analysis shows that among the remaining RR the patient SMP73 has a particularly high expression profile, as well as the PP patients SMP47 and SMP48. Both SMP47 and SMP48 have comorbidity (epilepsy) and an increase in follow-up EDSS (SMP47 6 to 7.5; SMP48 5 to 6). The clinic data for patient SMP73 is not available.

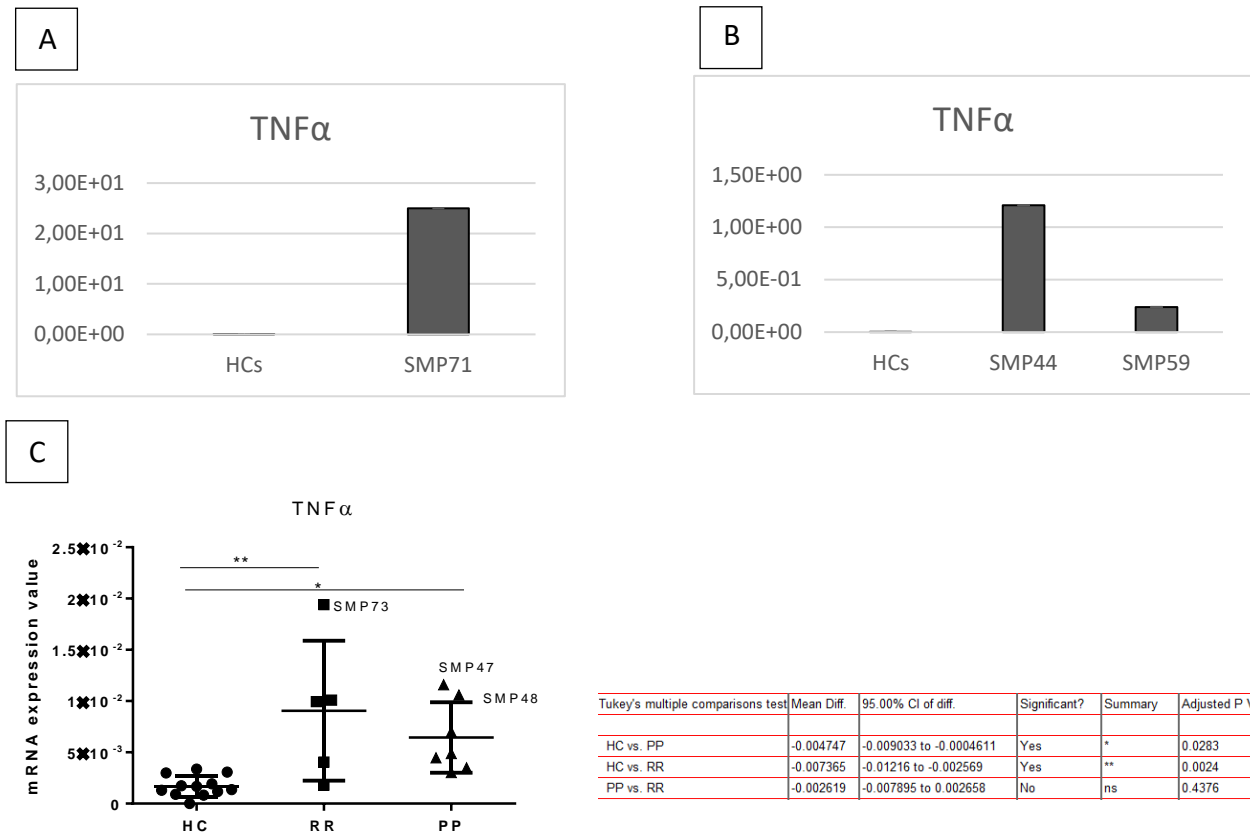


Figure 28. Statistical analysis of TNF α in cohort 2 subjects. A) Histogram obtained by the mean of each HC tested for TNF α and SMP71 mRNA expression value; B) Histogram obtained by the mean of each HC tested for TNF α and SMP44 and SMP59 mRNA expression value; C) Dot plot of tested samples without SMP71, SMP44 and SMP59. HCs, healthy controls; RR: Relapsing Remitting; PP: Primary Progressive; SMP: Multiple Sclerosis Patient. *pV < 0.03; ** pV =0.002

For the gene **PTX3** were tested **15 HCs** (HC11, HC27, HC32, HC41, HC52, HC53, HC01, HC02, HC03, HC04, HC05, HC10, HC11, HC13, HC14), **8 RR** (SMP44, SMP59, SMP69, SMO70, SMP71, SMP72, SMP73, SMP74), **7 PP** (SMP47, SMP51, SMP63, SMP65, SMP66, SMP68).

Figure 29 represents the statistical analysis of the validated samples. Once again, SMP44 turns out to be the RR patient with the highest level of deregulation for the analysed gene. Same thing for SMP48 and SMP47 among the PP patients. (Fig 29).

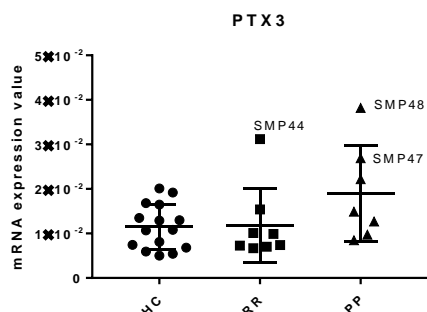


Figure 29. Statistical analysis of PTX3 in cohort 2 subjects. Dot plot of tested samples. HCs, healthy controls; RR: Relapsing Remitting; PP: Primary Progressive; SMP: Multiple Sclerosis Patient.

Summary about TNF α , IL1 β and PTX3 expression.

In conclusions, among the RR2 group, patients SMP17, SMP18 and SMP22 have higher levels of inflammatory genes. The clinical data that these patients have in common the presence of co-

morbidity (hypertension, cardiac waste, dyslipidemia, allergies). Furthermore, among RR2 MS patients, SMP22 has suffered the strongest disease progression in terms of EDSS score, rising from 2.5 to 7 from the time of collection to that of follow up, which highlights the important inflammatory state of the patient. The RR2 patients with the lowest profile were always SMP12 and SMP13: SMP12 is the only RR2 that had an improvement of its EDSS from 7 to 6.5 during the follow up. Among the RR1 patients, SMP16 and SMP29 have the highest induction profiles for TNF α gene. SMP28 upregulated both IL1 β and PTX3, and together with SMP29 have the highest number of relapses. SMP27 is the RR1 patient with the lowest gene expression profile both for TNF α and IL1 β genes. Summarizing the results in the cohort 1, we note that in both subgroups (RR1 and RR2) the patients with the longest disease duration corresponded to those with the lowest expression profile. For RR1 is the patient SMP 27 (16 years of disease compared to 1, 4 and 2 of patients SMP28, SMP16, SMP29), and for RR2 is the patient SMP12 (31 years of disease compared to 25, 6, 10, 27 and 12 of patients SMP11, SMP13, SMP17, SMP18 and SMP22). The PP SMP24 of cohort 1 always over-expresses all genes tested. By analysing the patients of cohort 2, SMP44, SMP71 and SMP73 stand out among RR and SMP47 and SMP48 patients among PP. What emerges from the clinic data is that in cohort 2, as observed for the cohort 1, patients with fewer years of disease have the highest deregulation profile.

4.2. CHEMOKINES GENES ARE INDUCED IN RR1 AND IN PP SMP 24

CXCL2 is a cell-signalling cytokine with chemoattractant properties¹³⁶. CXCL2 expression into the CNS leads neutrophil recruitment and EAE induction, nevertheless, little is known about CXCL2 in MS-monocytes context. As for CXCL2, also CXCL3 was poorly investigated in MS-peripheral cells context. Instead, CXCL8 is well characterized in MS-monocytes context. In fact, CXCL8 secretion from PBMCs is significantly higher in untreated MS patients compared to healthy subjects, and in addition it is significantly reduced in MS patients treated with interferon- β 1a¹³⁷. Interestingly, monocytes resulted the main responsible for the majority of this CXCL8 production¹³⁷. This suggests CXCL8 may be a biomarker of MS activity.

The Table 24 reports the main characteristics and the updated clinic data about cohort 1 MS patients tested for CXCL2, CXCL3 and CXCL8 genes.

Table 24. Cohort 1 information.

Phenotype	Age	EDSS	Disease duration	Treatment	Comorbidity	Updated clinic (EDSS; relapses)
HC3						

HC11						
HC13						
HC27						
HC29						
HC32	44					
HC35	37					
HC41	47					
HC52	40					
HC53	40					
HC57	41					
HC01	28					
HC02	36					
HC03	55					
HC04	40					
HC05	48					
HC10	49					
HC11N	49					
HC13N	41					
HC14	43					
SMP16 (RR1)	28	1	4			1; rel: 2011
SMP27 (RR1)	58	6.5	16	IFN		8
SMP28 (RR1)	49	5	1			5; rel: 2011,2012,2013,2014
SMP29 (RR1)	50	2.5	2			1; rel: 2011,2012,2016
SMP24 (PP)	68	6	13	Eutirox	Hypothyroidism	6.5
SMP11 (RR2)	55	3	25		Hashimoto Thyroiditis	3; rel: 2011
SMP12 (RR2)	51	7	31	AZA, Mito		6.5
SMP13 (RR2)	22	0	6			1; rel: 2010,2016 (x2),2017
SMP17 (RR2)	43	6	10	AZA, Methotrexate	LES	6
SMP18 (RR2)	55	5.5	27	AZA	Hypertension	5.5; rel: 2016
SMP22 (RR2)	39	2.5	12	AZA, GA		7; rel: 2017

HC: Healthy controls; RR1: Relapsing Remitting 1; RR2: Relapsing Remitting 2; PP: Primary Progressive; SMP: Multiple Sclerosis Patient. EDSS: Expanded Disability Status Scale; IFN: Interferon beta; Mito: Mitoxantrone; AZA: Azathioprine; GA: Glatiramer Acetate; LES: Systemic Lupus Erythematosus; rel: relapse.

Since we were able to test only **1PP** of the cohort 1 (SMP24), it was not included in the statistical analyses, but its expression was reported as the chart in comparison with HCs subjects.

For the **CXCL2** gene were tested **12 HCs** (HC11, HC27, HC41, HC01, HC02, HC03, HC04, HC05, HC10, HC11, HC13, HC14), **3 RR1** (SMP27, SMP28, SMP29), **6 RR2** (SMP11, SMP12, SMP13, SMP17, SMP18, SMP22), **1 PP** (SMP24).

The patients SMP17, SMP18 and SMP22 have higher mRNA expression values than the other RR2 patients. Whereas for RR1 MS, the SMP27 has the lowest expression value (Fig. 30A). Also in this case, PP patient SMP24 upregulate the gene in comparison to the HCs (Fig. 30B).

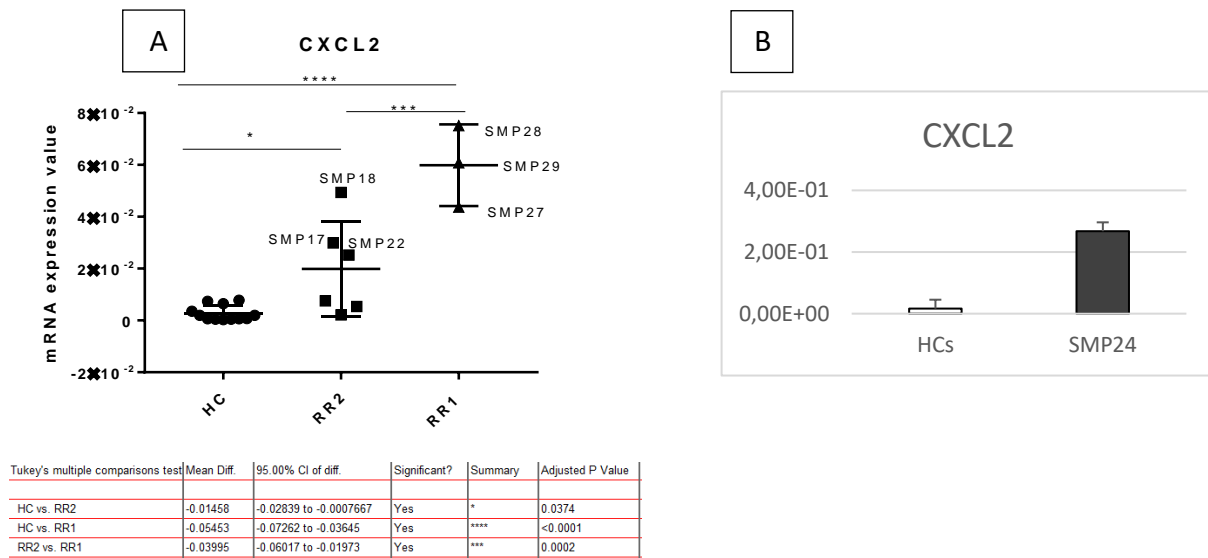


Figure 30. Statistical analysis of CXCL2 in cohort 1 subjects. A) Dot plot of tested samples, B) Histogram obtained by the mean of each HC tested for CXCL2, and SMP24 mRNA expression value. HCs, healthy controls; RR2, Relapsing Remitting 2; RR1, Relapsing Remitting 1; SMP: Multiple Sclerosis Patient. *pV =0.03; *** pV =0.0002; ****pV<0.0001.

For the **CXCL3** gene were tested **14 HCs** (HC11, HC32, HC52, HC35, HC57, HC01, HC02, HC03, HC04, HC05, HC10, HC11, HC13, HC14), **4 RR1** (SMP 16, SMP27, SMP28, SMP29), **6 RR2** (SMP11, SMP12, SMP13, SMP17, SMP18, SMP22), **1PP** (SMP24). The figures 31A and 31B represent the statistical analysis of the validated samples. As seen for TNF α , the most deregulated patients are SMP16 and SMP18. It is interesting to note that among the RR1, SMP27 is still the patient with the lower expression value. To appreciate better the differences observed between patients, the analysis was performed by removing SMP16 and SMP18 (Fig. 31B), considering the two patients as outliers (Fig.31B). It was so possible to appreciate the differences also in the other patients: SMP17 and SMP22 up-regulate the gene more than SMP11, SMP12 and SMP13. About PP patient, SMP24 has a higher expression profile than HCs (Fig. 31C).

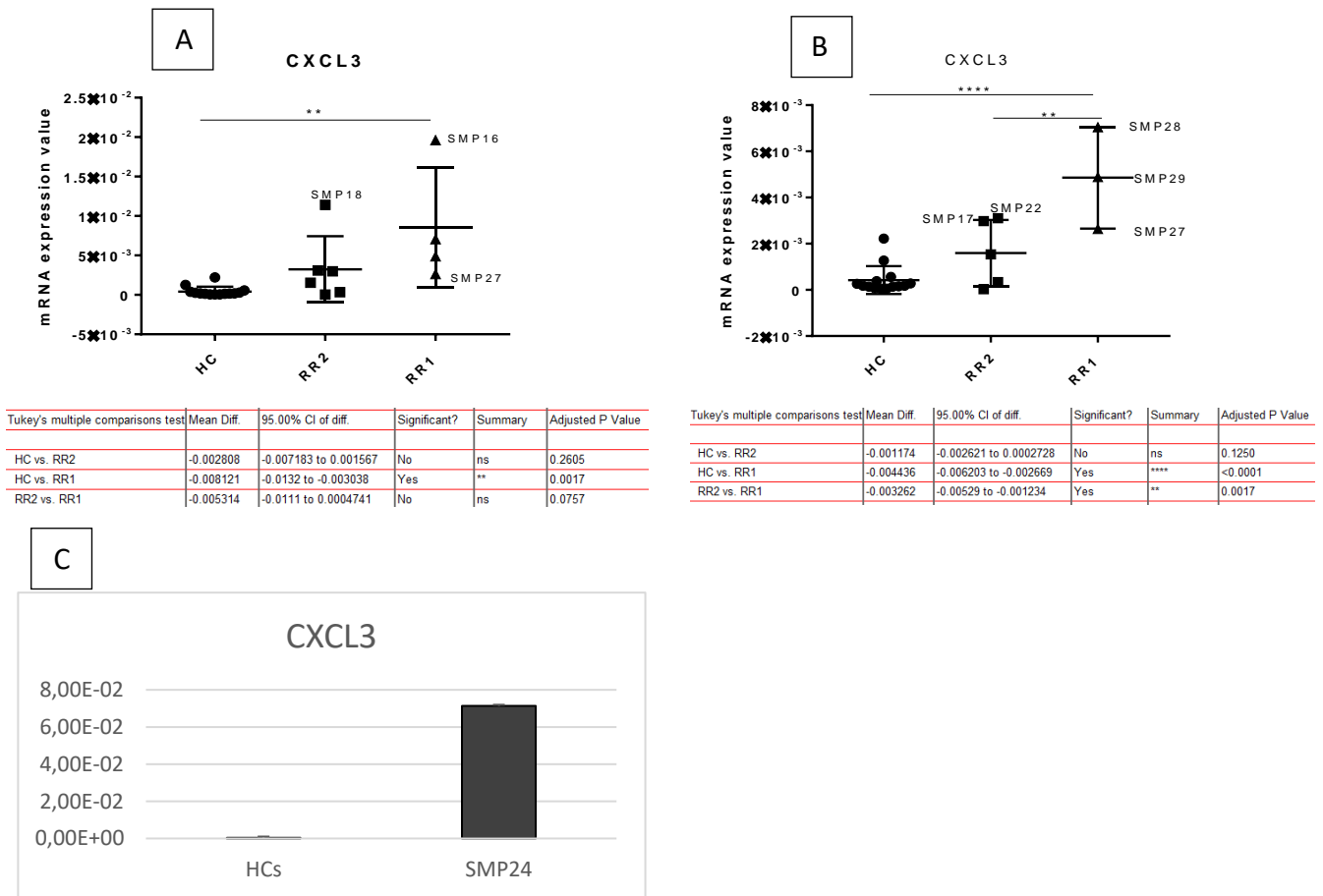
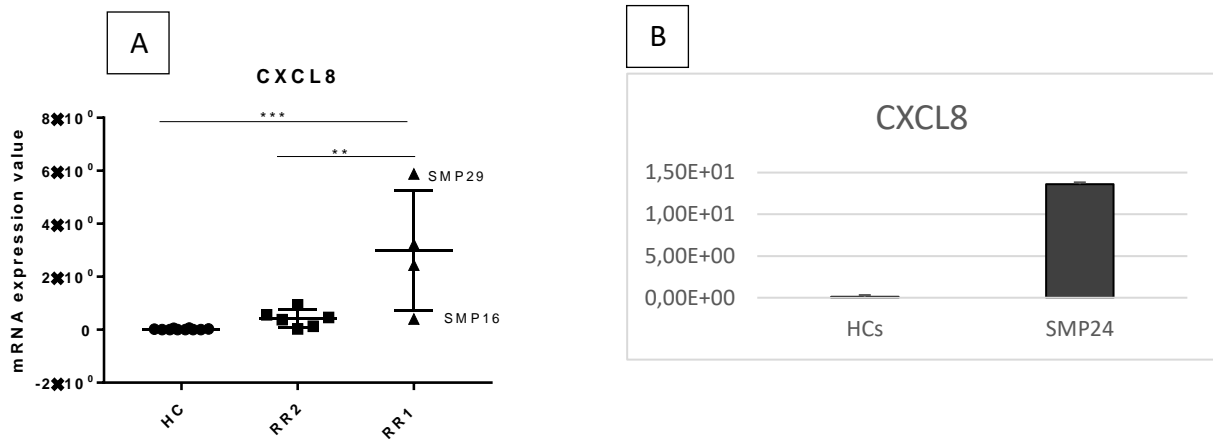


Figure 31. Statistical analysis of CXCL3 in cohort 1 subjects. A) Dot plot of tested samples, B) Dot plot by removing SMP16 and SMP18; C) Histogram obtained by the mean of each HC tested for CXCL3, and SMP24 mRNA expression value. HCs, healthy controls; RR2, Relapsing Remitting 2; RR1, Relapsing Remitting 1; SMP: Multiple Sclerosis Patient. **pV =0.00; ****pV<0.0001.

For the **CXCL8** gene were tested **10 HCs** (HC57, HC01, HC02, HC03, HC04, HC05, HC10, HC11, HC13, HC14), **4 RR1** (SMP 16, SMP27, SMP28, SMP29), **6 RR2** (SMP11, SMP12, SMP13, SMP17, SMP18, SMP22), **1 PP** (SMP24). It can be observed that for the CXCL8 the RR2 patients behave as the HCs. Patient SMP16 has a lower expression profile, contrary to what was observed for TNF α and CXCL3 genes. Instead, patient SMP29 has the highest level of induction (Fig. 32A). SMP24 over-expresses the gene as well (Fig. 32B).



Tukey's multiple comparisons test	Mean Diff.	95.00% CI of diff.	Significant?	Summary	Adjusted P Value
HC vs. RR2	-0.4002	-1.682 to 0.8819	No	ns	0.7076
HC vs. RR1	-2.967	-4.436 to -1.499	Yes	***	0.0002
RR2 vs. RR1	-2.567	-4.17 to -0.9645	Yes	**	0.0020

Figure 32. Statistical analysis of CXCL8 in cohort 1 subjects. A) Dot plot of tested samples, B) Histogram obtained by the mean of each HC tested for CXCL8, and SMP24 mRNA expression value.

HCs, healthy controls; RR2, Relapsing Remitting 2; RR1, Relapsing Remitting 1; SMP: Multiple Sclerosis Patient.

** pV =0.002, ****pV<0.0001.

CXCL2, CXCL3 and CXCL8 were additionally tested on MS samples from cohort 2. To verify whether CXCL2, CXCL3 and CXCL8 were indeed overexpressed in MS monocytes, we tested their upregulation on RR and PP samples derived from cohort 2.

The Table 25 reports the main characteristics and the updated clinic data about cohort 2 MS patients tested for CXCL2, CXCL3 and CXCL8 genes.

Table 25. Cohort 2 information.

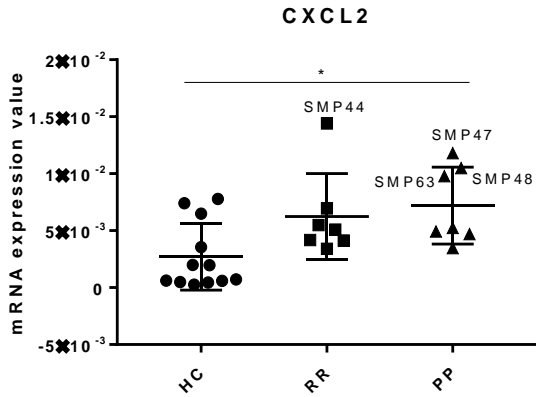
Phenotype	Age	EDSS	Disease duration	Treatment	Comorbidity	Updated clinic (EDSS; relapses)
HC3						
HC11						
HC13						
HC27						
HC29						
HC32	44					
HC35	37					
HC41	47					
HC52	40					
HC53	40					
HC57	41					
HC01	28					
HC02	36					
HC03	55					

HC04	40					
HC05	48					
HC10	49					
HC11N	49					
HC13N	41					
HC14	43					
SMP44 (RR)	50	1	6	NA		1
SMP59 (RR)	49	6.5	25	IFN, GA		8; rel: 2009,2010,2011,2013
SMP69 (RR)	40	1,5	14	IFN, GA		2.5; rel: 2013,2017
SMP70 (RR)	44	1	6	IFN	Endometriosis, Hypertension	4.5; rel: 2013 (x2), 2014, 2017
SMP71 (RR)	42	1	16	NA		3; rel: 2012,2013
SMP72 (RR)	58	6.5	36	Gabapentin, Clonazepam		
SMP73 (RR)	50	2.5	12	IFN, GA		
SMP74 (RR)	42	6	24	IFN, GA, AZA, Mitoxantrone		
SMP47 (PP)	52	6	5	Vit D	Epilepsy	7,5
SMP48 (PP)	47	5	9	Depakin, Vinpat	Epilepsy	6; rel: 2015
SMP51 (PP)	59	7	30	NA		8
SMP63 (PP)	55	7.5	16	NA		7.5
SMP65 (PP)	64	7.5	14	NA		8
SMP66 (PP)	63	6.5	39	Bacoflen, Amantadina		6.5
SMP68 (PP)	56	7	7	AZA	Raynaud Syndrome	7

HC: Healthy controls; RR: Relapsing Remitting; PP: Primary Progressive; SMP: Multiple Sclerosis Patients; EDSS: Expanded Disability Status Scale; IFN: Interferon beta; Mito: Mitoxantrone; AZA: Azathioprine; GA: Glatiramer Acetate; LES: Systemic Lupus Erythematosus; rel: relapse.

For the CXCL2 gene were tested **12 HCs** (HC11, HC27, HC41, HC01, HC02, HC03, HC04, HC05, HC10, HC11, HC13, HC14), **8 RR** (SMP44, SMP59, SMP69, SMO70, SMP71, SMP72, SMP73, SMP74), **7 PP** (SMP47, SMP48, SMP51, SMP63, SMP65, SMP66, SMP68).

The analysis shows again a high profile of the patient SMP44 compared to the other RR (Fig. 33). In general, patients and controls are not particularly homogeneous. Even for CXCL2 as for TNF α , patients SMP47 and SMP48 have the highest profile among PP, along with SMP63. The latter is stable at the current clinic.

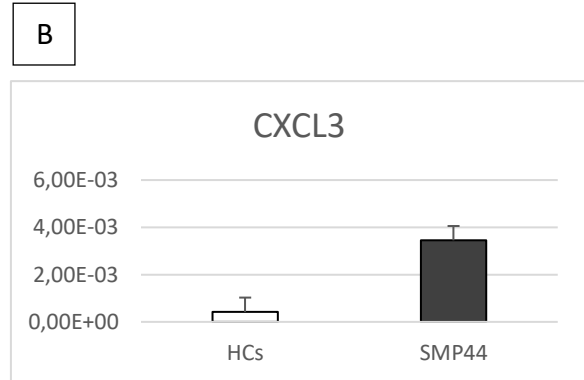
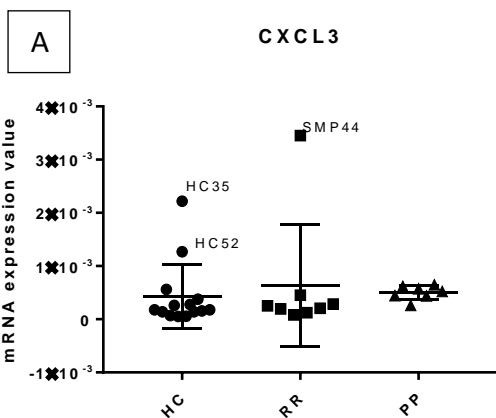


Tukey's multiple comparisons test	Mean Diff.	95.00% CI of diff.	Significant?	Summary	Adjusted P Value
HC vs. RR	-0.003541	-0.007442 to 0.0003595	No	ns	0.0800
HC vs. PP	-0.004508	-0.008409 to -0.0006077	Yes	*	0.0215
RR vs. PP	-0.0009671	-0.005351 to 0.003417	No	ns	0.8462

Figure 33. Statistical analysis of CXCL2 in cohort 2 subjects. Dot plot of tested samples. HCs, healthy controls; RR: Relapsing Remitting; PP: Primary Progressive.; SMP: Multiple Sclerosis Patient. *pV =0.02

For the **CXCL3** were tested **14 HCs** (HC11, HC32, HC52, HC35, HC57, HC01, HC02, HC03, HC04, HC05, HC10, HC11, HC13, HC14), **8 RR** (SMP44, SMP59, SMP69, SMP70, SMP71, SMP72, SMP73, SMP74), **7 PP** (SMP47, SMP51, SMP63, SMP65, SMP66, SMP68).

Again, the patient SMP44 has the higher induction profile, as shown in Figure 34A. Its expression value was so high that it flattened the trend of all other patients (Fig.34B). The general trend was most noticeable by removing SMP44, as seen in Figure C. Moreover, HC35 and HC52 deviate from the group of the other controls (Fig.34A). Therefore, in the successive analysis these subjects were removed: the most deregulated PP are still the patient SMP48, and then SMP66 and SMP65 (Fig.34C). The latter two show a worsening of EDSS from 6.5 to 7 and from 7.5 to 8 respectively.



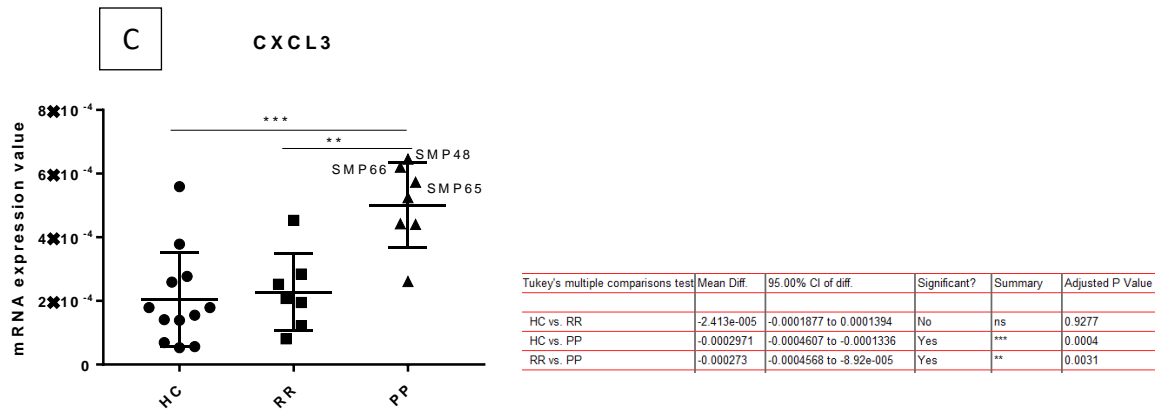


Figure 34. Statistical analysis of CXCL3 in cohort 2 subjects. A) Dot plot of tested samples, B) Histogram obtained by the mean of each HC tested for CXCL3 and SMP44 mRNA expression value; C) Dot plot without HC35, HC52 and SMP44. HCs, healthy controls; RR: Relapsing Remitting; PP: Primary Progressive; SMP: Multiple Sclerosis Patient. **pV =0.003; ***pV=0.0004.

For the **CXCL8** were tested **10 HCs** (HC57, HC01, HC02, HC03, HC04, HC05, HC10, HC11, HC13, HC14), **8 RR** (SMP44, SMP59, SMP69, SMP70, SMP71, SMP72, SMP73, SMP74), **7 PP** (SMP47, SMP48, SMP51, SMP63, SMP65, SMP66, SMP68).

From this analysis it can be observed that the patient SMP44 is still the most deregulated among the RR, while among the PP the most deregulated are still SMP48 and SMP47, along with SMP63 (Fig. 35A). Given these results, a later analysis by removing SMP44 and the four PP with the lowest expression values was performed – in order to identify if between the PP and the RR with the highest induction profile there were relevant differences (Fig. 35B). Important differences were observed between the controls and the remaining RR and PP, and between the three PP with the highest gene expression profile for CXCL8 and other RR (Fig.35B).

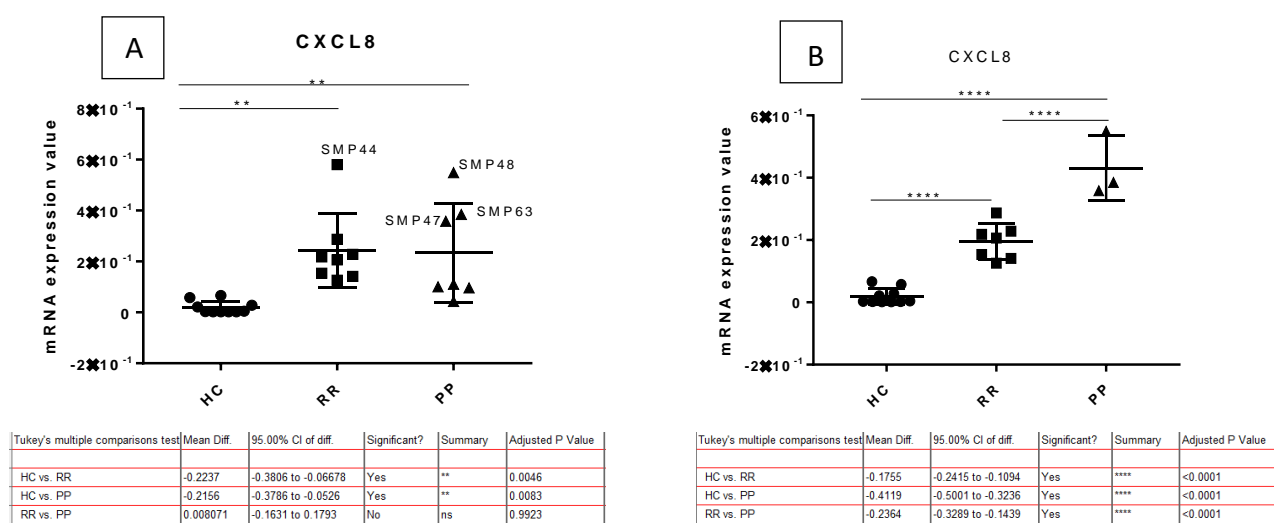


Figure 35. Statistical analysis of CXCL8 in cohort 2 subjects. A) Dot plot of tested samples, B) Dot plot without SMP44 and SMP51, SMP65, SMP66, SMP68. HCs, healthy controls; RR: Relapsing Remitting; PP: Primary Progressive; SMP: Multiple Sclerosis Patient. **pV < 0.008; ****pV<0.0001.

Summary about CXCL2, CXCL3 and CXCL8 expression.

In conclusion, as observed for TNF α and IL1 β , among the RR2 MS patients monocytes of SMP17 and SMP18 are still the most induced, especially for CXCL2 and CXCL3 genes. In addition, SMP22 patient also has a high gene expression profile for CXCL2.

In RR12 MS group, SMP16 is the patients with the highest gene expression profile for CXCL3 and the lowest for CXCL8. Patient SMP29 and SMP28 express high levels of CXCL8 and CXCL2 genes respectively. Again, SMP27 is the RR1 patient displayed lower expression levels especially for CXCL2 and CXCL3.

It is interesting to note that RR1 patients SMP16 and SMP27 seem to have an opposite trend to each other. The clinic characteristic, which could explain this trend, is the disease duration: SMP27 has a disease duration that is 4 times higher that of SMP16 (16 years vs 4).

In addition, also in this case the cohort 1 PP patient called SMP24 upregulates the tested genes.

By analysing the cohort 2, SMP44, SMP47 and SMP48 still remain the patients with the most deregulated profile. Hence, these results seem to be in line with previous results obtained for TNF α , IL1 β and PTX3 genes.

In general, we could confirm the expression profiles obtained by microarray analysis. Nevertheless, the genes signatures selected are specific for cohort 1 and there were not completed validated in cohort 2 subjects. Based on these results, we can select genetic signature that will help to stratify RRMS and PPMS patients by microarray analysis. Each profile is therefore cohort specific as the pattern selected could not be present on a different cohort.

5. CHOLESTEROL BIOSYNTHESIS PATHWAY IS INDUCED BOTH IN COHORT 1 AND IN COHORT 2 MS PATIENTS

As specified before, the Cholesterol Biosynthesis pathway is one of the most induced and interesting process deregulated in our patients' samples group (Fig. 24A). The cholesterol biosynthesis can be divided into two different parts: the first one involves the genes HMGCS1, HMGCR - through which Mevalonate production occurs - and IDI1, which plays a role in dimethylallyl diphosphate (DMAPP) formation; the second one is related to the cholesterol production itself, and involves the genes SQLE, SC4MOL, CYP51A1 and SC5DL. We found deregulated the gene INSIG-1 too that is involved in the homeostasis of the cholesterol process. Again, these genes were tested both on cohort 1 and cohort 2 of MS patients. HMGCS1 is a Protein Coding gene and catalyzes the condensation of acetyl-CoA with acetoacetyl-CoA to form HMG-CoA, which is converted by HMG-CoA reductase (HMGCR)

into mevalonate, a precursor for cholesterol synthesis. HMGCR (3-Hydroxy-3-Methylglutaryl-CoA Reductase) is a Protein Coding gene⁸⁶. The HMG-CoA-reductase enzyme is the rate-limiting enzyme of cholesterol biosynthesis and it is regulated through negative feedback mechanisms mediated by mevalonate derived metabolites. It has been demonstrated that in EAE model, treatment with Lovastatin - an inhibitor of HMGCR - significantly improved the disease severity and the demyelination¹³⁸. ID11 encodes a peroxisomally-localized enzyme that catalyzes the interconversion of isopentenyl diphosphate (IPP) to its highly electrophilic isomer, dimethylallyl diphosphate (DMAPP), which are the substrates for the successive reaction resulting in the synthesis of farnesyl diphosphate⁸⁶. About the MS context, RNA seq of spinal cord tissue from pEAE Biozzi ABH mice – animal model of secondary progressive MS – showed that ID11 gene is down-regulated¹³⁹. However, in our human study we have seen the opposite trend. SQLE gene encodes for Squalene Monooxygenase, which catalyzes the stereospecific oxidation of squalene to (S)-2,3-epoxysqualene. SC4MOL, also known as MSMO1 (Methylsterol Monooxygenase 1) is a protein coding gene and catalyzes the three-step monooxygenation required for the demethylation of 4,4-dimethyl and 4 α -methylsterols, which can be subsequently metabolized to cholesterol. It has been demonstrated that SC4MOL inhibition promote the oligodendrocytes formation, the glial cell type lost in MS¹⁴⁰. CYP51A1 (Cytochrome P450 Family 51 Subfamily A Member 1) encodes a member of the cytochrome P450 superfamily of enzymes. The cytochrome P450 proteins are monooxygenases which catalyze many reactions involved in drug metabolism and synthesis of cholesterol. As for SC4MOL, its inhibition is related to oligodendrocytes formation¹⁴⁰. SC5DL (Sterol-C5-Desaturase) encodes for the enzyme which catalyzes the conversion of lathosterol into 7-dehydrocholesterol and it plays a role in the last step of cholesterol biosynthesis. INSIG 1 gene encodes an endoplasmic reticulum membrane protein that regulates cholesterol metabolism, hence, it plays a role in the homeostasis of Cholesterol Biosynthesis process. Its regulation mechanism was described in the Introduction section of this thesis. The role of INSIG-1 in MS context has not been investigated, so the following data provide an additional information about its contribute in MS patients. Figures 36A and 36B correspond to the schemes of first and second part of cholesterol biosynthesis process, with the 1st one related to mevalonate/DMAPP production and the 2nd one related to the genes involved in the last phases of cholesterol production (Squalene pathway).

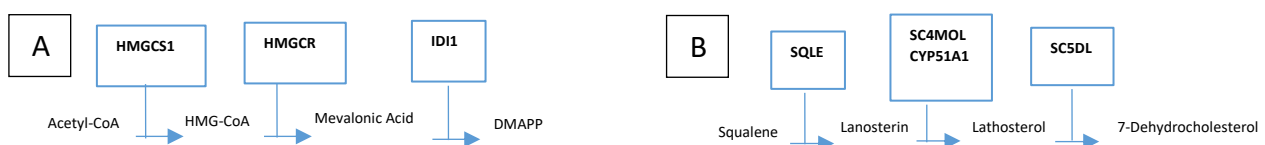


Figure 36. Schematic overview of Cholesterol Biosynthesis Process. A) Genes involved in the mevalonate/DMAPP pathway; B) Genes involved in the squalene pathway.

The Table 26 reports the main characteristics and the updated clinic data about cohort 1 MS patients tested for HMGCS1, HMGCR, IDI1, SQLE, SC4MOL, CYP51A1, SC5DL genes.

Table 26. Cohort 1 information.

Phenotype	Age	EDSS	Disease duration	Treatment	Comorbidity	Updated clinic (EDSS; relapses)
HC3						
HC11						
HC13						
HC32						
HC41	47					
HC30	47					
HC35	37					
HC38	38					
HC39	40					
HC40	49					
HC46	48					
HC57	41					
SMP16 (RR1)	28	1	4			1; rel: 2011
SMP27 (RR1)	58	6.5	16	IFN		8
SMP28 (RR1)	49	5	1			5; rel: 2011,2012,2013,2014
SMP29 (RR1)	50	2.5	2			1; rel: 2011,2012,2016
SMP24 (PP)	68	6	13	Eutirox	Hypothyroidism	6.5
SMP11 (RR2)	55	3	25		Hashimoto Thyroiditis	3; rel: 2011
SMP12 (RR2)	51	7	31	AZA, Mito		6,5
SMP13 (RR2)	22	0	6			1; rel: 2010,2016 (x2),2017
SMP17 (RR2)	43	6	10	AZA, Methotrexate	LES	6
SMP18 (RR2)	55	5.5	27	AZA	Hypertension	5.5; rel: 2016
SMP22 (RR2)	39	2.5	12	AZA, GA		7; rel: 2017

HC: Healthy controls; RR1: Relapsing Remitting 1; RR2: Relapsing Remitting 2; PP: Primary Progressive; SMP: Multiple Sclerosis Patient; EDSS: Expanded Disability Status Scale; IFN: Interferon beta; Mito: Mitoxantrone; AZA: Azathioprine; GA: Glatiramer Acetate; LES: Systemic Lupus Erythematosus; rel: relapse.

Since we were able to test only **1PP** of the cohort 1 (SMP24), it was not included in the statistical analyses, but its expression was reported as histogram in comparison to HCs subjects.

For the **HMGCS1, HMGCR, IDI1, SQLE, SC4MOL, CYP51A1, SC5SDL** genes were tested **12 HCs** (HC3, HC11, HC13, HC32, HC41, HC30, HC35, HC38, HC39, HC40, HC46, HC57), **4 RR1**

(SMP16, SMP27, SMP28, SMP29), **6 RR2** (SMP 11, SMP12, SMP13, SMP17, SMP18, SMP22), **1PP** (SMP24). The figures 37A and 37B represent the statistical analysis of the validated samples for the gene HMGCS1. Patient RR1 SMP28 has the most elevated induction among the RR1 patients, whereas SMP16 has the lower level (Fig.37A). PP patient SMP24 over-expressed the HMGCS1 gene in comparison to the mean of HCs tested (Fig.37B).

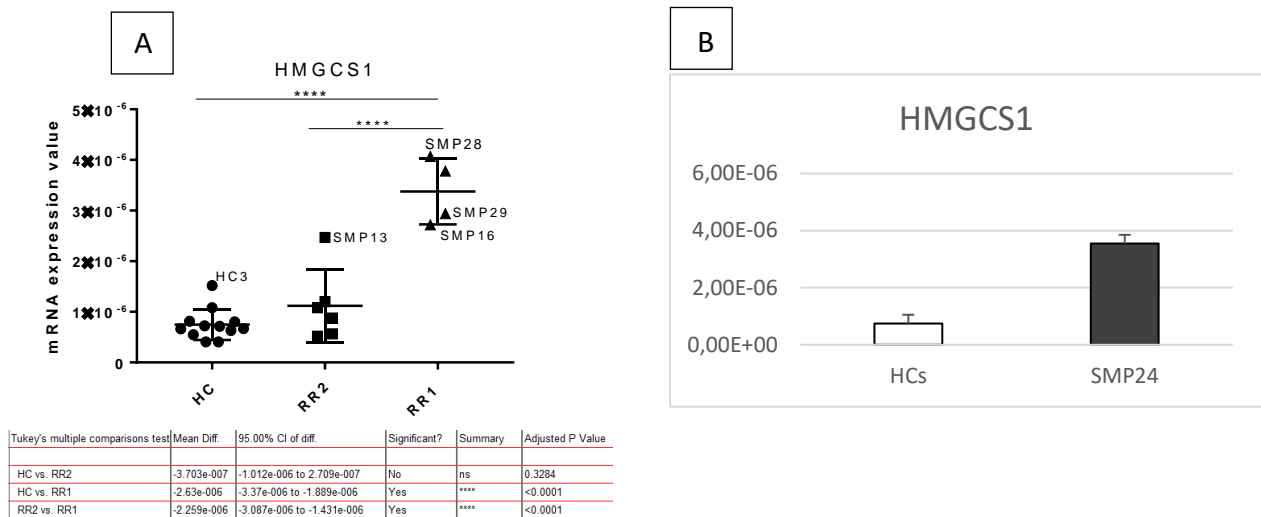


Figure 37. Statistical analysis of HMGCS1 in cohort 1 subjects. A) Dot plot of tested samples, B) Histogram obtained by the mean of each HC tested for HMGCS1, and SMP24 mRNA expression value. HCs, healthy controls; RR2: Relapsing Remitting 2; RR1: Relapsing Remitting 1; SMP: Multiple Sclerosis Patient. **** pV< 0.0001

For the **HMGCR** gene, it can be observed that two RR2 patients (SMP11 and SMP13) have a higher profile than the others. The same thing happens for the RR1 patients SMP16 and SMP28. On the other hand, the RR2 SMP18 and the RR1 SMP29 have the lower profiles (Fig.38A). It interesting to note that apparently SMP11 and SMP13 have important differences in terms of clinical data, both for age (55 vs 22) and disease duration (25 vs 6). PP SMP24 overexpresses the gene in comparison to the HCs (Fig.38 B).

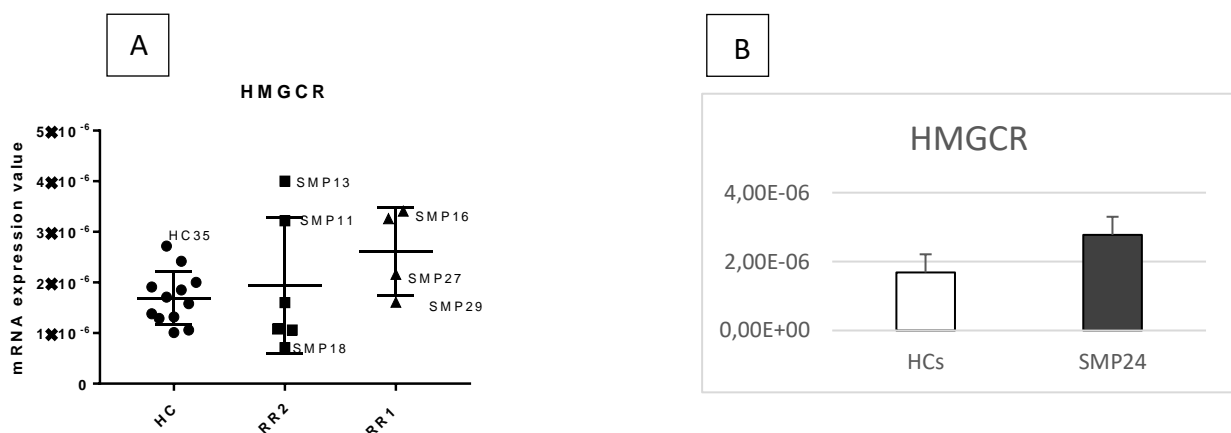


Figure 38. Statistical analysis of HMGCR in cohort 1 subjects. A) Dot plot of tested samples, B) Histogram obtained by the mean of each HC tested for HMGCR, and SMP24 mRNA expression value. HCs, healthy controls; RR2: Relapsing Remitting 2; RR1: Relapsing Remitting 1; SMP: Multiple Sclerosis Patient.

The Figures 39A represents the statistical analysis of the validated samples for **IDI1** gene. Figure 39B shows that PPMS patients overexpressed IDI1 gene, indicating that DMAPP accumulation could important for PPMS.

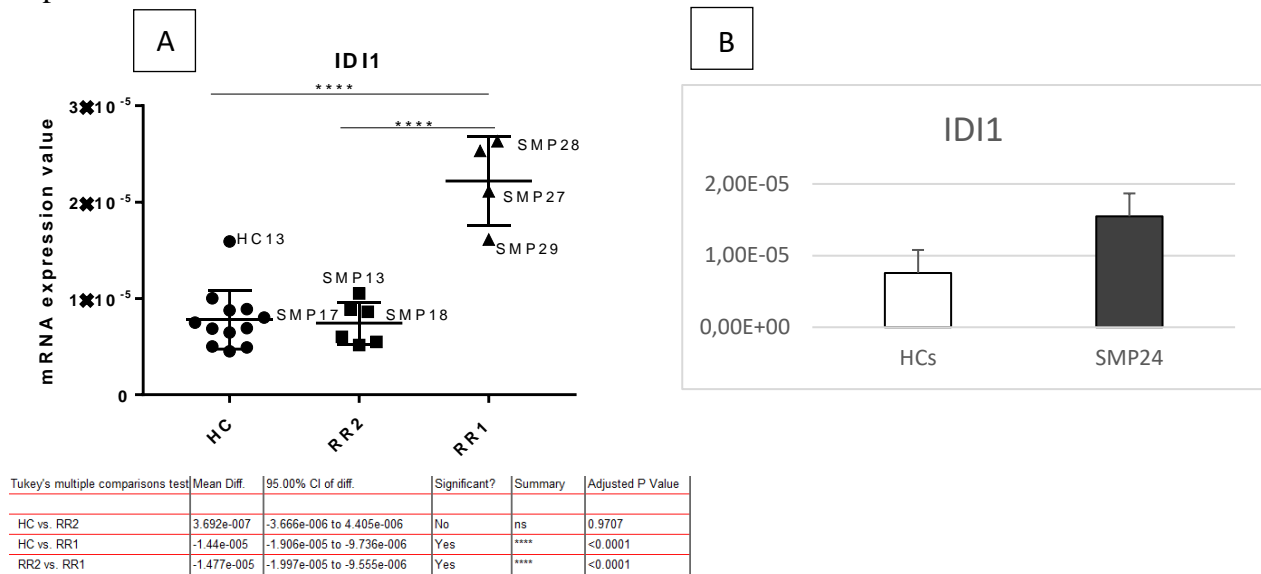


Figure 39. Statistical analysis of IDI1 in cohort 1 subjects. A) Dot plot of tested samples, B) Histogram obtained by the mean of each HC tested for IDI1, and SMP24 mRNA expression value. HCs, healthy controls; RR2: Relapsing Remitting 2; RR1: Relapsing Remitting 1; SMP: Multiple Sclerosis Patient. **** pV < 0.0001

The Figure 40 represents the statistical analysis of the validated samples for **SQLE** gene. The RR1 patient SMP28 has the highest expression profile (Fig.40A). The PP patient SMP24 over-expressed the gene (Fig.40B).

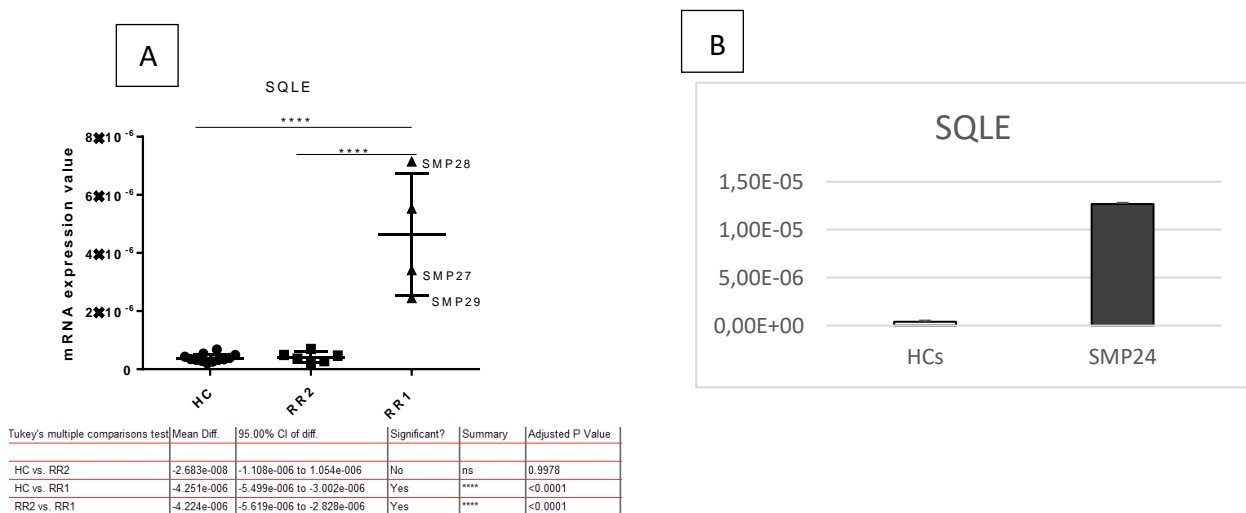


Figure 40. Statistical analysis of SQLE in cohort 1 subjects. A) Dot plot of tested samples, B) Histogram obtained by the mean of each HC tested for SQLE, and SMP24 mRNA expression value. HCs, healthy controls; RR2: Relapsing Remitting 2; RR1: Relapsing Remitting 1; SMP: Multiple Sclerosis Patient. **** pV < 0.0001

For the **SC4MOL** gene, both HCs and RR2 are homogeneous, as opposed to RR1 patients: SMP28

has the highest profile of induction, while SMP16 has the lowest one (Fig. 41A). SMP24 over-expresses also SC4MOL gene (Fig.41B).

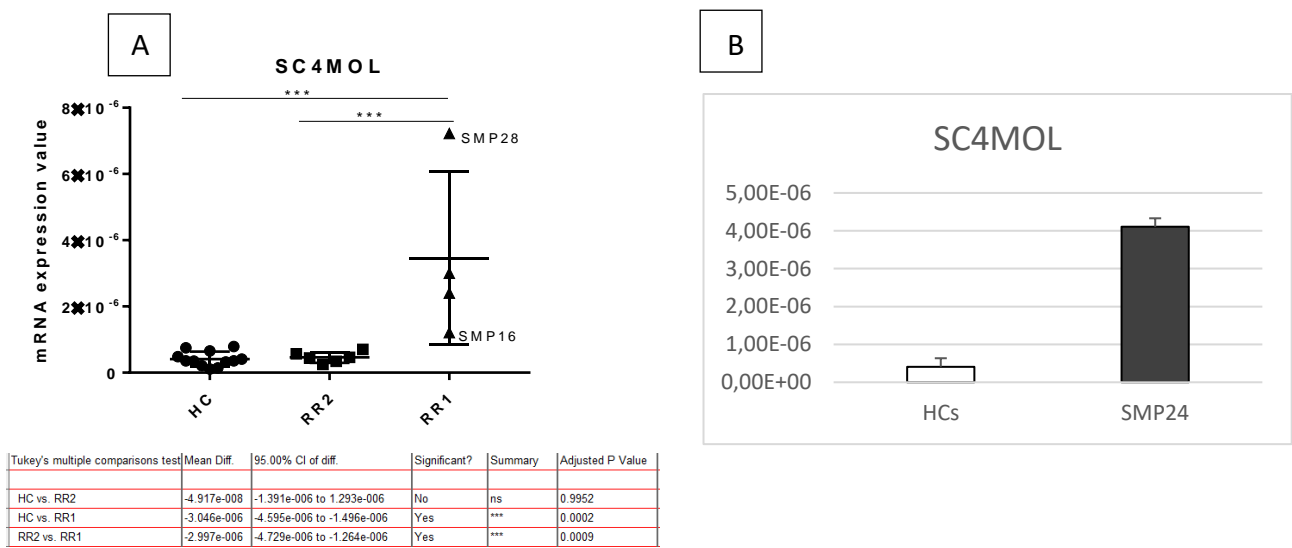


Figure 41. Statistical analysis of SC4MOL in cohort 1 subjects. A) Dot plot of tested samples, B) Histogram obtained by the mean of each HC tested for SC4MOL, and SMP24 mRNA expression value. HCs, healthy controls; RR2: Relapsing Remitting 2; RR1: Relapsing Remitting 1; SMP: Multiple Sclerosis Patient. **** pV < 0.0001.

CYP51A1 analysis shows that SMP28 is still the most upregulated for the RR1 (Fig.42A). SMP24 over-expresses CYP51A1 (Fig.42B).

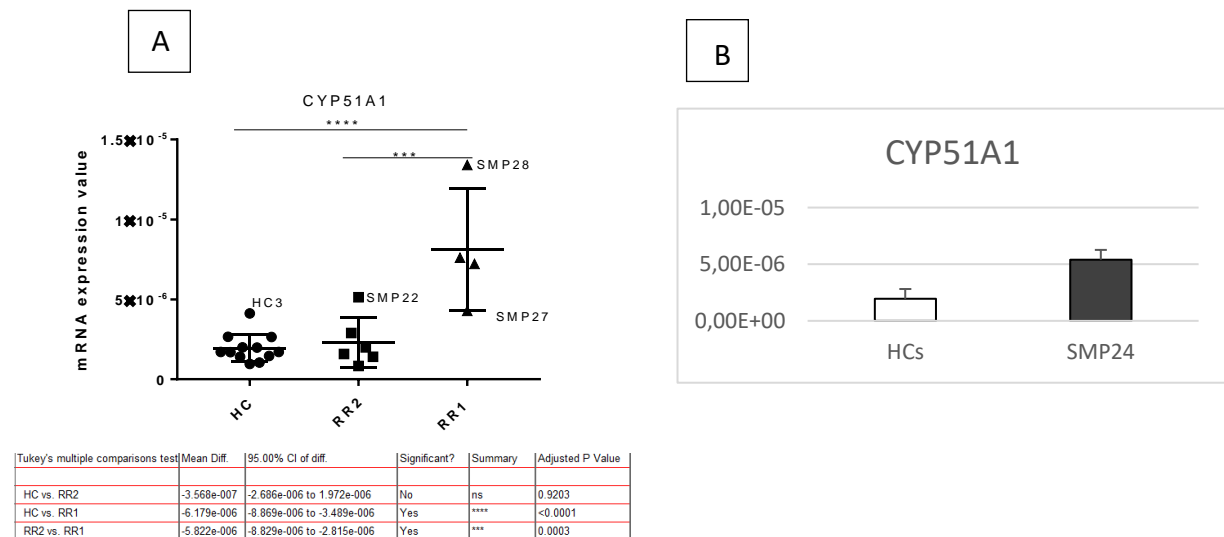


Figure 42. Statistical analysis of CYP51A1 in cohort 1 subjects. A) Dot plot of tested samples, B) Histogram obtained by the mean of each HC tested for CYP51A1, and SMP24 mRNA expression value. HCs, healthy controls; RR2: Relapsing Remitting 2; RR1: Relapsing Remitting 1; SMP: Multiple Sclerosis Patient. ***pV = 0.0003; **** pV < 0.0001

The HCs group is homogeneous for the SC5DL gene. Among the RR2, SMP13 is still the most induced, and also for RR1 the patients SMP27 and SMP28 have the higher profiles of induction.

Again, two different groups of RR1 patients are identified (Fig.43A). SMP24 over-expresses also this gene (Fig 43B).

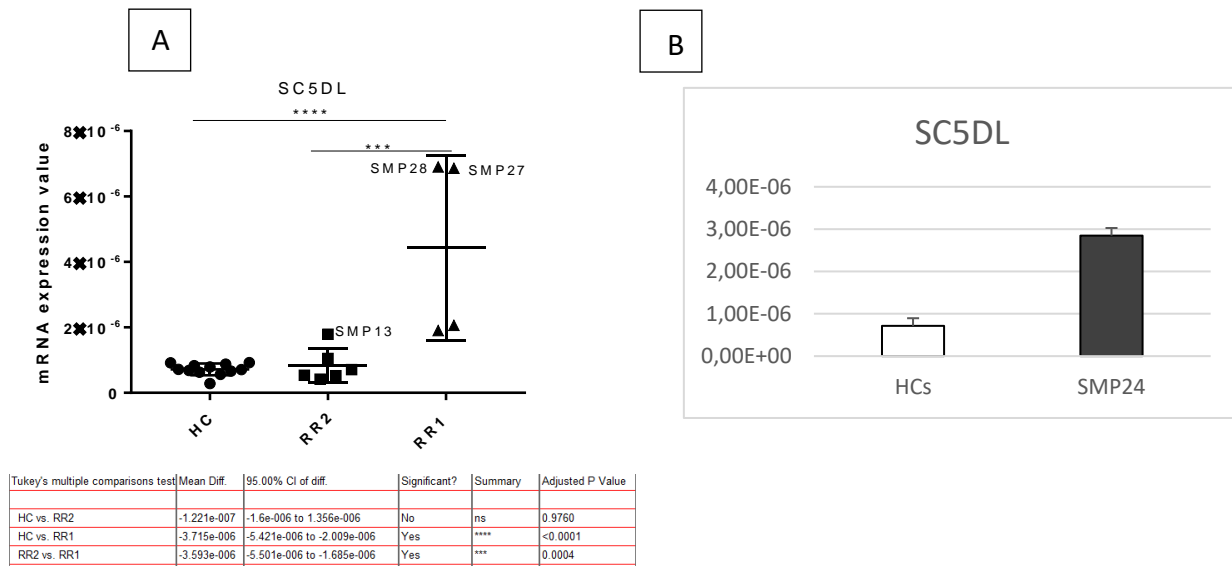


Figure 43. Statistical analysis of SC5DL in cohort 1 subjects. A) Dot plot of tested samples, B) Histogram obtained by the mean of each HC tested for SC5DL, and SMP24 mRNA expression value. HCs, healthy controls; RR2: Relapsing Remitting 2; RR1: Relapsing Remitting 1; SMP: Multiple Sclerosis Patient. ***pV =0.0004; **** pV< 0.0001

For the **INSIG1** gene were tested **9 HCs** (HC11, HC32, HC41, HC30, HC35, HC38, HC39, HC40, HC57), **4 RR1** (SMP16, SMP27, SMP28, SMP29), **6 RR2** (SMP 11, SMP12, SMP13, SMP17, SMP18, SMP22), **1PP** (SMP24). As observed until now, only the RR1 patients express high level of the analysed gene. In this case, the most induced RR1 is SMP28 and the lowest is SMP29 (Fig.44A). The PP patient SMP24 over-expresses INSIG-1 (Fig.44B).

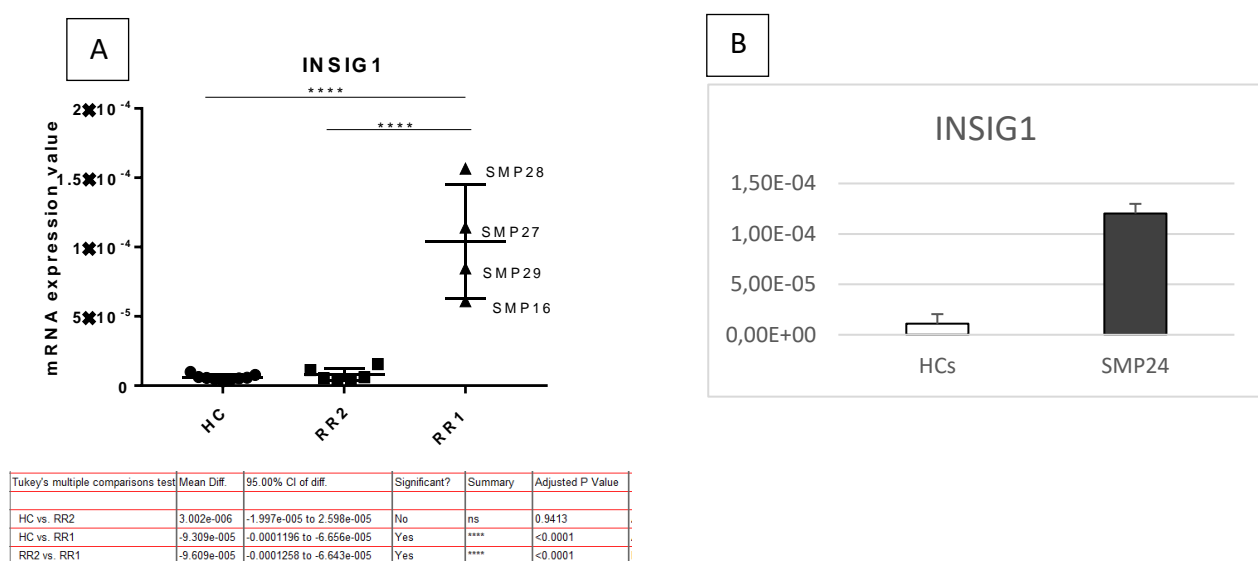


Figure 44. Statistical analysis of INSIG1 in cohort 1 subjects. A) Dot plot of tested samples, B) Histogram obtained by the mean of each HC tested for INSIG1, and SMP24 mRNA expression value. HCs, healthy controls; RR2: Relapsing Remitting 2; RR1: Relapsing Remitting 1; SMP: Multiple Sclerosis Patient. **** pV< 0.0001

Summary about the Cholesterol Biosynthesis genes expressed by cohort 1.

The Figures 45A and 45B represent the box plots of the Cholesterol Biosynthesis pathway divided into its two main parts. The first one provides the mevalonate production and DMAPP formation and involved the genes HMGCS1, HMGCR and IDI1; the second one ends with cholesterol production itself, and involves CYP51A1, SC5DL, SC4MOL and SQLE. The INSIG1 gene is not included since it is involved in the regulation of the cholesterol homeostasis.

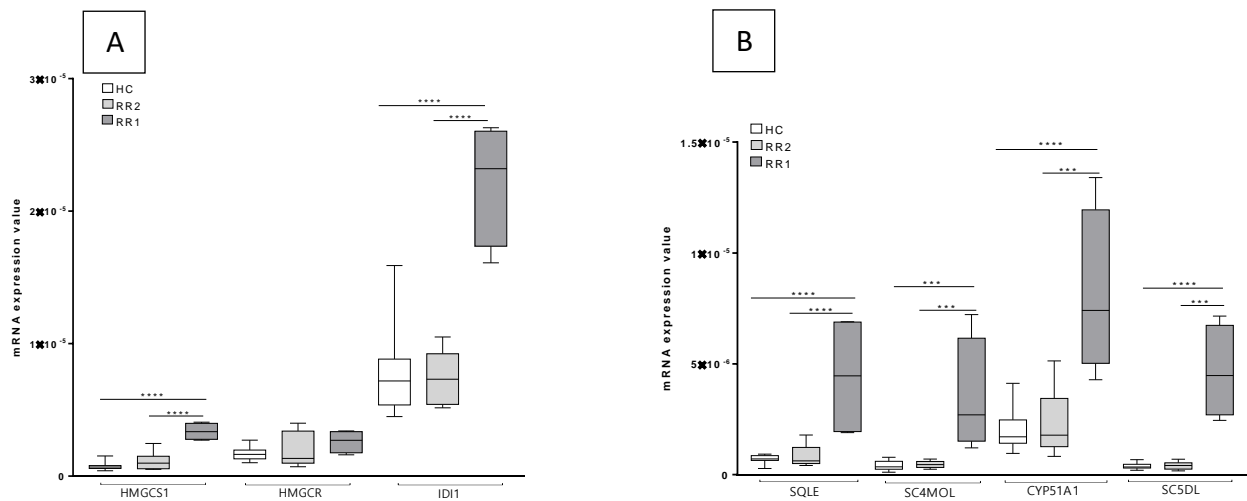


Figure 45. Trend of Cholesterol Biosynthesis genes on cohort 1 by dividing the pathway into its 2 parts. A) Genes related to the first part of Cholesterol Biosynthesis. B) Genes related to the second part of Cholesterol Biosynthesis. HC: healthy controls; RR2: Relapsing Remitting 2; RR1: Relapsing Remitting 1. ***pV<0.001; **** pV< 0.0001

The analysis clearly shows that the Cholesterol Biosynthesis pathway identifies a genetic signature that it is able to stratify RRMS into two functional groups named RR1 and RR2. The RR1 group is more similar to PPMS and the RR2 have an expression profiles for these genes that correlates with those of the HCs. The only gene that is not upregulated in this group of patients is the HMGCR gene.

Cholesterol Biosynthesis validation on cohort 2.

To verify whether the cholesterol gene signature was a general characteristic of MS, we tested the genetic pathway in cohort 2 subjects.

The Table 27 reports the main characteristics and the updated clinic data about cohort 2 MS patients tested for HMGCS1, HMGCR, IDI1, SQLE, SC4MOL, CYP51A1, SC5DL genes.

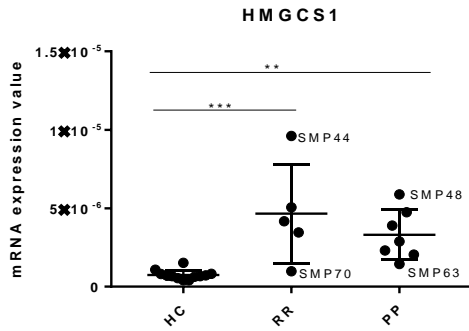
Table 27. Cohort 2 information

Phenotype	Age	EDSS	Disease duration	Treatment	Comorbidity	Updated clinic (EDSS; relapses)
HC3						
HC11						
HC13						
HC32						
HC41	47					
HC30	47					
HC35	37					
HC38	38					
HC39	40					
HC40	49					
HC46	48					
SMP44 (RR)	50	1	6	NA		1
SMP59 (RR)	49	6.5	25	IFN, GA		8; rel: 2009,2010,2011,2013
SMP69 (RR)	40	1.5	14	IFN, GA		2.5; rel: 2013,2017
SMP70 (RR)	44	1	6	IFN	Endometriosis, Hypertension	4.5; rel: 2013 (x2), 2014, 2017
SMP71 (RR)	42	1	16	NA		3; rel: 2012,2013
SMP47 (PP)	52	6	5	Vit D	Epilepsy	7.5
SMP48 (PP)	47	5	9	Depakin, Vin-pat	Epilepsy	6; rel: 2015
SMP51 (PP)	59	7	30	NA		8
SMP63 (PP)	55	7.5	16	NA		7.5
SMP65 (PP)	64	7.5	14	NA		8
SMP66 (PP)	63	6.5	39	Bacoflen, Amantadina		6.5
SMP68 (PP)	56	7	7	AZA	Raynaud Syndrome	7

HC: Healthy controls; RR: Relapsing Remitting; PP: Primary Progressive; SMP: Multiple Sclerosis Patient; EDSS: Expanded Disability Status Scale; IFN: Interferon beta; Mito: Mitoxantrone; AZA: Azathioprine; GA: Glatiramer Acetate; LES: Systemic Lupus Erythematosus; rel: relapse.

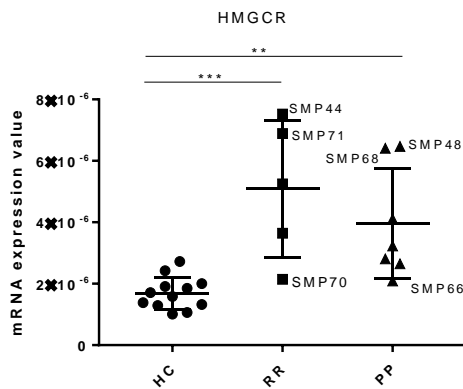
For the **HMGCS1**, **HMGCR**, **IDI1**, **SQLE**, **SC4MOL**, **CYP51A1**, **SC5DL** genes were tested **12 HCs** (HC3, HC11, HC13, HC32, HC41, HC30, HC35, HC38, HC39, HC40, HC46, HC57), **5 RR** (SMP44, SMP59, SMP69, SMP70, SMP71), **7 PP** (SMP47, SMP48, SMP51, SMP63, SMP65, SMP66, SMP68).

The Figure 46 represents the statistical analysis of the validated samples for **HMGCS1** gene. Both RR and PP patients significantly expressed HMGCS1, nevertheless the RR SMP44 patient expresses higher levels of this gene within the RR group.



Tukey's multiple comparisons test	Mean Diff.	95.00% CI of diff.	Significant?	Summary	Adjusted P Value
HC vs. RR	-3.905e-006	-6.1e-006 to -1.711e-006	Yes	***	0.0006
HC vs. PP	-2.562e-006	-4.523e-006 to -6.015e-007	Yes	**	0.0093
RR vs. PP	1.343e-006	-1.07e-006 to 3.757e-006	No	ns	0.3575

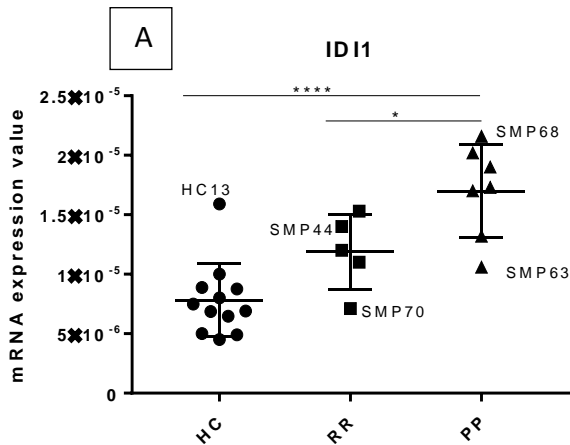
Figure 46. Statistical analysis of HMGS1 in cohort 2 subjects. Dot plot of tested samples. HC: healthy controls; RR: Relapsing Remitting; PP: Primary Progressive; SMP: Multiple Sclerosis Patient. **pV=0.009; ***pV= 0.0006
HMGCR is significantly over expressed by both RR and PP subjects with SMP44 expressing again the highest mRNA expression value, while SMP70 the lowest. On the contrary, PP patients could be divided into those that express high level of HMGCR gene and those that express lower levels. In particular SMP48 and SMP68 have the highest profiles and SMP66 the lowest (Fig. 47).



Tukey's multiple comparisons test	Mean Diff.	95.00% CI of diff.	Significant?	Summary	Adjusted P Value
HC vs. RR	-3.401e-006	-5.307e-006 to -1.494e-006	Yes	***	0.0006
HC vs. PP	-2.28e-006	-3.983e-006 to -5.763e-007	Yes	**	0.0077
RR vs. PP	1.121e-006	-9.762e-007 to 3.218e-006	No	ns	0.3858

Figure 47. Statistical analysis of HMGCR in cohort 2 subjects. Dot plot of tested samples. HC: healthy controls; RR: Relapsing Remitting; PP: Primary Progressive; SMP: Multiple Sclerosis Patient. **pV=0.007; ***pV= 0.0006

ID11 gene is significantly induced in RRMS and PPMS from cohort 2, especially by SMP44 (Fig. 48).

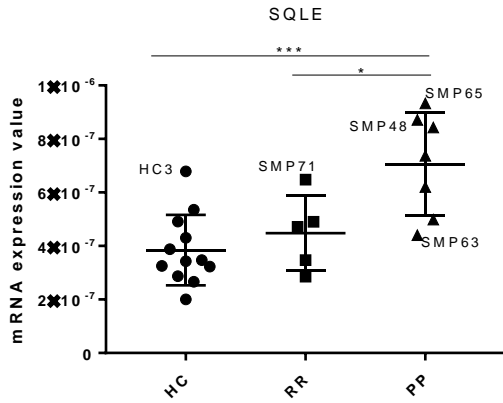


Tukey's multiple comparisons test	Mean Diff.	95.00% CI of diff.	Significant?	Summary	Adjusted P Value
HC vs. RR	-4.08e-006	-8.556e-006 to 3.966e-007	No	ns	0.0783
HC vs. PP	-9.182e-006	-1.318e-005 to -5.182e-006	Yes	****	<0.0001
RR vs. PP	-5.102e-006	-1.003e-005 to -1.775e-007	Yes	*	0.0414

Figure 48. Statistical analysis of ID11 in cohort 2 subjects. Dot plot of tested samples. HC: healthy controls; RR: Relapsing Remitting; PP: Primary Progressive; SMP: Multiple Sclerosis Patient.

*pV<0.05; ****pV< 0.0001

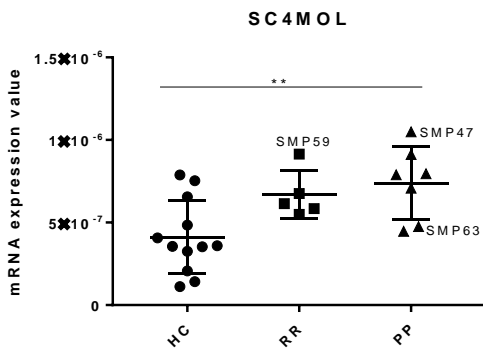
SQL gene is significantly expressed on PPMS but not in RRMS suggesting that the RRMS patients from cohort 2 shows a different regulation of this pathways in monocytes (Fig.49).



Tukey's multiple comparisons test	Mean Diff.	95.00% CI of diff.	Significant?	Summary	Adjusted P Value
HC vs. RR	-6.37e-008	-2.685e-007 to 1.411e-007	No	ns	0.7168
HC vs. PP	-3.216e-007	-5.046e-007 to -1.386e-007	Yes	***	0.0007
RR vs. PP	-2.579e-007	-4.832e-007 to -3.264e-008	Yes	*	0.0231

Figure 49. Statistical analysis of SQL in cohort 2 subjects. Dot plot of tested samples. HC: healthy controls; RR: Relapsing Remitting; PP: Primary Progressive; SMP: Multiple Sclerosis Patient. *pV=0.02; ****pV=0.0007

For the **SC4MOL** gene, out of the RR patients, SMP59 expresses the gene at higher level than the others; while for the PP the most deregulated for SC4MOL seems to be SMP47. Again, SMP63 expresses the lowest levels (Fig.50). Hence, The SCA4MOL gene is significantly upregulated in PPMS and RRMS although at lower level compared to cohort 1 subjects.



Tukey's multiple comparisons test	Mean Diff.	95.00% CI of diff.	Significant?	Summary	Adjusted P Value
HC vs. RR	-2.556e-007	-5.359e-007 to 2.476e-008	No	ns	0.0782
HC vs. PP	-3.279e-007	-5.784e-007 to -7.741e-008	Yes	**	0.0092
RR vs. PP	-7.231e-008	-3.807e-007 to 2.361e-007	No	ns	0.8264

Figure 50. Statistical analysis of SC4MOL in cohort 2 subjects. Dot plot of tested samples. HC: healthy controls; RR: Relapsing Remitting; PP: Primary Progressive; SMP: Multiple Sclerosis Patient. **pV=0.009

For the **CYP51A1** gene, as observed for the other genes, SMP44 has the highest profile and SMP70 the lowest among the RR. And again, SMP48 has the highest profile and SMP63 the lowest among the PP (Fig.51).

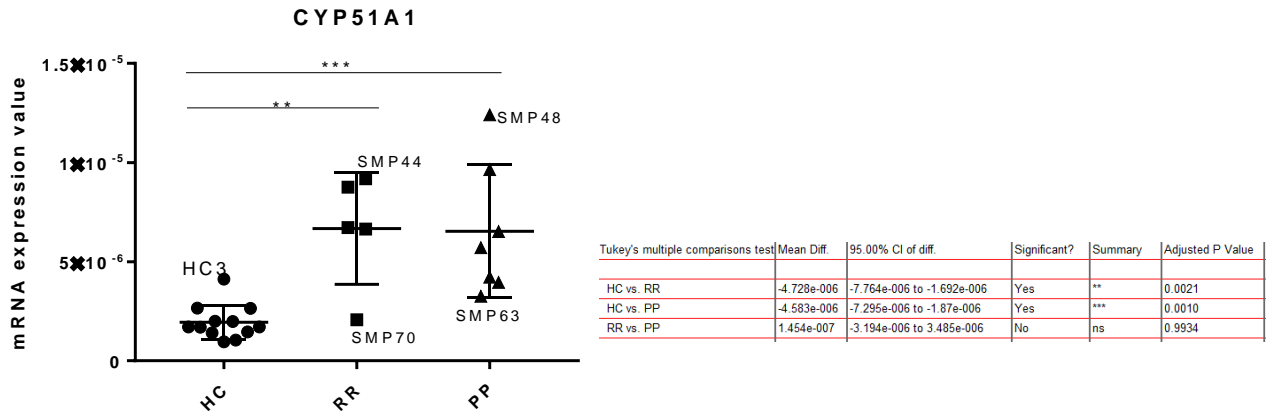


Figure 51. Statistical analysis of CYP51A1 in cohort 2 subjects. Dot plot of tested samples. HC: healthy controls; RR: Relapsing Remitting; PP: Primary Progressive; SMP: Multiple Sclerosis Patient. **pV=0.002; ***pV= 0.001

SC5DL expression in the RR patients is heterogeneous, with SMP44 presenting the highest profile of induction and SMP70 the lowest. The same for the PP group: SMP48 expresses SC5DL at higher levels than the others while SMP47 and SMP63 express the lowest levels. (Fig.52).

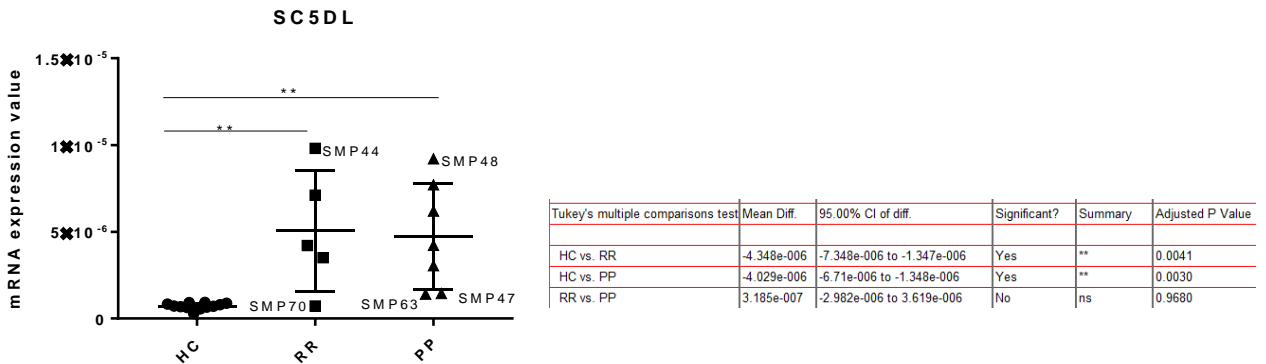


Figure 52. Statistical analysis of SC5DL in cohort 2 subjects. Dot plot of tested samples. HC: healthy controls; RR: Relapsing Remitting; PP: Primary Progressive; SMP: Multiple Sclerosis Patient. **pV<0.005

For the **INSIG1** gene were tested **9 HCs** (HC11, HC32, HC41, HC30, HC35, HC38, HC39, HC40, HC57), **5 RR** (SMP44, SMP59, SMP69, SMP70, SMP71), **7 PP** (SMP47, SMP48, SMP51, SMP63, SMP65, SMP66, SMP68). The figure 53 represents the statistical analysis of the validated samples. Concerning RR patients, the most deregulated is the SMP71, while for the PP patients is the SMP48.

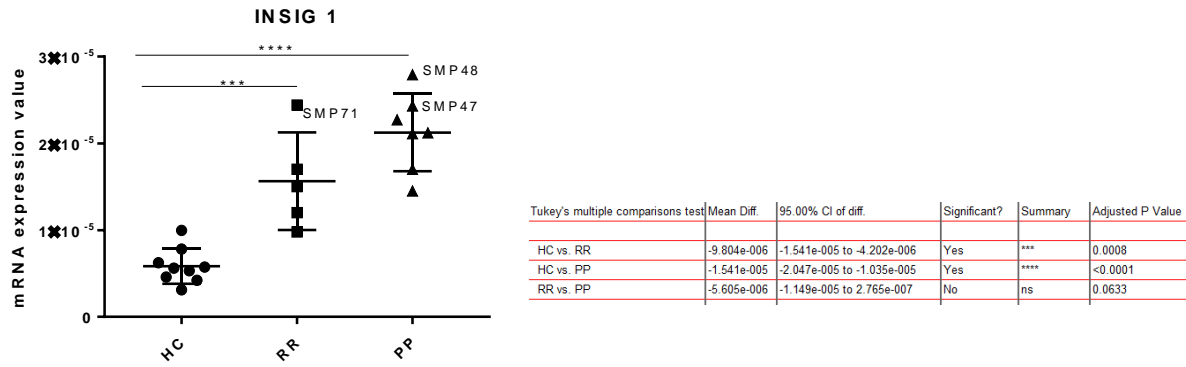


Figure 53. Statistical analysis of INSIG1 in cohort 2 subjects. Dot plot of tested samples. HCs, healthy controls; RR2: Relapsing Remitting 2; RR1: Relapsing Remitting 1; SMP: Multiple Sclerosis Patient. ****pV < 0.0001

Summary about the Cholesterol Biosynthesis genes expressed by cohort 2.

Just below is possible to observe the trend of the cohort 2 for both the first and the second part of Cholesterol Biosynthesis pathway (Fig. 54A and 54B). Again, INSIG-1 was not included into the box plot since it is involved into regulatory mechanisms of Cholesterol's homeostasis.

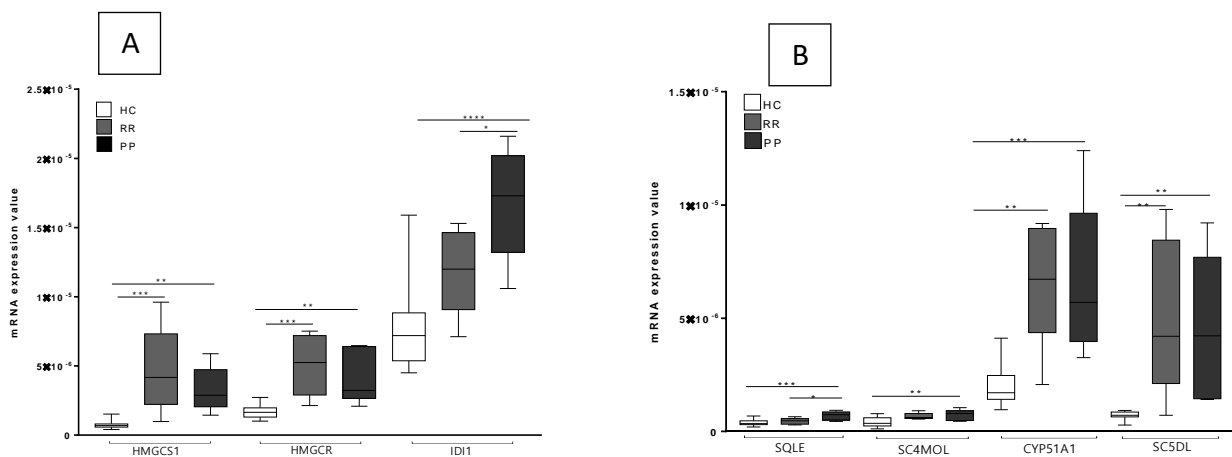


Figure 54. Trend of Cholesterol Biosynthesis genes on cohort 2 by dividing the pathway into its 2 parts. A) Genes related to the first part of Cholesterol Biosynthesis. B) Genes related to the second part of Cholesterol Biosynthesis. HC: healthy controls; RR2: Relapsing Remitting 2; RR1: Relapsing Remitting 1. *pV < 0.5; ** pV < 0.01; ***pV<0.001; **** pV< 0.0001

Analysis of the Cholesterol Biosynthesis pathway in the cohort 2 revealed that the RR resemble more the RR1 phenotype of cohort 1. The data on PP are in line with those of cohort 1 suggesting the Cholesterol pathway is generally dysregulated in PP patients. Moreover, two genes of the Squalene pathway, namely SQLE and SC4MOL are less expressed in both RR and PP from cohort 2. The functional role or this discrepancy need to be further investigated.

Interestingly the regulatory gene INSIG1 is well regulated in RR1 from cohort 1 whereas is overexpressed by both RR and PP from cohort 2 again suggesting again that monocytes from RR patients from cohort 2 are more activated compared to RR2 monocytes from cohort 1. Therefore, we

can conclude that by using a cholesterol signature we are able to stratify RR patients based on peripheral blood monocyte profiles.

Since the cholesterol pathway is reported to be essential for activation and/or amplification of the Trained Immunity phenotype¹⁰⁸, we suggest that the enhance activatory profiles observed in PPMS and RR1 patients of both cohort 1 and cohort 2 could be sustained by this molecular mechanism. Therefore, we suggest that the inhibition of the cholesterol biosynthesis pathway in MS is thus potentially relevant at least in those patients (RR1 and PP) where Trained Immunity may play a role.

6. MS TESTED SERA OVER-EXPRESS THE oxLDL IN COMPARISON TO THE HCS

Microarray analysis suggested that MS monocytes are activated in a subgroup of PP and RR patients. In addition, the qRT-PCR validation confirmed this trend showing the deregulation of Cholesterol Biosynthesis genes. It was particularly interesting to observe that the modulated pathways were those resembling a Trained Immunity phenotype¹⁴¹ recently described. Since Trained Immunity could be induced by oxLDL, we hypothesized that oxLDL was present in our samples, hence it has been tested whether oxLDL was actually present.

Sera of **16 HCs** (HC3, HC11, HC13, HC27, HC29, HC30, HC32, HC33, HC31, HC34, HC36, HC37, HC39, HC40, HC46, HC47), **6RR** (SMP59, SMP70, SMP71, SMP72, SMP73, SMP74) and **6PP** (SMP47, SMP51, SMP63, SMP65, SMP66, SMP68) female subjects of the cohort 2 patients were analyzed by performing the ELISA test. The Table 28 reports the main characteristics and the updated clinic data about female subjects.

Table 28: Female MS patients and female HCs tested for oxLDL detection.

Phenotype	Age	EDSS	Disease duration	Treatment	Comorbidity	Updated clinic (EDSS; relapses)
HC3						
HC11						
HC13						
HC27						
HC29						
HC30	47					
HC32	44					
HC33	44					
HC31	49					
HC34	34					
HC36	48					
HC37	41					

HC39	40					
HC40	49					
HC46	48					
HC47						
SMP59 (RR)	49	6,5	25	IFN, GA		8; rel: 2009,2010,2011,2013
SMP70 (RR)	44	1	6	IFN	Endometriosis, Hypertension	4.5; rel: 2013 (x2), 2014, 2017
SMP71 (RR)	42	1	16	NA		3; rel: 2012,2013
SMP72 (RR)	58	6.5	36	Gabapentin, Clonazepam		
SMP73 (RR)	50	2.5	12	IFN, GA		
SMP74 (RR)	42	6	24	IFN, GA, AZA, Mitoxantrone		
SMP47 (PP)	52	6	5	Vit D	Epilepsy	7.5
SMP48 (PP)	47	5	9	Depakin, Vinpat	Epilepsy	6; rel: 2015
SMP51 (PP)	59	7	30	NA		8
SMP63 (PP)	55	7.5	16	NA		7.5
SMP65 (PP)	64	7.5	14	NA		8
SMP66 (PP)	63	6.5	39	Bacoflen, Amantadina		6.5
SMP68 (PP)	56	7	7	AZA	Raynaud Syndrome	7

HC: Healthy controls; RR: Relapsing Remitting; PP: Primary Progressive; SMP: Multiple Sclerosis Patient; EDSS: Expanded Disability Status Scale; IFN: Interferon beta; Mito: Mitoxantrone; AZA: Azathioprine; GA: Glatiramer Acetate; LES: Systemic Lupus Erythematosus; rel: relapse.

In addition, were tested sera from male patients: **8HCs** (HC8, HC12, HC17, HC25, HC42, HC44, HC55) and **4PP** (SMP8, SM9, SMP19, SMP20). The Table 29 report the main characteristics and the updated clinic data about female subjects.

Table 29. Male MS patients and male HCs tested for oxLDL detection.

Phenotype	Age	EDSS	Disease duration	Treatment	Comorbidity	Updated clinic (EDSS; relapses)
HC8						
HC12						
HC17						
HC25						
HC42	40					
HC44						
HC55						
SMP8	52	7.5	12	IFN		
SMP9	51	7	16	Mito		
SMP19	45	6	3			
SMP20	55	6	12			

HC: Healthy controls; PP: Primary Progressive; SMP: Multiple Sclerosis Patient; EDSS: Expanded Disability Status Scale; IFN: Intereferon beta; Mito: Mitoxantrone.

All tested patients have higher oxLDL levels than HCs, in particular in RR patients SMP59 and in PP SMP51, SMP63 and SMP47. This experiment was performed by dividing MS samples based on sex (Fig.55A and Fig.55B). As shown, all the female MS patients have elevated level of oxLDL concentration in their blood, whereas only two out of four male PP patients have oxLDL overexpression.

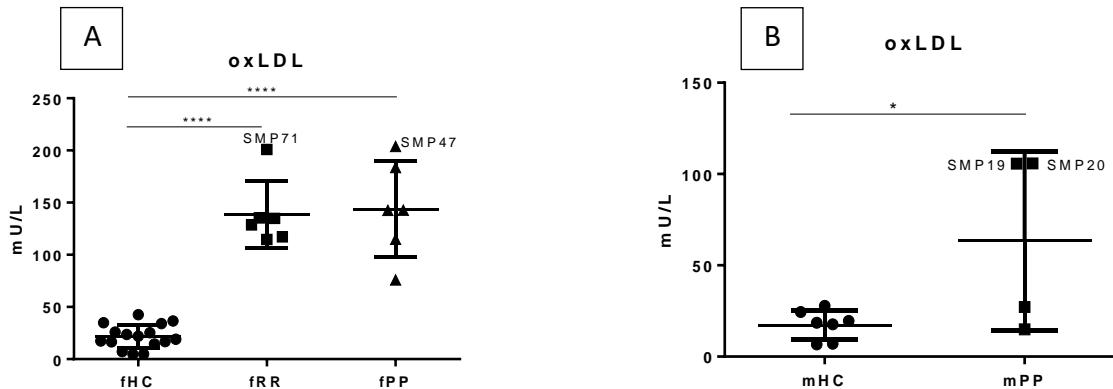


Figure 55. oxLDL in sera was detected through ELISA assay. A) female RR and PP patients have higher oxLDL level in sera in comparison to HCs subjects. B) male PP patients have higher oxLDL level in sera in comparison to HCs. **** $pV < 0.0001$

Summary about oxLDL detection.

Both RR and PP female over-express the oxLDL, in particular SMP71 and SMP63. This is in line with their trends observed during qRT-PCR validation. The male subjects, instead, are divided into two subgroups: SMP19 and SMP20 over-express the oxLDL, whereas the other two subjects do not. The clinical data do not explain this opposite trend.

6.1. CHARACTERIZATION OF RECEPTOR THAT MAY MEDIATE THE oxLDL UPTAKE

Since different scavenger receptors are able to recognize oxLDL, we tested the following putative receptors: CD36, SR-A and OLR1. CD36 is an innate immune receptor expressed in endothelial cells and microglia/macrophages cells. CD36 was poorly investigated in this specific context; however an important support to this topic comes from studies on Alzheimer's Disease (AD). In fact, it has been shown that AD patients have higher expression of CD36 in the cerebral cortex, whereas peripheral expression of CD36 was significantly reduced in AD patients¹⁴². It may suggest that the CD36 lower peripheral expression correlates with its accumulation in the CNS during neurodegenerative disease. The class A scavenger receptor (SRA), constitutively expressed by macrophages and dendritic cells in peripheral tissues and the CNS, seems to play a role in the phagocytosis of myelin¹⁴³. Nevertheless, its specific role in EAE development and in an autoimmune reaction in the periphery need further investigation. In a genome-wide approach aimed to study gene expression in rim and perilesional regions of chronic active and inactive MS lesions, the gene OLR1 resulted as one of the most induced

in active regions, accompanied by the presence of foamy macrophages¹⁴⁴. Taken together, all these results suggest that the lipid uptake in MS context might play a fundamental role.

The Table 30 report the main characteristics and the updated clinic data about cohort 1 MS patients tested for CD36, SR-A and OLR1 genes.

Table 30. Cohort 1 information

Pheno-type	Age	EDSS	Disease duration	Treatment	Comorbidity	Updated clinic (EDSS; relapses)
HC3						
HC11						
HC27						
HC29						
HC32	44					
HC52	40					
HC01	28					
HC02	36					
HC03	55					
HC04	40					
HC05	48					
HC10	49					
HC11N	49					
HC13N	41					
HC14	43					
SMP16 (RR1)	28	1	4			1; rel: 2011
SMP27 (RR1)	58	6,5	16	IFN		8
SMP28 (RR1)	49	5	1			5; rel: 2011,2012,2013,2014
SMP29 (RR1)	50	2,5	2			1; rel: 2011,2012,2016
SMP24 (PP)	68	6	13	Eutirox	Hypothyroidism	6,5
SMP11 (RR2)	55	3	25		Hashimoto Thyroiditis	3; rel: 2011
SMP12 (RR2)	51	7	31	AZA, Mito		6,5
SMP13 (RR2)	22	0	6			1; rel: 2010,2016 (x2),2017
SMP17 (RR2)	43	6	10	AZA, Methotrexate	LES	6
SMP18 (RR2)	55	5,5	27	AZA	Hypertension	5,5; rel: 2016
SMP22 (RR2)	39	2,5	12	AZA, GA		7; rel: 2017

HC: Healthy controls; RR1: Relapsing Remitting 1; RR2: Relapsing Remitting 2; PP: Primary Progressive; EDSS: Expanded Disability Status Scale; IFN: Interferon beta; Mito: Mitoxantrone; AZA: Azathioprine; GA: Glatiramer Acetate; LES: Systemic Lupus Erythematosus; rel: relapse.

Since we were able to test only **1PP** of the cohort 1 (SMP24), it was not included in the statistical analyses, but its expression was reported as histogram in comparison to HCs subjects.

For **CD36** were tested **15 HCs** (HC3, HC11, HC27, HC29, HC32, HC52, HC01, HC02, HC03, HC04, HC05, HC10, HC11, HC13, HC14); **6 RR2** (SMP11, SMP12, SMP13, SMP17, SMP18, SMP22); **4 RR1** (SMP16, SMP27, SMP28, SMP29), **1PP** (SMP24). The Figures 56A and 56B represent the statistical analysis of the validated samples. In general, CD36 is not expressed in PPMS and RRMS samples from cohort 1. Nevertheless, two RR2 SMP11 and SMP17 subjects express high levels of CD36 (Fig. 56A). The clinic data suggested that patient SMP11 had relapses over time, while patient SMP17 presented comorbidity (LES). SMP24 over-expresses the gene (Fig.56B).

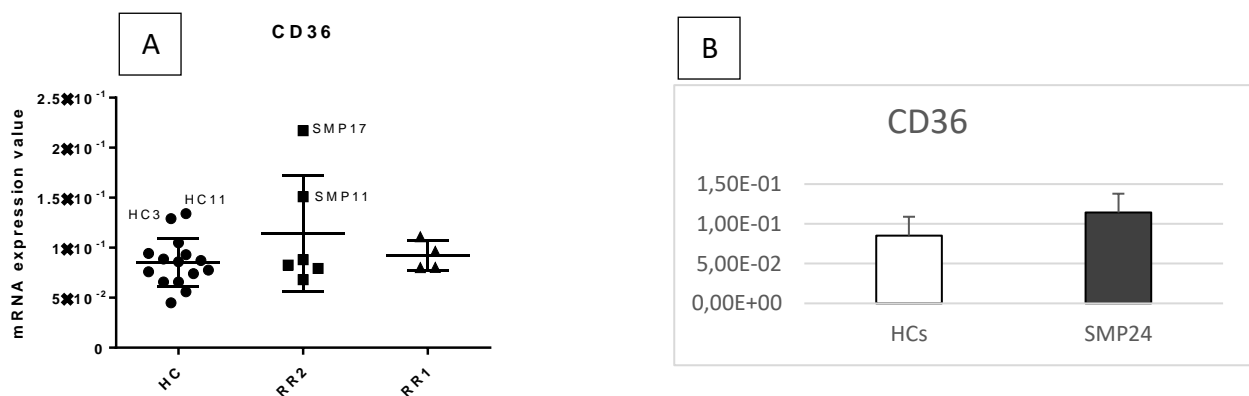


Figure 56. Statistical analysis of CD36 in cohort 1 subjects. A) Dot plot of tested samples, B) Histogram obtained by the mean of each HC tested for CD36, and SMP24 mRNA expression value
 HCs, healthy controls; RR2: Relapsing Remitting 2; RR1: Relapsing Remitting 1; SMP: Multiple Sclerosis Patient.

For the SR-A **12 HC** were tested (HC3, HC11, HC27, HC29, HC32, HC52, HC01, HC02, HC03, HC04, HC05, HC13); **6 RR2** (SMP11, SMP12, SMP13, SMP17, SMP18, SMP22); **4 RR1** (SMP16, SMP27, SMP28, SMP29), **1PP** (SMP24). The Figures 57A and 57B represent the statistical analysis of the validated samples. The SR-A is significantly expressed in SMP24 (Fig.57B) and in RR1 patients with the exception of SMP16 patient, who do not express the gene (Fig.57A). In RR2 samples, SR-A expression do not reached the significant level compared to the HCs subjects, therefore we conclude that SR-A is not expressed in the RR2MS patients.

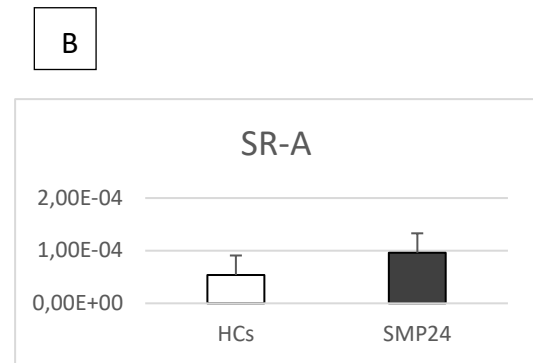
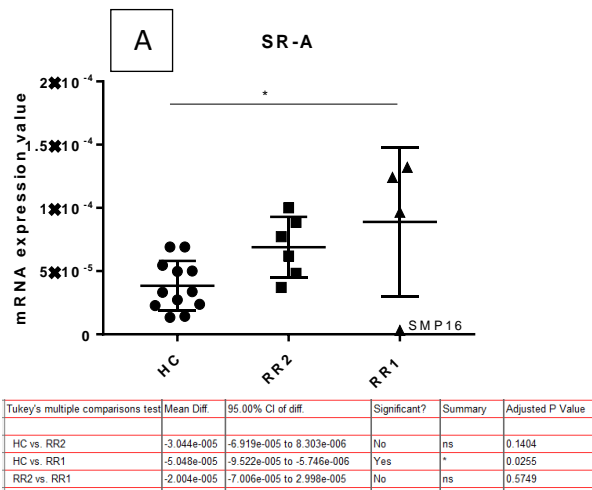


Figure 57. Statistical analysis of SR-A in cohort 1 subjects. A) Dot plot of tested samples, B) Histogram obtained by the mean of each HC tested for SR-A, and SMP24 mRNA expression value
 HCs, healthy controls; RR2: Relapsing Remitting 2; RR1: Relapsing Remitting 1; SMP: Multiple Sclerosis Patient.
 *pV=0.01; ** pV=0.008; ***pV<0.0001

For the **OLR-1** gene were tested **15 HCs** (HC3, HC11, HC27, HC29, HC32, HC52, HC01, HC02, HC03, HC04, HC05, HC10, HC11, HC13, HC14); **6 RR2** (SMP11, SMP12, SMP13, SMP17, SMP18, SMP22); **4 RR1** (SMP16, SMP27, SMP28, SMP29), **1PP** (SMP24). The expression of the OLR1 gene is not induced in RR2 and HCs whereas is upregulated in RR1 patients from cohort 1 although at variable expression levels (Fig.58A), and in the PP SMP24 (Fig.58B).

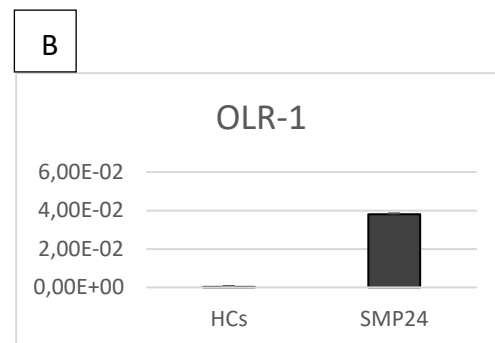
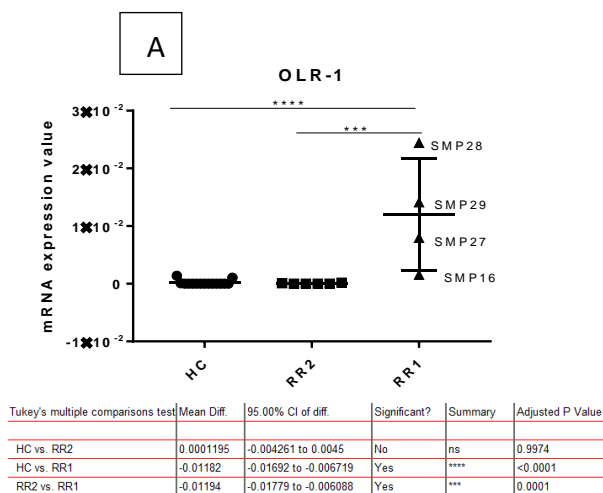


Figure 58. Statistical analysis of OLR-1 in cohort 1 subjects. A) Dot plot of tested samples, B) Histogram obtained by the mean of each HC tested for OLR-1, and SMP24 mRNA expression value
 HCs, healthy controls; RR2: Relapsing Remitting 2; RR1: Relapsing Remitting 1; SMP: Multiple Sclerosis Patient.
 pV=0.0001; *pV<0.0001

CD36, SR-A and OLR1 were additionally tested on MS samples from cohort 2.

To verify whether CD36, SR-A and OLR-1 were indeed overexpressed in MS monocytes, we tested their upregulation on RR and PP samples derived from cohort 2.

The Table 31 reports the main characteristics and the updated clinic data about cohort 2 MS patients tested for CD36, SR-A and OLR1 genes.

Table 31. Cohort 2 information

Phenotype	Age	EDSS	Disease duration	Treatment	Comorbidity	Updated clinic (EDSS; relapses)
HC3						
HC11						
HC27						
HC29						
HC32	44					
HC52	40					
HC01	28					
HC02	36					
HC03	55					
HC04	40					
HC05	48					
HC10	49					
HC11N	49					
HC13N	41					
HC14	43					
SMP44 (RR)	50	1	6	NA		1
SMP59 (RR)	49	6.5	25	IFN, GA		8; rel: 2009,2010,2011,2013
SMP69 (RR)	40	1.5	14	IFN, GA		2.5; rel: 2013,2017
SMP70 (RR)	44	1	6	IFN	Endometriosis, Hypertension	4.5; rel: 2013 (x2), 2014, 2017
SMP71 (RR)	42	1	16	NA		3; rel: 2012,2013
SMP72 (RR)	58	6.5	36	Gabapentin, Clonazepam		
SMP73 (RR)	50	2.5	12	IFN, GA		
SMP74 (RR)	42	6	24	IFN, GA, AZA, Mitoxantrone		
SMP47 (PP)	52	6	5	Vit D	Epilepsy	7.5
SMP48 (PP)	47	5	9	Depakin, Vinpat	Epilepsy	6; rel: 2015
SMP51 (PP)	59	7	30	NA		8
SMP63 (PP)	55	7.5	16	NA		7.5
SMP65 (PP)	64	7.5	14	NA		8
SMP66 (PP)	63	6.5	39	Bacoflen, Amantadina		6.5
SMP68 (PP)	56	7	7	AZA	Raynaud Syndrome	7

HC: Healthy controls; RR: Relapsing Remitting; PP: Primary Progressive; SMP: Multiple Sclerosis Patient; EDSS: Expanded Disability Status Scale; IFN: Intereferon beta; Mito: Mitoxantrone; AZA: Azathioprine; GA: Glatiramer Acetate; LES: Systemic Lupus Erythematosus; rel: relapse.

For **CD36** were tested **15 HC** (HC3, HC11, HC27, HC29, HC32, HC52, HC01, HC02, HC03, HC04, HC05, HC10, HC11, HC13, HC14); **8 RR** (SMP44, SMP59, SMP69, SMP70, SMP71, SMP72, SMP73, SMP74); **7 PP** (SMP47, SMP51, SMP63, SMP65, SMP66, SMP68, SMP48). The Figure 59 represents the statistical analysis of the validated samples. CD36 is significantly overexpressed although at very low level by RRMS patients but not in PPMS patients from cohort 2.

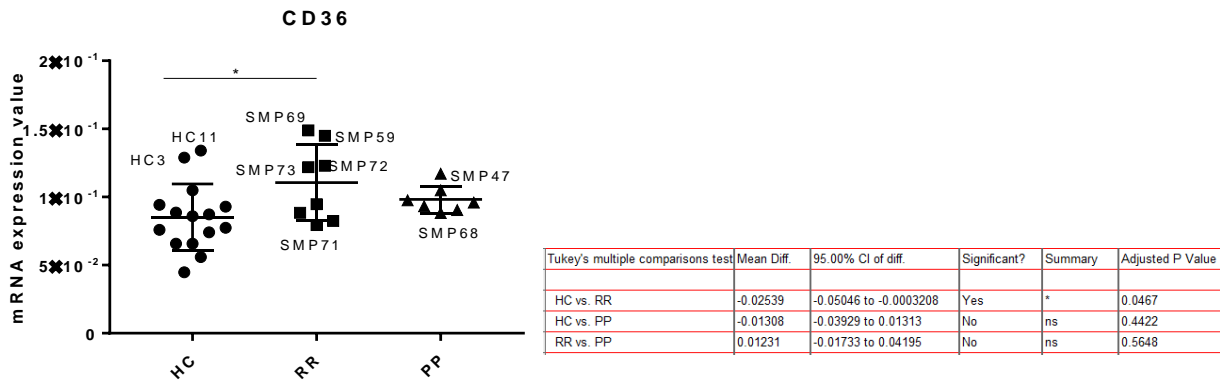


Figure 59. Statistical analysis of CD36 in cohort 2 subjects. Dot plot of tested samples. HC: healthy controls; RR: Relapsing Remitting; PP: Primary Progressive; SMP: Multiple Sclerosis Patient. *pV=0.04.

For **SR-A gene** were tested **12 HC** (HC3, HC11, HC27, HC29, HC32, HC52, HC01, HC02, HC03, HC04, HC05, HC13); **8 RR** (SMP44, SMP59, SMP69, SMP70, SMP71, SMP72, SMP73, SMP74); **7 PP** (SMP47, SMP51, SMP63, SMP65, SMP66, SMP68, SMP48). SR-A receptor is expressed by the RR sample SMP71 (Fig 60A) and by PP SMP48 and 47 (Fig. 60B), however, the overall SR-A expression did not reach significance levels in this cohort (pV=0.06).

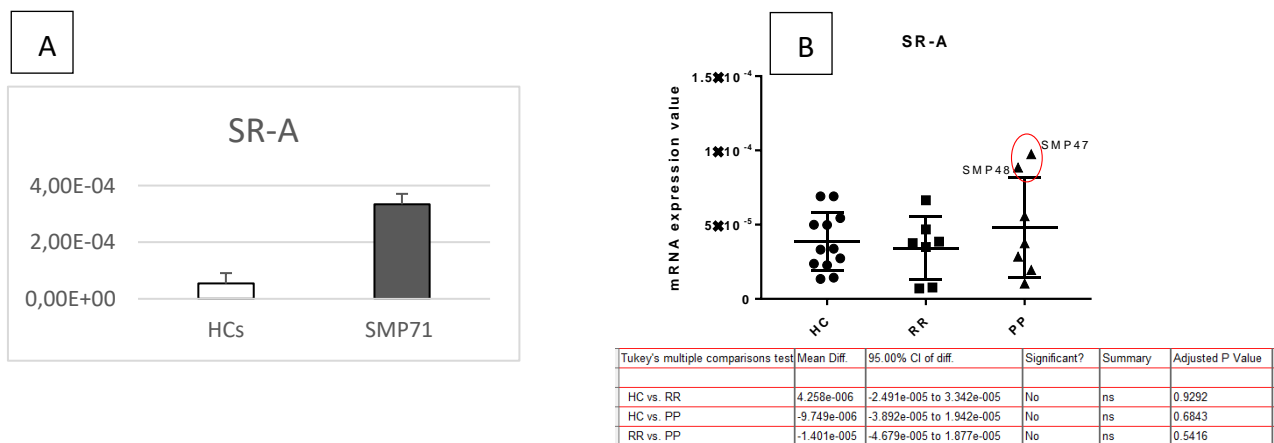


Figure 60. Statistical analysis of SR-A in cohort 2 subjects. A) Histogram obtained by the mean of each HC tested for SR-A, and SMP71 mRNA expression value; B) Dot plot of tested samples. HC: healthy controls; RR: Relapsing Remitting; PP: Primary Progressive; SMP: Multiple Sclerosis Patient.

For **OLR-1 gene** were tested **15 HC** (HC3, HC11, HC27, HC29, HC32, HC52, HC01, HC02, HC03, HC04, HC05, HC10, HC11, HC13, HC14); **8 RR** (SMP44, SMP59, SMP69, SMP70, SMP71,

SMP72, SMP73, SMP74); **7 PP** (SMP47, SMP51, SMP63, SMP65, SMP66, SMP68, SMP48) OLR-1 gene is not expressed at detectable level in RRMS and PPMS cohort 2 patients (Fig.61).

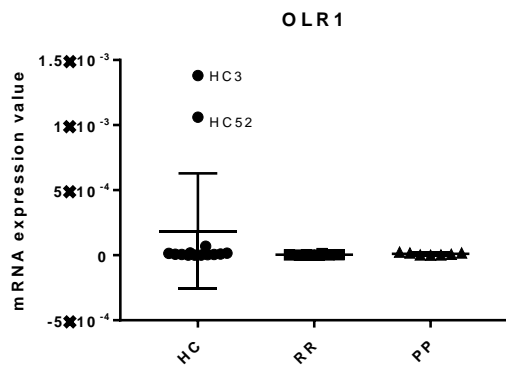


Figure 61. Statistical analysis of OLR1 in cohort 2 subjects. Dot plot of tested samples. HC: healthy controls; RR: Relapsing Remitting; PP: Primary Progressive; SMP: Multiple Sclerosis Patient.

Summary on CD36, SR-A and OLR-1 genes validation

Scavenger receptors (SRs) are a ‘superfamily’ of membrane-bound receptors that are known to bind and internalize oxidized low-density lipoprotein (oxLDL). More than ten families have been described in this class. oxLDL is able to stimulate its own uptake, presumably through induction of one or more scavenger receptors.

Since MS patients blood expressed increased levels of oxLDL, we sought to determine which scavenger receptor was regulated that could mediate the oxLDL-trained monocytes. For this reason, we analysed CD36, SR-A and OLR-1. OLR-1 was detected as differentially expressed in our microarray analysis.

The receptor analysis showed that we were able to measure expression of SR-A and OLR-1 on RR1 and PP SMP24 but not on RR2 patients from the cohort 1. On the contrary, the only gene that was significantly detectable in RR and PP from cohort 2 was the SR-A receptor. CD36 and OLR-1 receptors were overexpressed only on few patients from cohort 2 namely the RR SMP71, and PP SMP47 and SMP48. Therefore, we can conclude that the oxLDL receptors expression tested are only partially upregulated in cohort 2 patients and that oxLDL receptors expressed in MS monocytes deserve further investigation.

7. PUTATIVE TRAINED IMMUNITY RECEPTORS

It has been shown that monocytes can develop a Trained Immunity phenotype upon exposure to endogenous oxLDL particles but also after exposure of NLRP3 (uric acid) and DECTIN-1 ligands (β -glucan). Within the list of inflammatory genes grouped by GO analysis, the receptors NLRP3 and

DECTIN-1 were found differentially modulated in PP and RR1 compared to HCs (Fig.23). Therefore, in order to provide further data on these receptors, the genes NLRP3, DECTIN1 were selected for further validation in human monocytes MS-derived samples.

NLRP3 (NLR Family Pyrin Domain Containing 3) is a member of NLRP3 inflammasome complex. It has been recently demonstrated that the increased activity of NLRP3 in blood of Primary Progressive MS patient is related to the disease ¹⁴⁵. Dectin-1 is a pattern recognition receptor (PRR) that recognizes β -glucans and plays a major role in the immunity against fungal pathogens. Dectin-1 has been shown to ameliorate EAE upon the administration of Dectin-1 agonist¹⁴⁶.

The Table 32 reports the main characteristics and the updated clinic data about cohort 1 MS patients tested for NLRP3 and DECTIN1 genes.

Table 32. Cohort 1 information

Phenotype	Age	EDSS	Disease duration	Treatment	Comorbidity	Updated clinic (EDSS; relapses)
HC3						
HC11						
HC27						
HC29						
HC32	44					
HC52	40					
HC01	28					
HC02	36					
HC03	55					
HC04	40					
HC05	48					
HC10	49					
HC11N	49					
HC13N	41					
HC14	43					
SMP16 (RR1)	28	1	4			1; rel: 2011
SMP27 (RR1)	58	6.5	16	IFN		8
SMP28 (RR1)	49	5	1			5; rel: 2011,2012,2013,2014
SMP29 (RR1)	50	2.5	2			1; rel: 2011,2012,2016
SMP24 (PP)	68	6	13	Eutirox	Hypothyroidism	6.5
SMP11 (RR2)	55	3	25		Hashimoto Thyroiditis	3; rel: 2011
SMP12 (RR2)	51	7	31	AZA, Mito		6.5

SMP13 (RR2)	22	0	6			1; rel: 2010,2016 (x2), 2017
SMP17 (RR2)	43	6	10	AZA, Methotrexate	LES	6
SMP18 (RR2)	55	5.5	27	AZA	Hypertension	5.5; rel: 2016
SMP22 (RR2)	39	2.5	12	AZA, GA		7; rel: 2017

HC: Healthy controls; RR1: Relapsing Remitting 1; RR2: Relapsing Remitting 2; PP: Primary Progressive; SMP: Multiple Sclerosis Patient; EDSS: Expanded Disability Status Scale; IFN: Interferon beta; Mito: Mitoxantrone; AZA: Azathioprine; GA: Glatiramer Acetate; LES: Systemic Lupus Erythematosus; rel: relapse.

Since we were able to test only **1PP** of the cohort 1 (SMP24), it was not included in the statistical analyses, but its expression was reported as histogram comparison to HCs subjects.

For the **NLRP3** gene were tested **11 HC** (HC11, HC27, HC32, HC01, HC02, HC03, HC05, HC10, HC11, HC13, HC14); **6 RR2** (SMP11, SMP12, SMP13, SMP17, SMP18, SMP22); **4 RR1** (SMP16, SMP27, SMP28, SMP29), **1 PP** (SMP24).

As shown in Figure 62C and 62A, NLRP3 gene confirmed to be expressed in PP SMP24 and in RR1 SMP16 but not on RR1 patients SMP27, SMP28 and SMP29. To better appreciate the differences among the other patients, the SMP16 was removed from the analysis (Fig. 62B). Once again, the RR2MS patients SMP17 and SMP22 express high level of NLRP3 transcript within this phenotypic group.

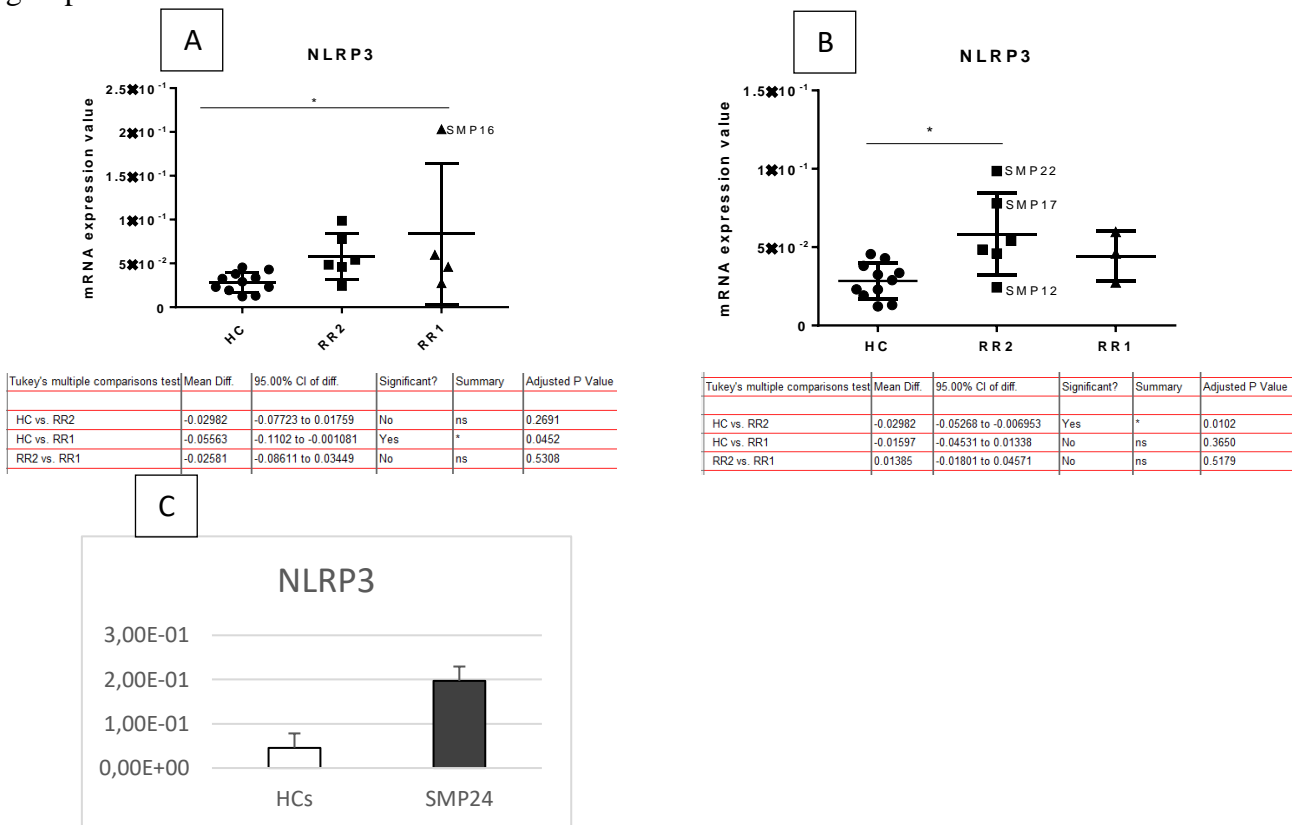


Figure 62. Statistical analysis of NLRP3 in cohort 1 subjects. A) Dot plot of tested samples, B) Dot plot without SMP16, C) Histogram obtained by the mean of each HC tested for NLRP3, and SMP24 mRNA expression value. HCs, healthy controls; RR2: Relapsing Remitting 2; RR1: Relapsing Remitting 1; SMP: Multiple Sclerosis Patient. *pV=0.03.

For the **DECTIN-1** gene were tested **15 HC** (HC3, HC27, HC01, HC02, HC03, HC04, HC05, HC10, HC11, HC13, HC14)), **6 RR2** (SMP11, SMP12, SMP13, SMP17, SMP18, SMP22); **4 RR1** (SMP16, SMP27, SMP28, SMP29), **1 PP** (SMP24).

DECTIN-1 was confirmed to be expressed by RR1 SMP16 and SMP29 but not on RR1 SMP27 and SMP28 (Fig.63A). Four subjects from the RR2MS group (SMP18, SMP11, SMP22 and SMP17) also expressed high level of DECTIN-1 (Fig.63B). SMP24 over-expresses DECTIN-1 too (Fig. 63C). Therefore, we can conclude that DECTIN-1 is differentially expressed in MS monocytes from cohort 1 but its expression is very variable within the MS subtypes and therefore we were unable to rule out a role for this gene.

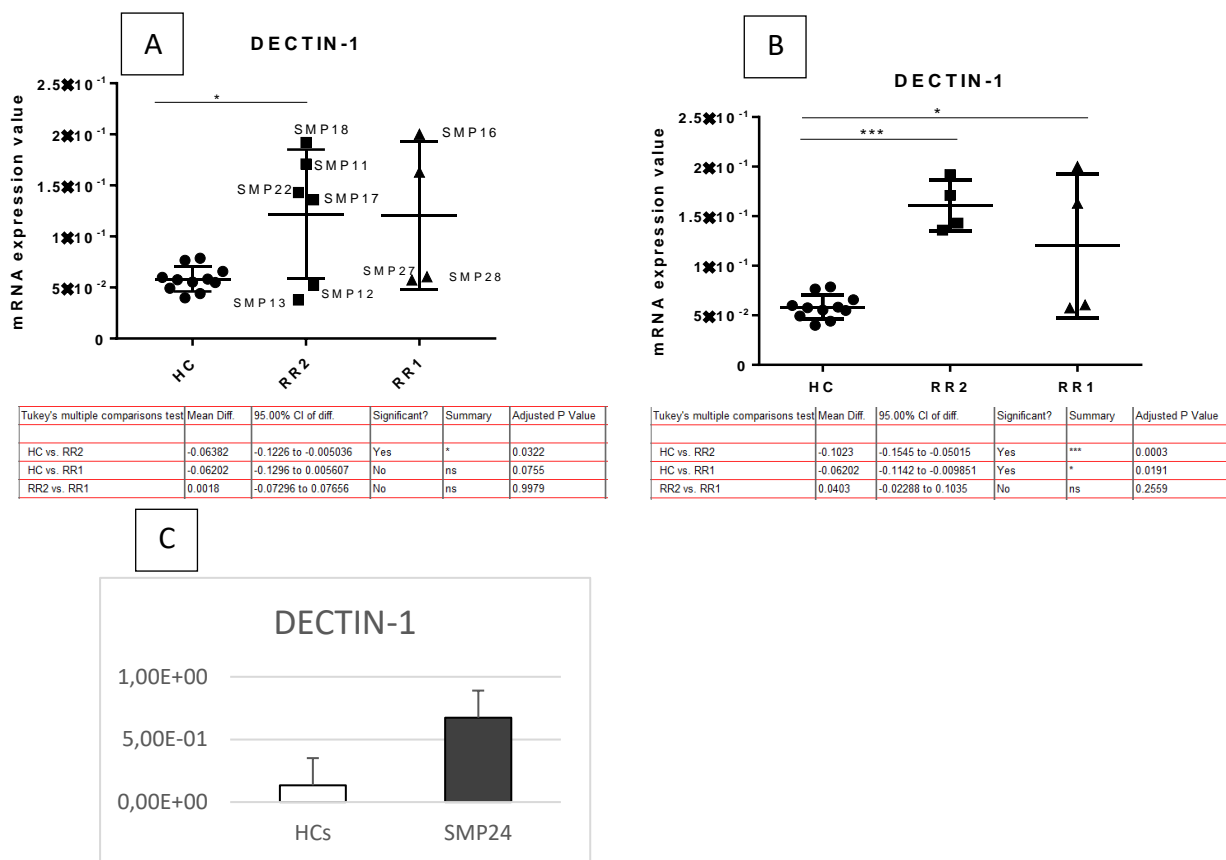


Figure 63. Statistical analysis of DECTIN-1 in cohort 1 subjects. A) Dot plot of tested samples, B) Dot plot without SMP12 and SMP13, C) Histogram obtained by the mean of each HC tested for DECTIN-1, and SMP24 mRNA expression value. HCs, healthy controls; RR2: Relapsing Remitting 2; RR1: Relapsing Remitting 1; SMP: Multiple Sclerosis Patient. *pV=0.03; ***pV=0.0003.

NLRP3 and DECTIN-1 were additionally tested on MS samples from cohort 2. To verify whether NLRP3 and DECTIN-1 were indeed overexpressed in MS monocytes, we tested their upregulation on RR and PP samples derived from cohort 2.

The Table 33 reports the main characteristics and the updated clinic data about cohort 2 MS patients tested for NLRP3 and DECTIN1 genes.

Table 33. Cohort 2 information

Phenotype	Age	EDSS	Disease duration	Treatment	Comorbidity	Updated clinic (EDSS; relapses)
HC3						
HC11						
HC27						
HC29						
HC32	44					
HC52	40					
HC01	28					
HC02	36					
HC03	55					
HC04	40					
HC05	48					
HC10	49					
HC11N	49					
HC13N	41					
HC14	43					
SMP44 (RR)	50	1	6	NA		1
SMP59 (RR)	49	6.5	25	IFN, GA		8; rel: 2009,2010,2011,2013
SMP69 (RR)	40	1.5	14	IFN, GA		2.5; rel: 2013,2017
SMP70 (RR)	44	1	6	IFN	Endometriosis, Hypertension	4.5; rel: 2013 (x2), 2014, 2017
SMP71 (RR)	42	1	16	NA		3; rel: 2012,2013
SMP72 (RR)	58	6.5	36	Gabapentin, Clonazepam		
SMP73 (RR)	50	2.5	12	IFN, GA		
SMP74 (RR)	42	6	24	IFN, GA, AZA, Mitoxantrone		
SMP47 (PP)	52	6	5	Vit D	Epilepsy	7,5
SMP48 (PP)	47	5	9	Depakin, Vinpat	Epilepsy	6; rel: 2015
SMP51 (PP)	59	7	30	NA		8
SMP63 (PP)	55	7.5	16	NA		7.5
SMP65 (PP)	64	7.5	14	NA		8
SMP66 (PP)	63	6.5	39	Bacoflen, Amantadina		6.5
SMP68 (PP)	56	7	7	AZA	Raynaud Syndrome	7

HC: Healthy controls; RR: Relapsing Remitting ; PP: Primary Progressive; SMP: Multiple Sclerosis Patient; EDSS: Expanded Disability Status Scale; IFN: Interferon beta; Mito: Mitoxantrone; AZA: Azathioprine; GA: Glatiramer Acetate; LES: Systemic Lupus Erythematosus; rel: relapse.

NLRP3 and **DECTIN-1** genes were tested in **11 HC** (HC11, HC27, HC32, HC01, HC02, HC03, HC05, HC10, HC11, HC13, HC14); **8 RR** (SMP44, SMP59, SMP69, SMP70, SMP71, SMP72, SMP73, SMP74); **7 PP** (SMP47, SMP51, SMP63, SMP65, SMP66, SMP68, SMP48) of cohort 2 patients.

Figures 64A and 64B show the statistical validation for **NLRP3** and **DECTIN-1** respectively. NLRP3

is not significantly expressed on PP and RR whereas DECTIN-1 is significantly expressed in both RR and PP of cohort 2 patients. Therefore, we were unable to rule out a role for these genes as their expression profiles were very variable within the cohort under study.

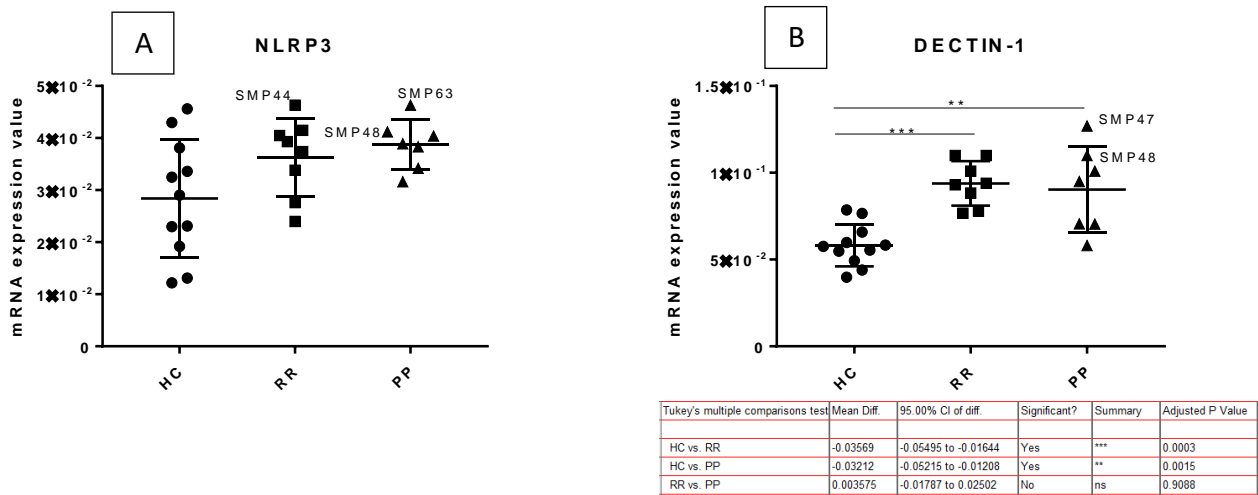


Figure 64. Statistical analysis of NLRP3 and DECTIN1 genes. A) Dot plot of tested samples for NLRP3 expression. B) Dot plot of tested samples for DECTIN-1 gene. HC: healthy controls; RR: Relapsing Remitting; PP: Primary Progressive; SMP: Multiple Sclerosis Patient. **pV=0.001; ***pV=0.0003

8. EPIGENETIC REGULATION ON MS MONOCYTES

Gene expression is tightly regulated at multiple layers by the action of transcription factors and regulatory elements such as promoters, enhancers, and repressors. An additional level of regulation is ensured at the epigenetic level. Epigenetic reprogramming can occur at the level of DNA methylation, histone modifications, or via the action of noncoding RNAs. Several studies have identified epigenetic signatures associated with Trained Immunity, the best studied of which is KDM5 (lysine demethylase 5) as the epigenetic enzymes involved in the regulation of β -glucan-induced Trained Immunity¹⁴⁷. In our microarray study, we found the gene KDM6B as differentially expressed in MS monocytes suggesting that this demethylase could mediate the induction of Trained Immunity in PPMS and RR1MS monocytes.

KDM6B is a lysine-specific demethylase that specifically demethylates the di- or tri-methylated lysine 27 of histone H3 (H3K27me₂ or H3K27me₃) and the result of its activation is the induction of gene transcription. Overexpression of KDM6B resulted in profound induction of innate immune genes¹⁴⁸. However, the regulation of this gene in monocytes in the context of MS remains to be investigated.

The Table 34 report the main characteristics and the updated clinic data about cohort 1 MS patients tested for KDM6B gene.

Table 34. Cohort 1 information

Phenotype	Age	EDSS	Disease duration	Treatment	Comorbidity	Updated clinic (EDSS; relapses)
HC11						
HC41	47					
HC35	37					
HC57	41					
HC01	28					
HC02	36					
HC03	55					
HC04	40					
HC05	48					
HC10	49					
HC11N	49					
HC13N	41					
HC14	43					
SMP27 (RR1)	58	6.5	16	IFN		8
SMP28 (RR1)	49	5	1			5; rel: 2011,2012,2013,2014
SMP29 (RR1)	50	2.5	2			1; rel: 2011,2012,2016
SMP24 (PP)	68	6	13	Eutirox	Hypothyroidism	6.5
SMP11 (RR2)	55	3	25		Hashimoto Thyroiditis	3; rel: 2011
SMP12 (RR2)	51	7	31	AZA, Mito		6.5
SMP13 (RR2)	22	0	6			1; rel: 2010,2016 (x2), 2017
SMP17 (RR2)	43	6	10	AZA, Methotrexate	LES	6
SMP18 (RR2)	55	5.5	27	AZA	Hypertension	5.5; rel: 2016
SMP22 (RR2)	39	2.5	12	AZA, GA		7; rel: 2017

HC: Healthy controls; RR1: Relapsing Remitting 1; RR2: Relapsing Remitting 2; PP: Primary Progressive; EDSS: Expanded Disability Status Scale; IFN: Interferon beta; Mito: Mitoxantrone; AZA: Azathioprine; GA: Glatiramer Acetate; LES: Systemic Lupus Erythematosus; rel: relapse.

For the gene **KDM6B** were tested **13 HCs** (HC11, HC41, HC57, HC01, HC02, HC10, HC11, HC13, HC14), **3 RR1** (SMP27, SMP28, SMP29), **6 RR2** (SMP11, SMP12, SMP13, SMP17, SMP18, SMP22), **1PP** (SMP24). KDM6B gene is highly expressed in RR1 SMP29 patients but not in RR2 and RR1MS SMP28 and SMP27 patients (Fig.65A). The PP of cohort 1 SMP24 over-expresses the gene (Fig.65B).

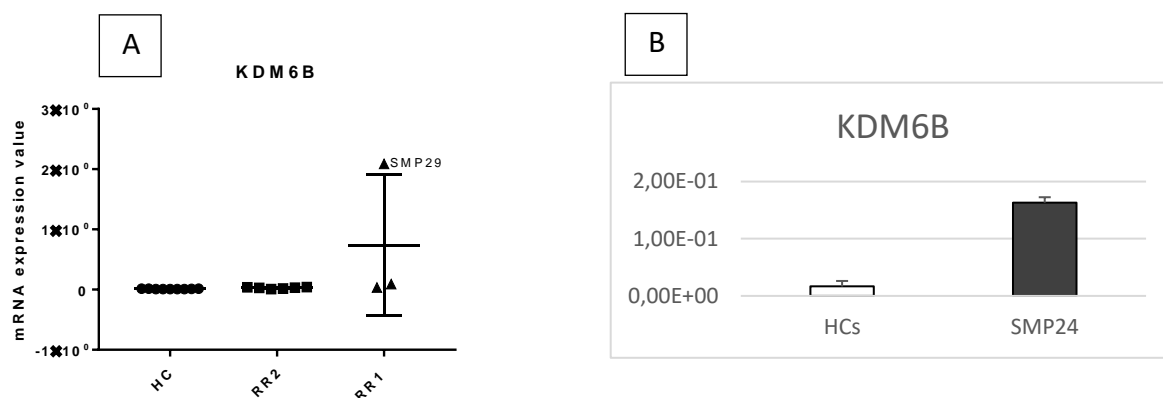


Figure 65. Statistical analysis of KDM6B in cohort 1 subjects. A) Dot plot of tested samples, B) Histogram obtained by the mean of each HC tested for KDM6B, and SMP24 mRNA expression value
HCs, healthy controls; RR2: Relapsing Remitting 2; RR1: Relapsing Remitting 1; SMP: Multiple Sclerosis Patient.

KDM6B gene was additionally tested on MS samples from cohort 2. Since we were unable to verify the KDM6B in all the PPMS subjects of cohort 1 we proceeded to test the expression of KDM6B on cohort 2 in order to define whether induction of transcription of this histone demethylase could play a more general role in MS monocytes.

The Table 35 report the main characteristics and the updated clinic data about cohort 2 MS patients tested for KDM6B gene.

Table 35. Cohort 2 information.

Phenotype	Age	EDSS	Disease duration	Treatment	Comorbidity	Updated clinic (EDSS; relapses)
HC11						
HC41	47					
HC35	37					
HC57	41					
HC01	28					
HC02	36					
HC03	55					
HC04	40					
HC05	48					
HC10	49					
HC11N	49					
HC13N	41					
HC14	43					
SMP44 (RR)	50	1	6	NA		1
SMP59 (RR)	49	6.5	25	IFN, GA		8; rel: 2009,2010,2011,2013
SMP69 (RR)	40	1.5	14	IFN, GA		2.5; rel: 2013,2017
SMP70 (RR)	44	1	6	IFN	Endometriosis, Hypertension	4.5; rel: 2013 (x2), 2014, 2017
SMP71 (RR)	42	1	16	NA		3; rel: 2012,2013

SMP72 (RR)	58	6.5	36	Gabapentin, Clo-nazepam		
SMP73 (RR)	50	2.5	12	IFN, GA		
SMP74 (RR)	42	6	24	IFN, GA, AZA, Mitoxantrone		
SMP47 (PP)	52	6	5	Vit D	Epilepsy	7,5
SMP48 (PP)	47	5	9	Depakin, Vinpat	Epilepsy	6; rel: 2015
SMP51 (PP)	59	7	30	NA		8
SMP63 (PP)	55	7.5	16	NA		7.5
SMP65 (PP)	64	7.5	14	NA		8
SMP66 (PP)	63	6.5	39	Bacoflen, Aman-tadina		6.5
SMP68 (PP)	56	7	7	AZA	Raynaud Syndrome	7

HC: Healthy controls; RR: Relapsing Remitting ; PP: Primary Progressive; SMP: Multiple Sclerosis Patient; EDSS: Expanded Disability Status Scale; IFN: Interferon beta; Mito: Mitoxantrone; AZA: Azathioprine; GA: Glatiramer Acetate; LES: Systemic Lupus Erythematosus; rel: relapse.

For KDM6B were tested **9 HCs** (HC11, HC41, HC57, HC01, HC02, HC10, HC11, HC13N, HC14N), **8 RR** (SMP44, SMP59, SMP69, SMP70, SMP71, SMP72, SMP73, SMP74), **7 PP** (SMP47, SMP51, SMP63, SMP65, SMP66, SMP68).

KDM6B is significantly expressed in PPMS patients confirming that this gene is specific for PPMS phenotype and may be responsible for monocytes immune activation observed in PPMS.

(Fig.66).

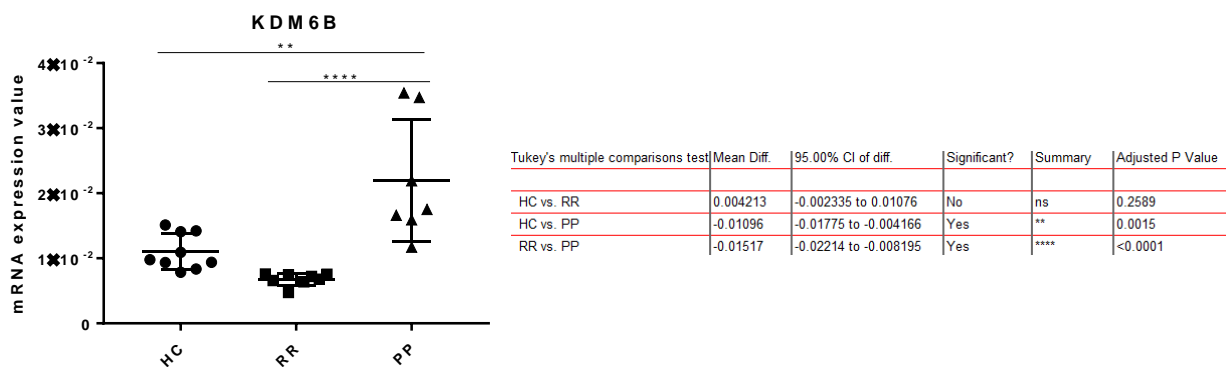


Figure 66. Statistical analysis of KDM6B in cohort 2 subjects: Dot plot of tested samples. HC: healthy controls; RR: Relapsing Remitting; PP: Primary Progressive; SMP: Multiple Sclerosis Patient. **pV=0.001; ****pV<0.0001.

9. SELECTION OF THE SUITABLE IN VITRO MODEL TO STUDY THE METABOLIC CHANGES OBSERVED IN MS MONOCYTES

From the previous results, we observed that a specific transcriptional signature is induced in monocytes derived from peripheral blood of MS patients. The most interesting aspect concerns the deregulation of genes involved in Cholesterol Biosynthesis and induction of innate immune genes encoding for receptors like NLRP3, DECTIN-1 and OLR-1. Since of dysregulation have been

associated to activation of innate immune memory, we hypothesize that Trained Immunity (TI) mechanisms are involved, at least in a subgroup of MS patients. TI consists of an enhanced immune response in monocytes upon nonspecific restimulation¹¹⁰. Up to now, β -Glucan has been shown to induce TI in monocytes via pattern recognition receptors (PRRs) DECTIN-1, leading to different metabolic modifications, including Cholesterol Biosynthesis pathways and epigenetic rewiring. Besides β -Glucan, also oxLDL has been shown to induce TI. Given these premises, during my doctorate I tried to develop an in vitro model that could stimulate cholesterol genes in monocytic cells in order to study the correlation between inflammation and cholesterol pathways. The cell line chosen was that of THP1, human monocytes derived from the blood of 1-year-old boys with acute monocytic leukemia (Tsuchiya et al. 1980). In particular, I tried to stimulate Cholesterol genes with lysophosphatidylcholine (LPC)¹⁴⁹. The latter is the principal component of oxLDL, and it has been demonstrated that is able to induce cholesterol genes in THP1 cells¹⁴⁹. All the protocols are described into Material and Methods section.

We observed that the stimulation of THP1 cells with LPC can upregulate all the genes involved in the mevalonate/DMAPP cholesterol pathway (HMGCS1, HMGCR, IDI1), but also the gene SQLE, which is responsible for squalene pathway. In addition, cholesterol's deregulation resulted connected to an upregulation of the pro-inflammatory cytokine TNF α . Moreover, NLRP3 and IL1 β genes resulted upregulated, confirming a strong correlation between the cholesterol and the inflammatory process.

9.1. CHOLESTEROL GENES RESULTED UP-REGULATED IN THP1 CELLS STIMULATED WITH LPC

The conditions used were those of untreated, treated with LPC 100 μ M and treated with the vehicle (0.1% methanol). Five experiments have been conducted using different biological replicates.

Above all, we investigated the genes involved into the mevalonate/DMAPP pathway (HMGCS1, HMGCR and IDI1) and successively the SQLE gene, involved into the last step of cholesterol production. All four of these genes resulted upregulated in THP1 treated with LPC 100 μ M in comparison to THP1 treated with the vehicle.

Once verified that we are able to induce the Cholesterol pathway, we also measured the expression of the cytokines TNF α and IL-1 β beside NLRP3 and OLR-1 receptor expression. As is shown in figures 68A-D, all the cholesterol genes were induced by LPC.

On the same samples, we tested the inflammatory cytokines TNF α and IL1 β (Fig 67E, 67F) and the receptors NLRP3 and OLR1 (Fig. 67G, 67H) confirming that LPC induces pro-inflammatory cytokines and receptors genes in THP1 cells.

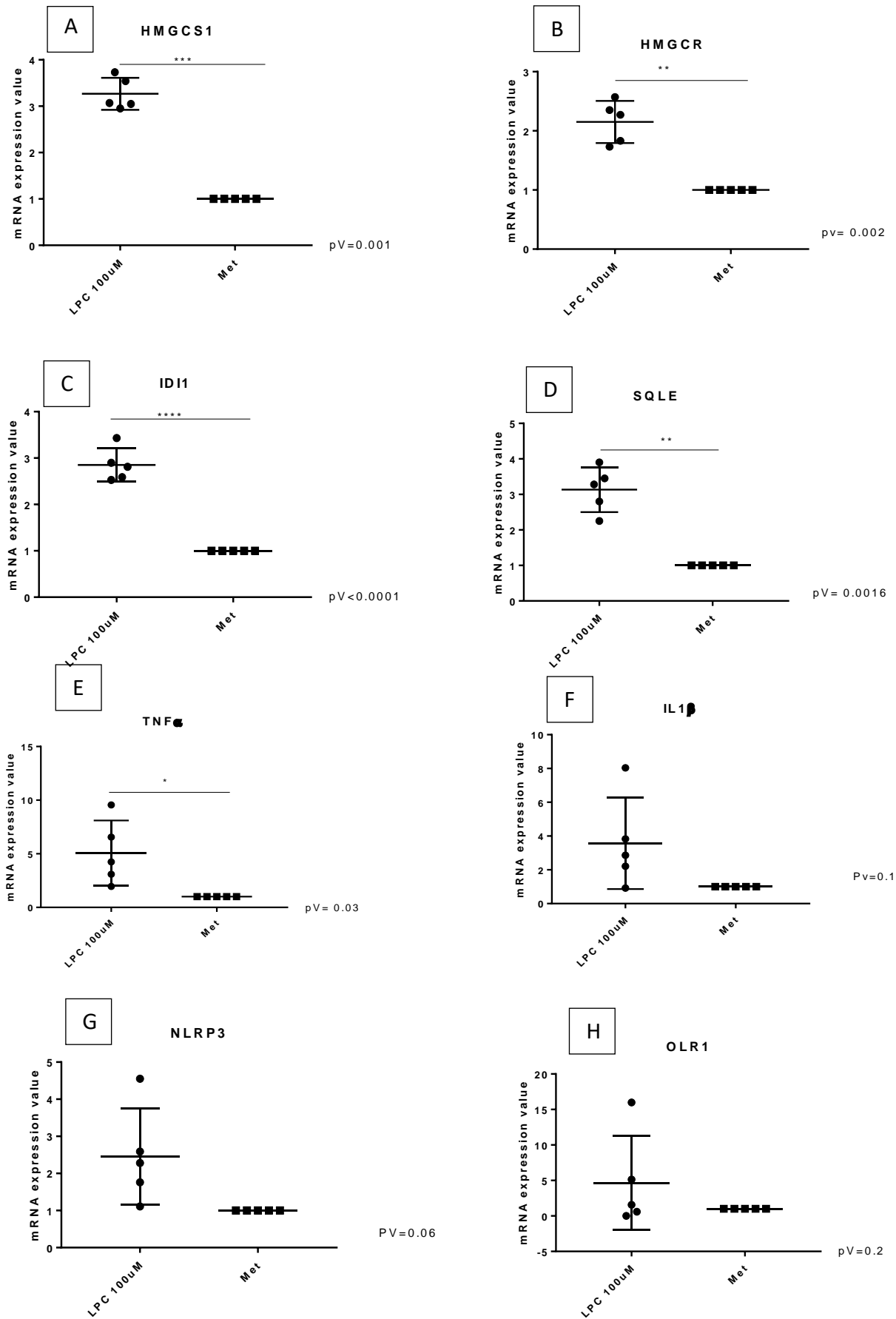


Figure 67. Statistical analysis of THP1 treated with LPC 100uM and Methanol as a vehicle. A) Dot plot analysis of HMGCS1 gene; B) Dot plot analysis of HMGCRC; C) Dot plot analysis for IDI1; D) Dot plot analysis of SQLE; E) Dot plot analysis of TNF α ; F) Dot plot analysis of IL1 β ; G) Dot plot analysis of NLRP3; H) Dot plot analysis of OLR1.

Conclusions and perspectives

In summary, it is likely that the activation of cholesterol genes is associated with the inflammatory pathway in monocytes. The most interesting fact of these results is related to that in our MS patients - among the most deregulated genes of the inflammatory pathway - there were genes related to the cholesterol biosynthetic pathway. We also found that oxLDL levels are increased in MS patients suggesting that this molecule could be responsible for the induction of oxLDL-induced monocyte activation. Several receptors can bound oxLDL. And indeed, in a subgroup of PP patients the OLR1 gene was found to be strongly induced, while in other cohort of MS patients a greater deregulation of CD36 and SR-A genes was observed.

All these results indicated that Trained Immunity may be involved in the pathogenesis of MS. Since we observed also a strong induction of the IDI1 gene which is responsible for DMAPP formation, we also hypothesised that, additionally, these metabolic-activated monocytes maybe prone to induce T γ δ cells activation which would lead to disease exacerbation¹⁵⁰. Currently, experiments are on their way to demonstrate this hypothesis.

Secondly, we identified a connection between induction of the cholesterol biosynthetic pathway and activation of the innate inflammatory responses in monocytes. Therefore, further studies will be concentrated to demonstrate the mechanisms by which the cholesterol biosynthesis pathways regulates TNF α , IL1 β , NLRP3 and OLR-1 expression in human monocytes. Preliminary experiments with cholesterol inhibitors (statins) have shown that if we block the cholesterol biosynthesis pathway we specifically block monocytes cytokine induction. In particular, we are planning to use the fluvastatin and zaragozic acid, which will inhibit the mevalonate/DMAPP pathway and the Squalene pathway respectively in order to define which part of the cholesterol biosynthesis pathway is required for immune activation in monocytes.

DISCUSSION

Multiple Sclerosis (MS) is an immune mediated, inflammatory and demyelinating disease of the Central Nervous System (CNS)¹⁵¹. Recently, the role of monocytes in MS was deeply investigated by Ajami and colleagues, which found that infiltrating monocytes trigger EAE progression¹⁵² and that monocytes depletion correlates with an improvement of the disease¹⁵³.

In addition, it has been recently demonstrated that alterations in endogenous interferon signalling occur in peripheral monocytes of MS patients.¹⁵⁴

Interestingly, one of the most up-regulated gene in monocytes resulted to be the IL-16, a chemotactic molecule specific for CD4⁺ T lymphocytes which regulate T cell activation. Furthermore, the IL-16 transcriptional regulator named STAT3 resulted over-expressed both at transcriptional and protein level in monocytes of RRMS patients analysed. These recent data support a specific role of monocytes in MS disease and our study is part of this panorama. In particular, we set up our study in order to further investigate the role of monocytes in MS by using a transcriptomic approach.

To do this, we collected peripheral blood from Relapsing Remitting Multiple Sclerosis (RR) and Primary Progressive Multiple Sclerosis Patient's (PP), and Healthy Controls (HC), and CD14⁺ monocytes were purified. To define the molecular pathways that were possible dysregulated in MS monocytes, a transcriptomics approach by Microarray Analysis was performed on 33 female subjects (13 HCs, 13 RR, 7 PP) and we discovered that the RR patients were very variable and that: based on this genetic profiles, two subgroups of RR samples (named RR1 and RR2) were evident. Specifically, the RR1 patients' expression pattern was closely correlated to those of the PP patients, whereas the RR2 profiles were clustering with the HCs.

Then, we proceeded to identify the Differentially Expressed Genes (DEGs) through the ANOVA test ($F_c=2$ and $FDR = 0.05$) and we were able to detect the DEGs between PP and HC (1491 DEGs, of which 1463 were upregulated) and to identify two different RR subgroups. Gene Ontology (GO) analysis of these genes pointed out the most dysregulated Biological Processes (BP) most as belonging to: *Cell Cycle*, *Anti-Apoptosis*, *Inflammation and Cholesterol*. In particular, the attention was focused on *Inflammation and Cholesterol pathway*, with this latter as the most clearly deregulated. QRT-PCR was chosen to validate our findings. To do this, we first validated the data by using the remained samples from the cohort 1 (16 samples: 5 HC; 6 RR2; 4 RR1; 1 PP) that was used to run the microarray analysis, and then we extended the analysis to a second cohort, named cohort 2 that was recruited for this purpose (22 samples: 7 HC; 8 RR; 7 PP). The inflammatory genes TNF α , IL-1 β and PTX3 were confirmed to be highly expressed in samples derived from cohort 1 and to a lesser extent on cohort 2. The chemokines genes belonging to the same inflammatory class namely CXCL2, CXCL3 and CXCL8 were also induced in PP and RR1 monocytes of cohort 1. CXCL8

known as IL-8, is known to chemo attract neutrophil and monocytes and it has already been shown to mediate the inflammatory response in MS patients¹³⁷ suggesting that monocytes recruitment to the brain may be mediated by this cytokine. Beside CXCL8 also other two neutrophils chemoattractants, namely CXCL2 and CXCL3 were induced in MS monocytes indicating that a crosstalk between monocytes and neutrophils may exist in the periphery of MS patients. Therefore, we suggest that monocytes may have an important role in the amplification of the inflammatory pattern observed in PP and RR1 patients. Interestingly, although in general CXCL2, 3 and 8 chemokines were generally induced in MS monocytes, we also observed that some MS patients had a more specific upregulation of CXCL3 (SMP16) and CXCL8 (SMP29), indicating that a specific inflammatory patient's profile may exist within MS patient subgroups. For example, among the RR2 patients subgroup, the patients SMP17 and SMP18 express high level of TNF α , IL1 β , PTX3, CXCL2, CXCL3; while within the RR1 patient's subgroup, SMP27 was characterized by a low expression profile for the gene TNF α , IL1 β , CXCL2, CXCL3. By analysing the clinical features of these patients, we observed that the RR2 patients showing dysregulation in the genes TNF α , IL1 β , PTX3, CXCL2, CXCL3, were those who also presented with comorbidities (hypertension and LES); while for the RR1's patients, those with a longer duration of the disease (SMP27) were characterized with lowest expression of the related genes. All genes analysed within the inflammatory profile were over-represented in the PP patient derived from cohort 1 (SMP24) that was available for the validation phase in our analysis. The second pathways we sought to investigate was the *Cholesterol Biosynthesis pathway*. The biosynthesis of cholesterol is a complex process, heavily regulated at several points throughout its progression. This process requires different enzymes, some of which are among the most regulated enzymes currently known. The first step in the synthesis of cholesterol is the formation of mevalonate from acetate, which begins with the condensation of two acetyl-coenzyme A (acetyl-CoA) molecules to form acetoacetyl-CoA, a process catalyzed by the enzyme thiolase. Next, HMG-CoA synthase (HMGCS1) catalyzes the reaction between acetoacetyl-CoA and another molecule of acetyl-CoA to form HMG-CoA⁸⁶. The final step in the synthesis of mevalonate is accomplished by HMG-CoA reductase (HMGR). The subsequent step in the biosynthesis of cholesterol comprises the conversion of mevalonate into two activated isoprenes (isopentanyl 5-pyrophosphate and dimethylallyl pyrophosphate). Following a series of successive condensations of activated isoprenes, squalene, is formed⁸⁶. To form cholesterol, squalene has shown to undergo a succession of changes, being initially converted to lanosterol, which is finally transformed into cholesterol after several sequential reactions⁸⁶. The key enzymes that were found dysregulated in MS in our microarray study, were those involved in the Mevalonate and DMAPP generation (HMGCS1 and HMGCR and IDI1) - that we named Mevalonate/DMAPP pathway - and those involved in the cholesterol biosynthetic pathway

starting from Squalene (SQLE, CYP51A1, SCAMOL and SC5DL) - that we named Squalene pathway. In addition, the regulatory gene INSIG1 which is an important cholesterol gene regulator was also found highly dysregulate in MS.

Analysis of the genes HMGCS1, HMGCR, IDI1, SQLE, CYP51A1, SC4MOL, SC5DL and INSIG1 in the MS subtypes revealed that the RR2 patients have a gene profile that correlates with those of the HCs, while the RR1 and PP SMP24 over-express all the genes tested with the exception of the gene HMGCR. This latter was not significantly regulated, nevertheless two RR2 patients, (SMP11 and SMP13) expressed high values for HMGCR suggesting a specific gene expression profiles for this gene. These two subjects were extremely different in terms of clinical parameters. The SMP11 has 55 years old, EDSS of 3, disease duration of 25 years and Hashimoto Thyroiditis; on the contrary, the patient SMP13 has 22 years old, an EDSS of 0 and a disease duration of 6 years which does not correlate with the observed HMGCR gene expression pattern. However, a closer look at the clinical course updates evidenced that these two patients had several clinical relapses, especially patient SMP13 experienced additional 3 relapses over a time of 2 years. In conclusion, the MS patients from cohort 1 displayed a dysregulation of both the Mevalonate/DMAPP and the Squalene pathways in RR1 and in the PP SMP24.

A different pattern of Cholesterol gene expression was observed in MS patients from cohort 2. Specifically, the mevalonate/DMAPP pathway was in general significantly upregulated by both RR and PP patients, indicating that indeed the RR form cohort 2 resembled more the RR1 phenotype of cohort 1, nevertheless the squalene pathway was dysregulated primarily in PP patients except for the gene CYP51A1 that was upregulated in the RR and PP patients from cohort 2. These data indicated that the MS patient's cohort 2 may represent a distinct phenotypical group although the RR of cohort 2 seem to be more correlated with the RR1 phenotype identified in cohort 1. Interestingly, the gene INSIG1 confirmed that RR of cohort 2 possess high gene expression profile for this gene.

In conclusion, we have identified genetic signatures that can be used to stratify MS patients in different RR and possibly PP subgroups. Since the observed pattern was not completely constant in the two cohorts of MS patients analysed we envisage to perform a detailed microarray analysis also on the cohort 2 in order to identify the specific molecular pathways that are indeed related to this cohort.

Because PP and RR1 monocytes displayed an enhanced pro-inflammatory phenotype and upregulation of the cholesterol pathway, we hypothesized that a form of Trained Immunity (TI) ¹⁰⁹ phenotype could operate in MS, at least in a subgroup of MS patients.

Up to now, β -Glucan has been deeply characterized as TI inducer in monocytes via pattern recognition receptors (PRRs) DECTIN-1, leading to different metabolic modifications that include

the Cholesterol Biosynthesis pathways and epigenetic rewiring. Besides β -Glucan, also oxLDL and BGC have been shown to induce TI. To identify the endogenous ligand that could be responsible for the Trained Immunity-like phenotype in MS, we tested the concentration of oxLDL in the blood of our MS subjects. Surprisingly, both the RR and PP from the cohort 2 expressed high level of oxLDL in their blood. Interestingly, all the female samples had high levels of oxLDL concentration whereas only two out of four males analyzed had measurable levels of oxLDL. The data suggested that different mechanisms may likely operate between male and female MS patients although we can not rule out this possibility as a small group of male patients have been analyzed. Nevertheless, we suggest that it is important to molecularly characterize each MS cohort under study to identify the specific pattern operating in each subgroup.

To define the receptor that could mediate the induction of TI in monocytes, we studied the oxLDL receptor family which is composed by several receptors including the scavenger receptors SR-A and CD36 beside the well-known OLR-1¹⁵⁵. Because the binding of oxLDL to its receptor has been shown to induce its gene expression, we tested CD36 and SR-A, together with OLR-1 gene by qRT-PCR both in cohort 1 and cohort 2.

In general, RR1 and the PP SMP24 monocytes expressed OLR-1 and SR-A but not CD36. OLR-1 receptor was not expressed by RR2 group which showed a variable degree of expression for the CD36. Again those sample expressing high level of CD36 and SR-A receptors were those who carried comorbidity such as Hashimoto's thyroiditis (SMP11) and LES (SMP17). Moreover, SR-A gene expression was dysregulated also on the patient SMP12 who was characterized by having a long disease duration (25 years and 31 years respectively). Analysis of the cohort 2 RR and PP patients receptor expression indicated that in this cohort the oxLDL receptor expression was probably mediated by the SR-A and CD36 receptors, at least in a subgroup of PP (SMP47 and SMP48) and RR (SMP59, SMP72, SMP73) as it was mostly overexpressed compared to the other receptor types (Fig. 59 and Fig.60).

Induction of the enhanced activation in monocytes has been reported to be mediated by receptors belonging to the family of C-type lectins (DECTIN-1) and those controlling the inflammasome response (NLRP3)¹⁵⁶. Interestingly, these receptor's types were found to be dysregulated in MS and were grouped within the list of inflammatory genes derived from the microarrays analysis. Again, NLRP3 and DECTIN-1 genes were overexpressed on cohort 1 MS patients although to very variable levels whereas only DECTIN-1 was overexpressed in RR and PP patients from cohort 2. These results pointed out again the need to thoroughly molecular characterized the cohort under study because specific disease molecular mechanisms can account for the observed disease phenotypes.

Finally, the gene KDM6B that encode for Lysine (K)-Specific Demethylase 6B was also selected for differentially expression in MS compared to controls. KDM6B is one of the histone demethylase which activate gene expression via demethylating H3K27me3 to H3K27me2 or H3K27me1 suggesting that it could be responsible for aberrant epigenetic reprogramming observed in RR1 and PP MS monocytes¹⁵⁷.

In conclusion, we were able to confirm the genetic signatures derived from microarrays analysis on RR and PP MS patients and on the only PP patient that remained available for the real-time experiments (SMP24) on cohort 1. In addition, we were able to stratify RR patients into two distinct phenotypic groups named RR1 and RR2. The signature selected could identify a subgroup of RR patients that presents a much stronger monocytes activatory profiles not only for what concern the inflammatory genes but also for what concern the metabolic changes in their monocytes. The selected signature was also tested on a second cohort of RR and PP patients (cohort 2) revealing that although we were able to confirm part of the signature, we also observed a specific cohort 2 pattern for these genes, suggesting that a microarray analysis should be performed on each independent recruited cohort in order to identify a cohort specific gene signature.

Indeed, we observed that three patients from cohort 2 (SMP44, SMP47 and SMP48) were overexpressing the signature genes significantly higher than other members of the same group.

Trained immunity seems to be induced by both cohorts of subjects but the mechanism inducing this phenotype maybe different. We observed higher OLR-1 expression in cohort 1 patients whereas cohort 2 was characterized by higher levels for the SR-A and CD36 receptors indicating that the metabolic changes can be induced by different receptor's types.

Finally, to test whether we could mimic in vitro the signature observed in ex vivo MS patient's monocytes, we initiated experiments by using the well-known THP-1 cell line. These cells derive from the blood of 1-year- old boys with acute monocytic leukemia (Tsuchiya et al. 1980). To induce the Cholesterol genes, THP-1 cells we treated with LPC, a component of oxLDL which was shown to be able to induce cholesterol genes in THP-1 cells. We could measure induction of the mevalonate/DMAPP pathway genes (HMGCS1, HMGCR, IDI1), but also the squalene pathway (SQLE). At the same time, we measured the ability of LPC to induce the upregulation of the pro-inflammatory cytokine TNF α and IL1 β and the NLRP3 receptor implicating that a strong correlation between cholesterol and inflammatory pathways may exist. Experiments in the laboratory are underway to demonstrate that the cholesterol pathways regulated pro-inflammatory gene expression in monocytes.

Moreover, since we measured a strong upregulation of the IDI1 gene which lead to the accumulation of the dimethylallyl diphosphate (DMAPP) metabolite, we hypothesized that MS monocytes may affect T $\gamma\delta$ cells activation and differentiation as this cell type, is indeed regulated by DMAPP concentrations released by activated monocytes¹⁵⁰. Therefore, we suggest that this pathway may additionally contribute to the PP phenotype exacerbation, at least in a subgroup of PP patients.

So, to summarize the overall data, we propose to perform gene expression studies in order to derived cohort-specific genetic signatures that will be important for patient's stratification - as it was shown for the different phenotypic RR groups identified in this study. Moreover, gene expression analysis also will allow to identify the patient's specific molecular mechanisms operating as it was the case of the identified Trained Immunity signatures described in this study. Therefore, we suggest that inhibition of the cholesterol synthesis pathway in inflammatory conditions is thus potentially very relevant for those MS patients that present a Trained Immunity-type of phenotype as shown by our PP group. Inhibition of the cholesterol synthesis pathway could therefore be an effective therapy in those MS patients in which Trained Immunity may play a role. In support of this hypothesis, a phase III of clinical trial testing simvastatin in Secondary Progressive MS patients is presently ongoing (<https://www.msociety.org.uk>).

Finally, we suggest that a personalized Immunology approach must begin to be considered as fundamental and necessary for the management for MS and in general for other autoimmune diseases.

BIBLIOGRAPHY

1. McFarland, H. F. & Martin, R. Multiple sclerosis: A complicated picture of autoimmunity. *Nature Immunology* **8**, 913–919 (2007).
2. Weiner, H. L. Multiple sclerosis is an inflammatory T-cell-mediated autoimmune disease. *Archives of Neurology* **61**, 1613–1615 (2004).
3. Bar-Or, A., Oliveira, E. M. L., Anderson, D. E. & Hafler, D. A. Molecular pathogenesis of multiple sclerosis. *J. Neuroimmunol.* **100**, 252–259 (1999).
4. Díaz, C., Zarco, L. A. & Rivera, D. M. Highly active multiple sclerosis: An update. *Multiple Sclerosis and Related Disorders* **30**, 215–224 (2019).
5. Kumar, D. R., Aslinia, F., Yale, S. H. & Mazza, J. J. Jean-martin charcot: The father of neurology. *Clin. Med. Res.* **9**, 46–49 (2011).
6. Pearce, J. M. S. Historical Descriptions of Multiple Sclerosis. *Eur. Neurol.* **54**, 49–53 (2005).
7. Reich, D. Multiple Sclerosis. *Nejm* **176**, 139–148 (2017).
8. Phadke, J. G. Survival pattern and cause of death in patients with multiple sclerosis: Results from an epidemiological survey in north east Scotland. *J. Neurol. Neurosurg. Psychiatry* **50**, 523–531 (1987).
9. Federation, M. S. I. Atlas of MS 2013: Mapping multiple sclerosis around the world. *Mult Scler Int Fed* **2013**, 1–28 (2013).
10. Ysrraelit, M. C. & Correale, J. Impact of sex hormones on immune function and multiple sclerosis development. *Immunology* **156**, 9–22 (2019).
11. Belbasis, L. Environmental risk factors and multiple sclerosis: an umbrella review of systematic reviews and meta-analyses. *The Lancet. Neurology* vol. **14**, 3, 263-73 (2015).
12. Ascherio, A. & Munger, K. L. Epstein-barr virus infection and multiple sclerosis: A review. *Journal of Neuroimmune Pharmacology* **5**, 271–277 (2010).
13. Sintzel, M. B., Rametta, M. & Reder, A. T. Vitamin D and Multiple Sclerosis: A Comprehensive Review. *Neurology and Therapy* **7**, 59–85 (2018).
14. Baranzini, S. E. & Oksenberg, J. R. The Genetics of Multiple Sclerosis: From 0 to 200 in 50 Years. *Trends in Genetics* **33**, 960–970 (2017).
15. Sawcer, S., Franklin, R. J. M. & Ban, M. Multiple sclerosis genetics. *The Lancet Neurology* **13**, 700–709 (2014).
16. Koch, M. W., Metz, L. M. & Kovalchuk, O. Epigenetic changes in patients with multiple sclerosis. *Nature Reviews Neurology* **9**, 35–43 (2013).
17. Savinetti, I., Papagna, A. & Foti, M. Human monocytes plasticity in neurodegeneration.

Biomedicines **9**, (2021).

18. Graves, M. C. *et al.* Methylation differences at the HLA-DRB1 locus in CD4+ T-Cells are associated with multiple sclerosis. *Mult. Scler. J.* **20**, 1033–1041 (2014).
19. Rhead, B. *et al.* Increased DNA methylation of SLFN12 in CD4 + and CD8 + T cells from multiple sclerosis patients. *PLoS One* **13**, (2018).
20. Maltby, V. E. *et al.* Genome-wide DNA methylation profiling of CD8+ T cells shows a distinct epigenetic signature to CD4+ T cells in multiple sclerosis patients. *Clin. Epigenetics* **7**, (2015).
21. Ewing, E. *et al.* Combining evidence from four immune cell types identifies DNA methylation patterns that implicate functionally distinct pathways during Multiple Sclerosis progression. *EBioMedicine* **43**, 411–423 (2019).
22. Mangano, K. *et al.* Hypomethylating agent 5-Aza-2'-deoxycytidine (DAC) ameliorates multiple sclerosis in mouse models. *J. Cell. Physiol.* **229**, 1918–1925 (2014).
23. Popescu, B. F. G., Pirko, I. & Lucchinetti, C. F. Pathology of multiple sclerosis: Where do we stand? *CONTINUUM Lifelong Learning in Neurology* **19**, 901–921 (2013).
24. Hauser, S. L. *et al.* Immunohistochemical analysis of the cellular infiltrate in multiple sclerosis lesions. *Ann. Neurol.* **19**, 578–587 (1986).
25. Ludwin, S. K. The neuropathology of multiple sclerosis. *Neuroimaging Clinics of North America* **10**, 625–648 (2000).
26. Peterson, J. W., Bö, L., Mörk, S., Chang, A. & Trapp, B. D. Transected neurites, apoptotic neurons, and reduced inflammation in cortical multiple sclerosis lesions. *Ann. Neurol.* **50**, 389–400 (2001).
27. Kuhlmann, T. *et al.* An updated histological classification system for multiple sclerosis lesions. *Acta Neuropathol.* **133**, 13–24 (2017).
28. Lassmann, H. Pathogenic mechanisms associated with different clinical courses of multiple sclerosis. *Frontiers in Immunology* **10**, (2019).
29. Friese, M. A., Schattling, B. & Fugger, L. Mechanisms of neurodegeneration and axonal dysfunction in multiple sclerosis. *Nature Reviews Neurology* **10**, 225–238 (2014).
30. Klineova, S. & Lublin, F. D. Clinical course of multiple sclerosis. *Cold Spring Harb. Perspect. Med.* **8**, (2018).
31. Rommer, P. S. *et al.* Relapsing and progressive MS: the sex-specific perspective. *Ther. Adv. Neurol. Disord.* **13**, (2020).
32. Torkildsen, O., Myhr, K. M. & Bø, L. Disease-modifying treatments for multiple sclerosis - a review of approved medications. *Eur. J. Neurol.* **23**, 18–27 (2016).

33. European Medicines Agency. Assessment report: Gilenya (EMEA/H/C/2202). *Assessment* **44**, 1–117 (2011).
34. Brandstadter, R. & Sand, I. K. The use of natalizumab for multiple sclerosis. *Neuropsychiatric Disease and Treatment* **13**, 1691–1702 (2017).
35. Syed, Y. Y. Ocrelizumab: A Review in Multiple Sclerosis. *CNS Drugs* **32**, 883–890 (2018).
36. Louveau, A. *et al.* Structural and functional features of central nervous system lymphatic vessels. *Nature* **523**, 337–341 (2015).
37. Hemmer, B., Kerschensteiner, M. & Korn, T. Role of the innate and adaptive immune responses in the course of multiple sclerosis. *The Lancet Neurology* **14**, 406–419 (2015).
38. Ji, Q., Castelli, L. & Goverman, J. M. MHC class I-restricted myelin epitopes are cross-presented by Tip-DCs that promote determinant spreading to CD8 + T cells. *Nat. Immunol.* **14**, 254–261 (2013).
39. McMahon, E. J., Bailey, S. L., Castenada, C. V., Waldner, H. & Miller, S. D. Epitope spreading initiates in the CNS in two mouse models of multiple sclerosis. *Nat. Med.* **11**, 335–339 (2005).
40. Racke, M. K. Immunopathogenesis of multiple sclerosis. *Annals of Indian Academy of Neurology* **12**, 215–220 (2009).
41. Malpass, K. Multiple sclerosis: ‘Outside-in’ demyelination in MS. *Nature Reviews Neurology* **8**, 61 (2012).
42. Van Oosten, B. W. *et al.* Treatment of multiple sclerosis with the monoclonal anti-CD4 antibody cM-T412 : 351–357 (1997).
43. Lu, L. F. & Rudensky, A. Molecular orchestration of differentiation and function of regulatory T cells. *Genes and Development* **23**, 1270–1282 (2009).
44. Gregori, S., Goudy, K. S. & Roncarolo, M. G. The cellular and molecular mechanisms of immuno-suppression by human type 1 regulatory T cells. *Frontiers in Immunology* **3**, (2012).
45. Cosantino, C. M., Baecher-Allan, C. M. & Hafler, D. A. Human regulatory T cells and autoimmunity. *Eur. J. Immunol.* **38**, 921–924 (2008).
46. Sasaki, K. *et al.* Relapsing–Remitting Central Nervous System Autoimmunity Mediated by GFAP-Specific CD8 T Cells. *J. Immunol.* **192**, 3029–3042 (2014).
47. Howell, O. W. *et al.* Meningeal inflammation is widespread and linked to cortical pathology in multiple sclerosis. *Brain* **134**, 2755–2771 (2011).
48. Choi, S. R. *et al.* Meningeal inflammation plays a role in the pathology of primary progressive multiple sclerosis. *Brain* **135**, 2925–2937 (2012).
49. Lim, M., Hacohen, Y. & Vincent, A. Autoimmune Encephalopathies. *Pediatric Clinics of*

- North America* **62**, 667–685 (2015).
50. Cencioni, M. T., Mattosio, M., Magliozzi, R., Bar-Or, A. & Muraro, P. A. B cells in multiple sclerosis — from targeted depletion to immune reconstitution therapies. *Nature Reviews Neurology* **17**, 399–414 (2021).
 51. Lisak, R. P. *et al.* B cells from patients with multiple sclerosis induce cell death via apoptosis in neurons in vitro. *J. Neuroimmunol.* **309**, 88–99 (2017).
 52. Mishra, M. K. & Wee Yong, V. Myeloid cells—targets of medication in multiple sclerosis. *Nature Reviews Neurology* **12**, 539–551 (2016).
 53. Chanvillard, C., Jacolik, R. F., Infante-Duarte, C. & Nayak, R. C. The role of natural killer cells in multiple sclerosis and their therapeutic implications. *Front. Immunol.* **4**, (2013).
 54. Quintana, F. J., Yeste, A. & Mascalfroni, I. D. Role and therapeutic value of dendritic cells in central nervous system autoimmunity. *Cell Death and Differentiation* **22**, 215–224 (2015).
 55. Gandhi, R., Laroni, A. & Weiner, H. L. Role of the innate immune system in the pathogenesis of multiple sclerosis. *Journal of Neuroimmunology* **221**, 7–14 (2010).
 56. Chu, F. *et al.* The roles of macrophages and microglia in multiple sclerosis and experimental autoimmune encephalomyelitis. *Journal of Neuroimmunology* **318**, 1–7 (2018).
 57. Bennett, M. L. *et al.* New tools for studying microglia in the mouse and human CNS. *Proc. Natl. Acad. Sci. U. S. A.* **113**, E1738–E1746 (2016).
 58. Butovsky, O. *et al.* Modulation of inflammatory monocytes with a unique microRNA-gene signature ameliorates ALS mice. *J. Neuroimmunol.* **253**, 63 (2012).
 59. Jurga, A. M., Paleczna, M. & Kuter, K. Z. Overview of General and Discriminating Markers of Differential Microglia Phenotypes. *Front. Cell. Neurosci.* **14**, (2020).
 60. Gordon, S. & Taylor, P. R. Monocyte and macrophage heterogeneity. *Nature Reviews Immunology* **5**, 953–964 (2005).
 61. Yona, S. & Jung, S. Monocytes: Subsets, origins, fates and functions. *Current Opinion in Hematology* **17**, 53–59 (2010).
 62. Aguilar-Ruiz, S. R. *et al.* Human CD16 + and CD16 - monocyte subsets display unique effector properties in inflammatory conditions in vivo . *J. Leukoc. Biol.* **90**, 1119–1131 (2011).
 63. Passlick, B., Flieger, D. & Loms Ziegler-Heitbrock, H. W. Identification and characterization of a novel monocyte subpopulation in human peripheral blood. *Blood* **74**, 2527–2534 (1989).
 64. Cros, J. *et al.* Human CD14dim Monocytes Patrol and Sense Nucleic Acids and Viruses via TLR7 and TLR8 Receptors. *Immunity* **33**, 375–386 (2010).
 65. Ziegler-Heitbrock, L. *et al.* Nomenclature of monocytes and dendritic cells in blood. *Blood*

- 116**, (2010).
66. Mukherjee, R. *et al.* Non-Classical monocytes display inflammatory features: Validation in Sepsis and Systemic Lupus Erythematosus. *Sci. Rep.* **5**, (2015).
 67. Ancuta, P. *et al.* Fractalkine preferentially mediates arrest and migration of CD16+ monocytes. *J. Exp. Med.* **197**, 1701–1707 (2003).
 68. Semple, B. D., Kossman, T. & Morganti-Kossmann, M. C. Role of chemokines in CNS health and pathology: A focus on the CCL2/CCR2 and CXCL8/CXCR2 networks. *Journal of Cerebral Blood Flow and Metabolism* **30**, 459–473 (2010).
 69. Chu, H. X. *et al.* Role of CCR2 in inflammatory conditions of the central nervous system. *Journal of Cerebral Blood Flow and Metabolism* **34**, 1425–1429 (2014).
 70. Glabinski, A. R., Bielecki, B., O’Bryant, S., Selmaj, K. & Ransohoff, R. M. Experimental autoimmune encephalomyelitis: CC chemokine receptor expression by trafficking cells. *J. Autoimmun.* **19**, 175–181 (2002).
 71. Nicholson, L., Raveney, B. & Munder, M. Monocyte Dependent Regulation of Autoimmune Inflammation. *Curr. Mol. Med.* **9**, 23–29 (2009).
 72. Ajami, B. & Steinman, L. Nonclassical monocytes: Are they the next therapeutic targets in multiple sclerosis? *Immunology and Cell Biology* (2018). doi:10.1111/imcb.12004
 73. Waschbisch, A. *et al.* Pivotal Role for CD16 + Monocytes in Immune Surveillance of the Central Nervous System . *J. Immunol.* **196**, 1558–1567 (2016).
 74. Makhlof, K., Weiner, H. L. & Khoury, S. J. Increased percentage of IL-12 + monocytes in the blood correlates with the presence of active MRI lesions in MS. *J. Neuroimmunol.* **119**, 145–149 (2001).
 75. Patel, V. K., Williams, H., Li, S. C. H., Fletcher, J. P. & Medbury, H. J. Monocyte inflammatory profile is specific for individuals and associated with altered blood lipid levels. *Atherosclerosis* **263**, 15–23 (2017).
 76. Aguilar-Ballester, M., Herrero-Cervera, A., Vinué, Á., Martínez-Hervás, S. & González-Navarro, H. Impact of cholesterol metabolism in immune cell function and atherosclerosis. *Nutrients* **12**, 1–19 (2020).
 77. Pineda-Torra, I., Siddique, S., Waddington, K. E., Farrell, R. & Jury, E. C. Disrupted Lipid Metabolism in Multiple Sclerosis: A Role for Liver X Receptors? *Frontiers in Endocrinology* **12**, (2021).
 78. Luo, J., Yang, H. & Song, B. L. Mechanisms and regulation of cholesterol homeostasis. *Nature Reviews Molecular Cell Biology* **21**, 225–245 (2020).
 79. Narwal, V. *et al.* Cholesterol biosensors: A review. *Steroids* **143**, 6–17 (2019).

80. Schade, D. S., Shey, L. & Eaton, R. P. Cholesterol review: A metabolically important molecule. *Endocrine Practice* **26**, 1514–1523 (2020).
81. Shibuya, Y., Chang, C. C. Y. & Chang, T. Y. ACAT1/SOAT1 as a therapeutic target for Alzheimer's disease. *Future Med. Chem.* **7**, 2451–2467 (2015).
82. Kuzu, O. F., Noory, M. A. & Robertson, G. P. The role of cholesterol in cancer. *Cancer Research* **76**, 2063–2070 (2016).
83. Silvente-Poirot, S. & Poirot, M. Cholesterol and cancer, in the balance. *Science* **343**, 1445–1446 (2014).
84. Bloch, K. The biological synthesis of cholesterol. *Science (80-.)*. **150**, 19–28 (1965).
85. Zhang, J. & Liu, Q. Cholesterol metabolism and homeostasis in the brain. *Protein Cell* **6**, 254–264 (2015).
86. Berg, J., Tymoczko, J. & Stryer, L. *Biochemistry. 5th Edition, New York: W H Freeman. New York: W H Freeman* (2002).
87. Nohturfft, A., Brown, M. S. & Goldstein, J. L. Topology of SREBP cleavage-activating protein, a polytopic membrane protein with a sterol-sensing domain. *J. Biol. Chem.* **273**, 17243–17250 (1998).
88. Weber, L. W., Boll, M. & Stampfl, A. Maintaining cholesterol homeostasis: Sterol regulatory element-binding proteins. *World Journal of Gastroenterology* **10**, 3081–3087 (2004).
89. Iqbal, J., Qarni, A. Al & Hawwari, A. Regulation of Intestinal Cholesterol Absorption: A Disease Perspective. *Adv. Biol. Chem.* **7**, 60–75 (2017).
90. Gylling, H. & Miettinen, T. A. Inheritance of cholesterol metabolism of probands with high or low cholesterol absorption. *J. Lipid Res.* **43**, 1472–1476 (2002).
91. Feingold, K. R. Introduction to Lipids and Lipoproteins. *Endotext* 1–19 (2021).
92. Powell, L. M. *et al.* A novel form of tissue-specific RNA processing produces apolipoprotein-B48 in intestine. *Cell* **50**, 831–840 (1987).
93. Eisenberg, S. & Sehayek, E. Remnant particles and their metabolism. *Baillieres. Clin. Endocrinol. Metab.* **9**, 739–753 (1995).
94. Cohn, J. S., Marcoux, C. & Davignon, J. Detection, quantification, and characterization of potentially atherogenic triglyceride-rich remnant lipoproteins. *Arterioscler. Thromb. Vasc. Biol.* **19**, 2474–2486 (1999).
95. Elshourbagy, N. A., Meyers, H. V. & Abdel-Meguid, S. S. Cholesterol: The good, the bad, and the ugly-therapeutic targets for the treatment of dyslipidemia. *Medical Principles and Practice* **23**, 99–111 (2014).
96. Gil, G., Faust, J. R., Chin, D. J., Goldstein, J. L. & Brown, M. S. Membrane-bound domain

- of HMG CoA reductase is required for sterol-enhanced degradation of the enzyme. *Cell* **41**, 249–258 (1985).
97. Song, B. L., Javitt, N. B. & DeBose-Boyd, R. A. Insig-mediated degradation of HMG CoA reductase stimulated by lanosterol, an intermediate in the synthesis of cholesterol. *Cell Metab.* **1**, 179–189 (2005).
 98. Jin, U., Park, S. J. & Park, S. M. Cholesterol metabolism in the brain and its association with Parkinson's disease. *Experimental Neurobiology* **28**, 554–567 (2019).
 99. J., C. *et al.* Effect of high-dose simvastatin on brain atrophy and disability in secondary progressive multiple sclerosis (MS-STAT): A randomised, placebo-controlled, phase 2 trial. *The Lancet* **383**, 2213–2221 (2014).
 100. Sorensen, P. S. *et al.* Simvastatin as add-on therapy to interferon beta-1a for relapsing-remitting multiple sclerosis (SIMCOMBIN study): A placebo-controlled randomised phase 4 trial. *Lancet Neurol.* **10**, 691–701 (2011).
 101. Gafson, A. R. *et al.* Lipoprotein markers associated with disability from multiple sclerosis. *Sci. Rep.* **8**, (2018).
 102. Tall, A. R. & Yvan-Charvet, L. Cholesterol, inflammation and innate immunity. *Nature Reviews Immunology* **15**, 104–116 (2015).
 103. Manzel, A. *et al.* Role of 'western diet' in inflammatory autoimmune diseases. *Curr. Allergy Asthma Rep.* **14**, (2014).
 104. Duewell, P. *et al.* NLRP3 inflammasomes are required for atherogenesis and activated by cholesterol crystals. *Nature* **464**, 1357–1361 (2010).
 105. Fontana, L., Ghezzi, L., Cross, A. H. & Piccio, L. Effects of dietary restriction on neuroinflammation in neurodegenerative diseases. *Journal of Experimental Medicine* **218**, (2021).
 106. Jordan, S. *et al.* Dietary Intake Regulates the Circulating Inflammatory Monocyte Pool. *Cell* **178**, 1102–1114.e17 (2019).
 107. Stambanoni Bassi, M. *et al.* Obesity worsens central inflammation and disability in multiple sclerosis. *Mult. Scler. J.* **26**, 1237–1246 (2020).
 108. Bekkering, S. *et al.* Metabolic Induction of Trained Immunity through the Mevalonate Pathway. *Cell* **172**, 135–146.e9 (2018).
 109. Netea, M. G. *et al.* Trained immunity: A program of innate immune memory in health and disease. *Science* **352**, 427 (2016).
 110. Netea, M. G. *et al.* Defining trained immunity and its role in health and disease. *Nature Reviews Immunology* **20**, 375–388 (2020).

111. Christ, A. *et al.* Western Diet Triggers NLRP3-Dependent Innate Immune Reprogramming. *Cell* **172**, 162–175.e14 (2018).
112. Ghisletti, S. *et al.* Identification and Characterization of Enhancers Controlling the Inflammatory Gene Expression Program in Macrophages. *Immunity* **32**, 317–328 (2010).
113. Smale, S. T., Tarakhovsky, A. & Natoli, G. Chromatin contributions to the regulation of innate immunity. *Annual Review of Immunology* **32**, 489–511 (2014).
114. Natoli, G. & Ostuni, R. Adaptation and memory in immune responses. *Nature Immunology* **20**, 783–792 (2019).
115. Mulder, W. J. M., Ochando, J., Joosten, L. A. B., Fayad, Z. A. & Netea, M. G. Therapeutic targeting of trained immunity. *Nat. Rev. Drug Discov.* **18**, 553–566 (2019).
116. Cheng, S. C. *et al.* mTOR- and HIF-1 α -mediated aerobic glycolysis as metabolic basis for trained immunity. *Science* (80-.). **345**, (2014).
117. Mitroulis, I. *et al.* Modulation of Myelopoiesis Progenitors Is an Integral Component of Trained Immunity. *Cell* **172**, 147–161.e12 (2018).
118. Casamassimi, A., Federico, A., Rienzo, M., Esposito, S. & Ciccodicola, A. Transcriptome profiling in human diseases: New advances and perspectives. *International Journal of Molecular Sciences* **18**, (2017).
119. De Jager, P. L. Multiple Sclerosis Genomic Map implicates peripheral immune cells & microglia in susceptibility International Multiple Sclerosis Genetics Consortium * HHS Public Access. *Science* (80-.). **365**, (2019).
120. Serrano-Fernández, P. *et al.* Time course transcriptomics of IFN β drug therapy in multiple sclerosis. *Autoimmunity* **43**, 172–178 (2010).
121. Kemmerer, C. L. *et al.* Differential effects of disease modifying drugs on peripheral blood B cell subsets: A cross sectional study in multiple sclerosis patients treated with interferon- β , glatiramer acetate, dimethyl fumarate, fingolimod or natalizumab. *PLoS One* **15**, (2020).
122. Menon, R. *et al.* Gender-based blood transcriptomes and interactomes in multiple sclerosis: Involvement of SP1 dependent gene transcription. *J. Autoimmun.* **38**, (2012).
123. Mohammed, E. M. Environmental Influencers, MicroRNA, and Multiple Sclerosis. *J. Cent. Nerv. Syst. Dis.* **12**, 117957351989495 (2020).
124. Otaegui, D. *et al.* Differential micro RNA expression in PBMC from multiple sclerosis patients. *PLoS One* **4**, (2009).
125. Wang, Y. F. *et al.* The identification of up-regulated ebv-miR-BHRF1-2-5p targeting MALT1 and ebv-miR-BHRF1-3 in the circulation of patients with multiple sclerosis. *Clin. Exp. Immunol.* **189**, 120–126 (2017).

126. Bonauer, A. & Dimmeler, S. The microRNA-17~92 cluster: Still a miRacle? *Cell Cycle* **8**, 3866–3873 (2009).
127. Lorenzi, J. C. C. *et al.* miR-15a and 16-1 are downregulated in CD4+ T cells of multiple sclerosis relapsing patients. *Int. J. Neurosci.* **122**, 466–471 (2012).
128. Guerau-De-Arellano, M. *et al.* Micro-RNA dysregulation in multiple sclerosis favours pro-inflammatory T-cell-mediated autoimmunity. in *Brain* **134**, 3575–3586 (2011).
129. Amoruso, A. *et al.* Immune and central nervous system-related miRNAs expression profiling in monocytes of multiple sclerosis patients. *Sci. Rep.* **10**, (2020).
130. Koch, M., Kingwell, E., Rieckmann, P. & Tremlett, H. The natural history of primary progressive multiple sclerosis. *Neurology* **73**, 1996–2002 (2009).
131. Grath, S. & Parsch, J. Sex-Biased Gene Expression. *Annual Review of Genetics* **50**, 29–44 (2016).
132. Fresegna, D. *et al.* Re-Examining the Role of TNF in MS Pathogenesis and Therapy. *Cells* **9**, (2020).
133. Lin, C.-C. & Edelson, B. T. New Insights into the Role of IL-1 β in Experimental Autoimmune Encephalomyelitis and Multiple Sclerosis. *J. Immunol.* **198**, 4553–4560 (2017).
134. Brunetta, E. *et al.* Macrophage expression and prognostic significance of the long pentraxin PTX3 in COVID-19. *Nat. Immunol.* **22**, 19–24 (2021).
135. Wang, H. *et al.* Increased plasma levels of pentraxin 3 in patients with multiple sclerosis and neuromyelitis optica. *Mult. Scler. J.* **19**, 926–931 (2013).
136. Tsutsui, M. *et al.* TRPM2 exacerbates central nervous system inflammation in experimental autoimmune encephalomyelitis by increasing production of CXCL2 chemokines. *J. Neurosci.* **38**, 8484–8495 (2018).
137. Lund, B. T. *et al.* Increased CXCL8 (IL-8) expression in Multiple Sclerosis. *J. Neuroimmunol.* **155**, 161–171 (2004).
138. Nath, N., Giri, S., Prasad, R., Singh, A. K. & Singh, I. Potential Targets of 3-Hydroxy-3-Methylglutaryl Coenzyme A Reductase Inhibitor for Multiple Sclerosis Therapy. *J. Immunol.* **172**, 1273–1286 (2004).
139. Sevastou, I., Pryce, G., Baker, D. & Selwood, D. L. Characterisation of transcriptional changes in the spinal cord of the progressive experimental autoimmune encephalomyelitis Biozzi ABH mouse model by RNA sequencing. *PLoS One* **11**, 1–28 (2016).
140. Pleshinger, M. J. *et al.* Inhibition of SC4MOL and HSD17B7 shifts cellular sterol composition and promotes oligodendrocyte formation. *RSC Chem. Biol.* (2021).
doi:10.1039/d1cb00145k

141. Netea, M. G. & van der Meer, J. W. M. Trained Immunity: An Ancient Way of Remembering. *Cell Host and Microbe* **21**, 297–300 (2017).
142. Dobri, A. M., Dudău, M., Enciu, A. M. & Hinescu, M. E. CD36 in Alzheimer's Disease: An Overview of Molecular Mechanisms and Therapeutic Targeting. *Neuroscience* **453**, 301–311 (2021).
143. Levy-Barazany, H. & Frenkel, D. Expression of Scavenger receptor A on antigen presenting cells is important for CD4+ T-cells proliferation in EAE mouse model. *J. Neuroinflammation* **9**, (2012).
144. Hendrickx, D. A. E. *et al.* Gene expression profiling of multiple sclerosis pathology identifies early patterns of demyelination surrounding chronic active lesions. *Front. Immunol.* **8**, (2017).
145. Lemprière, S. NLRP3 inflammasome activity as biomarker for primary progressive multiple sclerosis. *Nature Reviews Neurology* **16**, 350 (2020).
146. Deerhake, M. E., Biswas, D. D., Barclay, W. E. & Shinohara, M. L. Pattern Recognition Receptors in Multiple Sclerosis and Its Animal Models. *Frontiers in Immunology* **10**, (2019).
147. Arts, R. J. W. *et al.* Glutaminolysis and Fumarate Accumulation Integrate Immunometabolic and Epigenetic Programs in Trained Immunity. *Cell Metab.* **24**, 807–819 (2016).
148. De Santa, F. *et al.* The Histone H3 Lysine-27 Demethylase Jmjd3 Links Inflammation to Inhibition of Polycomb-Mediated Gene Silencing. *Cell* **130**, 1083–1094 (2007).
149. Cha, M. H., Lee, S. M. & Jung, J. Lysophosphatidylcholine induces expression of genes involved in cholesterol biosynthesis in THP-1 derived macrophages. *Steroids* **139**, 28–34 (2018).
150. Roelofs, A. J. *et al.* Peripheral blood monocytes are responsible for $\gamma\delta$ T cell activation induced by zoledronic acid through accumulation of IPP/DMAPP. *Br. J. Haematol.* **144**, 245–250 (2009).
151. Ghasemi, N., Razavi, S. & Nikzad, E. Multiple sclerosis: Pathogenesis, symptoms, diagnoses and cell-based therapy. *Cell Journal* **19**, 1–10 (2017).
152. Ajami, B., Bennett, J. L., Krieger, C., McNagny, K. M. & Rossi, F. M. V. Infiltrating monocytes trigger EAE progression, but do not contribute to the resident microglia pool. *Nat. Neurosci.* **14**, 1142–1150 (2011).
153. Ajami, B. & Steinman, L. Nonclassical monocytes: Are they the next therapeutic targets in multiple sclerosis. *Immunology and Cell Biology* **96**, 125–127 (2018).
154. Severa, M. *et al.* A cell type-specific transcriptomic approach to map B cell and monocyte type I interferon-linked pathogenic signatures in Multiple Sclerosis. *J. Autoimmun.* **101**, 1–16

(2019).

155. Lara-Guzmán, O. J. *et al.* Oxidized LDL triggers changes in oxidative stress and inflammatory biomarkers in human macrophages. *Redox Biol.* **15**, 1–11 (2018).
156. Kankkunen, P. *et al.* (1,3)- β -Glucans Activate Both Dectin-1 and NLRP3 Inflammasome in Human Macrophages. *J. Immunol.* **184**, 6335–6342 (2010).
157. Gang Xiao, Z. *et al.* The Roles of Histone Demethylase UTX and JMJD3 (KDM6B) in Cancers: Current Progress and Future Perspectives. *Curr. Med. Chem.* **23**, 3687–3696 (2016).